



UNIVERSITAT POLITÈCNICA DE CATALUNYA
BARCELONATECH

Escola Tècnica Superior d'Enginyeria
Industrial de Barcelona



Master Thesis

Master's degree in Energy Engineering

Hydrogen production with photocatalysts prepared by
mechanochemical methods

Author: Verónica Anadón Martínez
Directors: Jordi Llorca Piqué
Isabel Serrano Carreño

September 2020

Resum

L'objectiu d'aquesta tesi és l'estudi de l'obtenció d'hidrogen amb fotocatalitzadors preparats amb mètodes mecanoquímics a partir de semiconductors com el diòxid de titani.

La preparació dels fotocatalitzadors i el seu assaig es van realitzar en un fotoreactor al laboratori. D'aquesta manera es va poder determinar mitjançant les diferents tècniques i composicions químiques utilitzades, quina formulació era la més eficaç.

Els mètodes mecanoquímics són simples i respectuosos amb el medi ambient perquè no s'utilitzen dissolvents; són més ràpids i reproduïbles. La tècnica mitjançant la qual s'han dut a terme els experiments és el "ball milling". Aquest mètode és una tècnica mecànica àmpliament utilitzada per moldre les mostres de pols de diferents composicions químiques en una barreja homogènia de les partícules d'aquests materials.

Les mostres utilitzades per aquest estudi han sigut una barreja de diòxid de titani o titania (TiO_2) amb diferents composicions químiques d'un altre semiconductor. Aquests han estat el diòxid d'estany (SnO_2), òxid de zinc (ZnO), òxid de coure (II) (CuO), sulfur de cadmi (CdS) i sulfur de zinc (ZnS). Un cop obtinguda la mostra mitjançant "ball milling" a partir de diferents composicions de 90 % TiO_2 més 10 % de l'altre semiconductor, s'ha analitzat la seva reactivitat en un fotoreactor de laboratori per determinar quina quantitat d'hidrogen produeix cada fotocatalitzador.

Mitjançant aquest anàlisi s'ha determinat que el fotocatalitzador que obté els millors resultats quant a producció d'hidrogen és la combinació de 90 % TiO_2 10 % CuO . Degut a que el semiconductor de CuO té un band gap més petit que la resta de semiconductors analitzats. Per tant, els semiconductors que presentaven un band gap més elevat com el ZnO o el SnO_2 , han sigut aquells que han obtingut pitjors resultats, exceptuant el fotocatalitzador de SnO_2 , ja que ha sigut el segon fotocatalitzador que millor ha funcionat.

Per tant, segons els resultats obtinguts, s'ha determinat que no només s'ha de tenir en compte el band gap del semiconductor a l'hora de preparar un fotocatalitzador, sinó que també la posició de la CB i VB de cada semiconductor, per poder determinar quina combinació d'elements és més adient.

Paraules clau:

Hidrogen, Fotocatalitzador, "Ball milling", "Band gap", "Valence band" (VB), "Conduction band" (CB), Semiconductor, Mètode mecanoquímic, Fotoreactor.

Resumen

El objetivo de esta tesis es el estudio de la obtención de hidrógeno con fotocatalizadores preparados con métodos mecanoquímicos a partir de semiconductores como el dióxido de titanio.

La preparación de los fotocatalizadores y su ensayo se realizaron en un fotoreactor en un laboratorio de la universidad. De este modo se pudo determinar mediante las diferentes técnicas y composiciones químicas utilizadas, qué formulación era la más eficaz.

Los métodos mecanoquímicos son simples y respetuosos con el medio ambiente porque no se utilizan disolventes; son más rápidos y reproducibles. La técnica mediante la cual se han llevado a cabo los experimentos es el "ball milling". Este método es una técnica mecánica ampliamente utilizada para moler las muestras de polvo de diferentes composiciones químicas en una mezcla homogénea de las partículas de estos materiales.

Las muestras utilizadas para este estudio han sido una mezcla de dióxido de titanio o titania (TiO_2) con diferentes composiciones químicas de otro semiconductor. Estos han sido: el dióxido de estaño (SnO_2), óxido de zinc (ZnO), óxido de cobre (II) (CuO), sulfuro de cadmio (CdS) y sulfuro de zinc (ZnS). Una vez obtenida la muestra mediante "ball milling" a partir de diferentes composiciones de 90% TiO_2 más 10% del otro semiconductor, se ha analizado su reactividad en un fotoreactor del laboratorio para determinar qué cantidad de hidrógeno produce cada fotocatalizador.

Mediante este análisis se ha determinado que el fotocatalizador que obtiene los mejores resultados en cuanto a producción de hidrógeno es la combinación de 90 % TiO_2 10% CuO . Debido a que el semiconductor de CuO tiene un band gap más pequeño que el resto de semiconductores analizados. Por lo tanto, los semiconductores que presentaban un band gap más elevado como el ZnO o lo ZnS , han sido aquellos que han obtenido peores resultados, exceptuando el fotocatalizador de SnO_2 , ya que ha sido el segundo fotocatalizador que mejor ha funcionado.

Por lo tanto, según los resultados obtenidos, se ha determinado que no solo se tiene que tener en cuenta el band gap del semiconductor en el momento de preparar un fotocatalizador, sino que también se tiene que considerar la posición de la CB y VB de cada semiconductor, para poder determinar qué combinación de elementos es más adecuada.

Palabras clave:

Hidrogeno, Fotocatalizador, "Ball milling", "Band gap", "Valence band" (VB), "Conduction band" (CB), Semiconductor, Método mecanoquímico, Fotoreactor.

Abstract

The objective of this thesis is to study the hydrogen production according to the preparation of photocatalysts with mechanochemical methods from semiconductors such as titanium dioxide.

The preparation of the photocatalysts and their assay were performed in a laboratory with a photoreactor. In this way it was possible to determine by the different techniques and chemical compositions, which formulation was the most effective.

The mechanochemical methods are simple and environmentally friendly because no solvents are used; they are faster and easily reproducible. The technique by which the experiments were performed is called ball milling. This method is a mechanical technique widely used to grind powders into fine particles and blend materials.

The samples used for this study were a mixture of titanium dioxide (TiO_2) with different chemical compositions of another semiconductor. These were tin (IV) oxide (SnO_2), zinc oxide (ZnO), copper (II) oxide (CuO), cadmium sulphide (CdS) and zinc sulphide (ZnS). Once the sample was obtained by ball milling from different compositions of 90% TiO_2 plus 10% from another semiconductor mentioned before, its reactivity was analysed in a laboratory photoreactor to determine how much hydrogen produces each photocatalyst.

This analysis has determined that the photocatalyst that achieves the best results in terms of hydrogen production is the combination of 90% TiO_2 and 10% CuO , since CuO semiconductor has a smaller band gap than the other semiconductors analysed. Therefore, the semiconductors that had a higher band gap, such as ZnO or ZnS , were the ones that obtained the worst results, except for the SnO_2 photocatalyst, as it was the second photocatalyst that worked best.

Therefore, according to the results obtained, it has been determined that not only the semiconductor band gap must be considered when preparing a photocatalyst, but also the position of the CB and VB of each semiconductor, to be able to determine which combination of elements is most suitable.

Keywords:

Hydrogen, Photocatalyst, Ball milling, Band gap, Valence band (VB), Conduction band (CB), Semiconductor, Mechanochemical method, Photoreactor.

Acknowledgement

I would like to thank to all those who made possible for me to complete this thesis.

I want to thank...

... Prof. Jordi Llorca for giving me the possibility to work in this subject, to develop a practise thesis, with research and experimental part. Thank you also for the help to acquire all the required knowledge for this thesis.

... Isabel Serrano, thanks for your help, and for all your time dedicated to me, for teaching me how all the equipment and the photocatalytic system works and patience with me throughout the process.

... my family, for those who are here, but specially all for those who are no longer, thanks for your support.

List of Figures

Figure 1. Global energy-related carbon dioxide emissions by source, 1990-2018 adapted from [3]	18
Figure 2. Current policy support for hydrogen deployment in 2018 adapted from [7].....	19
Figure 3. Hydrogen sources and integration of renewable sources into end uses by means of hydrogen adapted from [8].....	21
Figure 4. Scheme of steam reforming of natural gas. [11].....	23
Figure 5. Scheme of the process of hydrogen production with biomass or biofuels.	24
Figure 6. Scheme of hydrogen production through electrolysis. [12]	26
Figure 7. Scheme of the three main technologies used for the electrolysis process [13].	27
Figure 8. Scheme of the basic principle of the overall water-splitting reaction on a semiconductor photocatalyst adapted from [15].....	28
Figure 9. Schematic representation of a ball mill with two powder material to grind.	32
Figure 10. Scheme of the system used to develop the thesis.	33
Figure 11. Type of recipient to do ball milling.....	34
Figure 12. Preparation of one sample in the laboratory balance.....	34
Figure 13. Preparation of one sample for ball milling.....	35
Figure 14. Last steps in the preparation of the sample for the photochemical reactor.....	36
Figure 15. Photocatalytic system.....	36
Figure 16. Tubular photoreactor without the sample (left) and with the sample (right).	37
Figure 17. Micro GC and burette of flow measurement. [46]	39
Figure 18. Placing the sample in the photoreactor.....	39
Figure 19. Evolution of the O ₂ concentration during the experiment.....	44
Figure 20. Evolution of H ₂ concentration and CH ₃ CHO concentration during the experiment.	44

Figure 21. Evolution of the O ₂ concentration and the H ₂ produced for a catalyst of 100 % TiO ₂ .	46
Figure 22. Evolution of the O ₂ concentration and the H ₂ produced for a catalyst of 90 % TiO ₂ 10 % ZnO.....	47
Figure 23. Evolution of the O ₂ concentration and the H ₂ produced for a catalyst of 90 % TiO ₂ 10 % ZnO.....	48
Figure 24. Evolution of the O ₂ concentration and the H ₂ produced for a catalyst of 90 % TiO ₂ 10 % CuO.....	48
Figure 25. Evolution of the O ₂ concentration and the H ₂ produced for a catalyst of 90 % TiO ₂ 10 % CdS.....	49
Figure 26. Evolution of the O ₂ concentration and the H ₂ produced for a catalyst of 90 % TiO ₂ 10 % ZnS.....	49
Figure 27. Evolution of the O ₂ concentration and the H ₂ produced for a catalyst of 90 % TiO ₂ 10 % SnO ₂	50
Figure 28. Evolution of the O ₂ concentration and the H ₂ produced for a catalyst of 90 % TiO ₂ 10 % SnO ₂	50
Figure 29. Comparison between the H ₂ and the CH ₃ CHO produced for 100 % TiO ₂	51
Figure 30. Comparison between the H ₂ and the CH ₃ CHO produced for 90 % TiO ₂ 10 % ZnO.....	52
Figure 31. Comparison between the H ₂ and the CH ₃ CHO produced for 90 % TiO ₂ 10 % ZnO.....	52
Figure 32. Comparison between the H ₂ and the CH ₃ CHO produced for 90 % TiO ₂ 10 % CuO.....	53
Figure 33. Comparison between the H ₂ and the CH ₃ CHO produced for 90 % TiO ₂ 10 % CdS.....	54
Figure 34. Comparison between the H ₂ and the CH ₃ CHO produced for 90 % TiO ₂ 10 % ZnS.....	54
Figure 35. Comparison between the H ₂ and the CH ₃ CHO produced for 90 % TiO ₂ 10 % SnO ₂	55
Figure 36. Comparison between the H ₂ and the CH ₃ CHO produced for 90 % TiO ₂ 10 % SnO ₂	56
Figure 37. Comparison between the evolution of O ₂ concentration of the ZnO compound.	57
Figure 38. Comparison between the amount of H ₂ produced of ZnO compound.....	57
Figure 39. Comparison between the evolution of O ₂ concentration of the SnO ₂ compound.....	58

Figure 40. Comparison between the amount of H₂ produced of SnO₂ compound. 58

Figure 41. Comparison between all the catalysts analysed regarding H₂ production. 59

Figure 42. Band energies of the photocatalysts consider in the thesis with respect to TiO₂. 60

Figure 43. Schematic diagram of the photogeneration of H₂ on the TiO₂-CuO system. [47] 61

Figure 44. Gantt Diagram of the thesis..... 67

List of Tables

Table 1. Hydrogen generation sources adapted from [6].	22
Table 2. Comparative of the techniques.	23
Table 3. Physical characteristics of the semiconductors used in this work.	29
Table 4. Experimental data.	41
Table 5. Comparison between all the catalysts analysed reagrding H ₂ production.	59
Table 6. Personnel costs associated to the thesis.	69
Table 7. Cost of the equipment associated to the thesis.	69
Table 8. Economic budget associated to the thesis.	70
Table 9. Project final cost.	70
Table 10. Data from Channel 1.	94
Table 11. Data from Channel 3.	108

Index

RESUM	2
RESUMEN	3
ABSTRACT	4
ACKNOWLEDGEMENT	5
LIST OF FIGURES	7
LIST OF TABLES	11
1. PREFACE	15
1.1. Origin of the work.....	15
1.2. Motivation.....	15
1.3. Prerequisites.....	15
2. INTRODUCTION	17
2.1. Objectives of this work.....	20
2.2. Scope of the work.....	20
3. LITERATURE SURVEY	21
3.1. Hydrogen production.....	21
3.1.1. Reforming and gasification processes.....	22
3.1.2. Biological process.....	25
3.1.3. Thermal cycles.....	25
3.1.4. Electrolysis.....	26
3.2. Photocatalysis.....	27
3.2.1. Semiconductor materials.....	29
4. EXPERIMENTAL SETUP AND CONDITIONS	33
4.1. Preparation of the photocatalyst.....	34
4.2. Photocatalytic system.....	36
4.2.1. Photoreactor.....	37
4.2.2. Micro Gas Chromatograph.....	37
4.2.3. Experimental plan and method.....	38
4.3. Realization of the experiments.....	39
4.3.1. Data collection of the photocatalysts.....	40

5. HYDROGEN PRODUCTION WITH PHOTOCATALYSTS PREPARED BY MECHANOCHEMICAL METHODS	43
5.1. Data analysis.....	43
5.2. Results.....	46
5.2.1. Influence of the compounds of the photocatalyst prepared.....	46
5.2.2. Verification of the H ₂ obtained with the amount of CH ₃ CHO produced.....	51
5.2.3. Comparison of the results between preparing the photocatalyst with different conditions of ball milling.....	56
5.2.4. Analysis of the results.....	59
CONCLUSIONS	63
FUTURE WORK	65
TEMPORAL PLANNING	67
ECONOMIC ANALYSIS	69
ENVIRONMENTAL IMPACT	71
NOMENCLATURE	73
BIBLIOGRAPHY	75
A EXCEL CALCULATIONS	79
B DATASHEETS	109
B1. FRITSCH Ball Mills - Mini-Mill PULVERISETTE 23 [44].....	109
B2. Agilent 490 Micro Gas Chromatograph [43].....	110

1. Preface

In this study, the hydrogen production using photocatalysts prepared by mechanochemical methods, as ball milling, will be investigated. This research includes the preparation of the photocatalysts and their assay in a laboratory photoreactor. The best formulation will be characterized by different techniques. Hydrogen is an energy vector that allows better energy management. One method of obtaining it is from the Sun with photocatalysts made of semiconductors.

This work was performed at the campus of *Escola d'Enginyeria de Barcelona Est (EEBE)*, *Universitat Politècnica de Catalunya (UPC)*. The content of this thesis is part of the investigation carried out in the research group focussed on the production of hydrogen by different methods and applications (*Nanoengineering of materials applied to energy, NEMEN*). Therefore, this thesis is related to the previous work done there, showing continuity with respect to the research activity performed.

1.1. Origin of the work

The present work was performed in a research group working in the hydrogen production. As it was mentioned, hydrogen is thought to be a clean and renewable energy vector. In this thesis, the hydrogen production by photocatalysis by semiconductor formulations in the presence of sunlight, simulated with ultraviolet (UV) light in a laboratory photoreactor is analysed.

1.2. Motivation

Currently, it has been declared climate emergency, admitting by the governments that global warming exists and that the measures taken up to this point are not enough. Moreover, today's societies attempt to keep improving their quality of life by searching for new energy systems that meet the demands of society at attainable prices. That's why every development made in terms of renewable energy production, in this case with hydrogen production, it is essential.

1.3. Prerequisites

To accomplish the thesis some knowledge in chemistry and hydrogen production could be helpful in order to develop some of the hypothesis to analyse in this study. Additionally, understanding how this energy vector works will be also useful for developing the thesis.

2. Introduction

One of the objectives of today's society, in all its sectors, is sustainable improvement of the quality of life and, more precisely, the search for new energy systems that meet the demands of society (reducing contaminating agents and ensuring the energy supply) at attainable prices.

Furthermore, these days governments and scientists have stated a climate emergency declaration, an action taken to acknowledge humanity is in a climate emergency. In declaring a climate emergency, a government admits that global warming exists and that the measures taken up to this point are not enough to limit the changes brought by it.

The science of climate change is well established [1]:

- » Climate change is real and human activities are the main cause. (IPCC)
- » The concentration of greenhouse gases in the earth's atmosphere is directly linked to the average global temperature on Earth. (IPCC)
- » The concentration has been rising steadily, and mean global temperatures along with it, since the time of the Industrial Revolution. (IPCC)
- » The most abundant greenhouse gas, accounting for about two-thirds of greenhouse gases, carbon dioxide (CO₂), is largely the product of burning fossil fuels. (IPCC)

It is known that the energy sector is essential to combat climate change. Promoting sustainable development and combating climate change have become integral aspects of energy planning, analysis and policy making. Energy accounts for two-thirds of total greenhouse gas, so efforts to reduce emissions and mitigate climate change must include the energy sector [2].

Global energy-related CO₂ emissions grew 1.7% in 2018 to reach a historic high of 33.1 Gt CO₂. It was the highest rate of growth since 2013, as it is illustrated in Figure 1. Moreover, the increase in emissions was determined by higher energy consumption resulting from a robust global economy, as well as from weather conditions that led to increased energy demand for heating and cooling in some parts of the world [3].

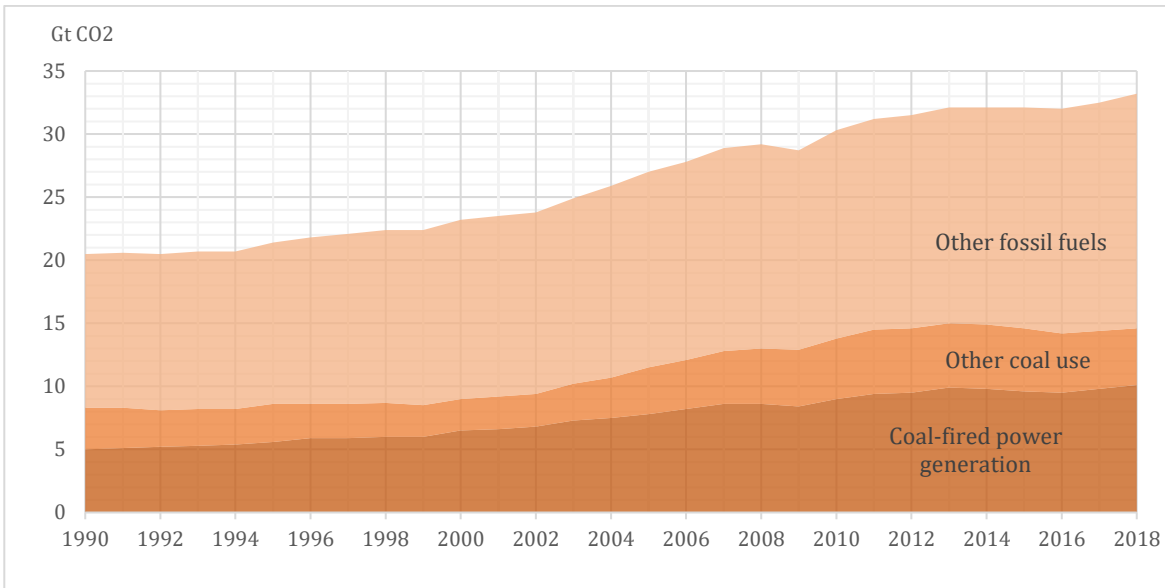


Figure 1. Global energy-related carbon dioxide emissions by source, 1990-2018 adapted from [3]

Regarding renewables, an increase of their use in 2018 had a considerable impact on CO₂ emissions, avoiding 215 Mt of emissions, due to the transition to renewables in the power sector. Therefore, emissions growth would have been 50% higher, without the transition to low-carbon sources of energy in 2018. Nonetheless the energy efficiency contribution was lower, mainly because of a continued slowdown in implementing energy efficiency policies [3].

Furthermore, for the current situation carbon emissions are falling abruptly due to coronavirus [4]. In relation to the global pandemic CO₂ emissions are decreasing promptly [5], nonetheless experts have said that the decline will not last if governments do not start moving to cleaner energy, as it was announced with the climate emergency declaration.

For example, in China, carbon emissions were decreasing approximately 18 % between early February and mid-March due to falls in coal consumption and industrial output. Nevertheless, as consequence of the number of coronavirus cases have been reducing, China has been working hard to restart its economy, which means that China's emissions are already rebounding as the country restarts its factories [4].

For this reason, if that absence of strong government support for clean energy moving forward, experts have said the pandemic will not reverse the upward March of global carbon emissions, something that requests to happen immediately in order to help the world meet its climate targets.

Therefore, renewables have to continue growing, in order to become a robust and indispensable resource for energy generation industries. The challenge to meet the goals in all sectors (transport, industry, buildings, etc.) is enormous, especially in electricity generation [6]. That is why hydrogen can be a decisive part in the shift to a net-zero-emission future because of its cleanness and flexibility to act as a fuel in various applications as well as energy storage.

Hydrogen is known as a technically viable and benign energy vector. However, with hydrogen being naturally unavailable in its pure form, traditionally industries such as oil refining and fertilisers have sourced it through processes such as gasification and reforming of fossil fuels [6].

In the long term, for hydrogen to be seen as a clean fuel that can be produced on a large scale, it should have to be provided by renewable energy sources, which are capable of producing it. Figure 2 demonstrates the trend on the number of countries with policies that directly support investment in hydrogen technologies is increasing, along with the number of sectors [7].

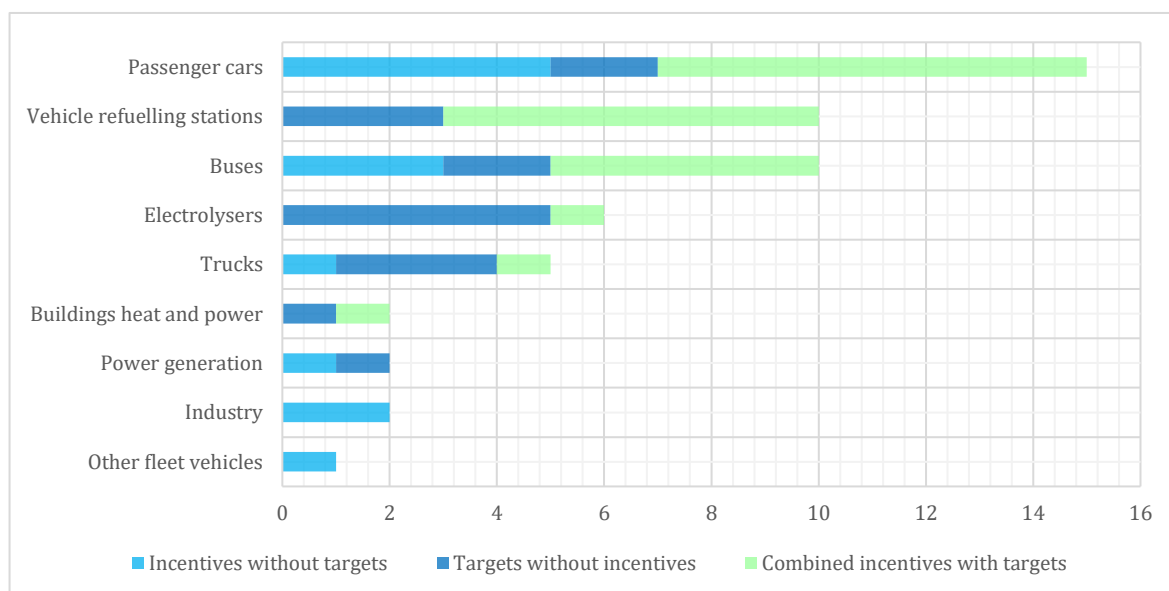


Figure 2. Current policy support for hydrogen deployment in 2018 adapted from [7]

Therefore, the production of hydrogen from these renewable sources could permit distributed generation in accordance with local economies, by means of the cleanest and most appropriate method in each case; but also, it releases regions and countries of the need to import fossil fuels and their derivatives because, in many cases, local production of the required hydrogen will be possible. For this reason, over the past few years, global spending on hydrogen energy research, development and demonstration by national governments has risen.

On the other hand, a common consideration is that, in the short to medium term, the best way to propitiate renewable hydrogen's entering the market will be its production using wind or solar photovoltaic energy, or by reforming biofuels, mainly due to the possibilities presented by implementation of decentralized production.

The recent tipping point in the cost of some renewable energy technologies such as wind and solar photovoltaics (PV) has mobilised continuing sustained interest in renewable hydrogen through water splitting [6]. Accordingly, the method used in this thesis for hydrogen production is by photocatalysis that in the presence of sunlight are potential future methods to produce hydrogen.

2.1. Objectives of this work

The main objective of this thesis is to study the hydrogen production according to the preparation of photocatalysts with mechanochemical methods from semiconductors such as titanium dioxide. Additionally, this project includes the preparation of photocatalysts and their testing in a laboratory photoreactor. Therefore, the aim is to find the most efficient formulation by characterizing it with different techniques.

2.2. Scope of the work

Hydrogen is an energy vector that allows better management of energy. One of its methods of obtaining is from the Sun with photocatalysts made of semiconductors. Photons of energy above the band gap give rise to electron-hole pairs that can be used to carry out reduction-oxidation reactions and obtain hydrogen.

The aim of this study is to prepare photocatalysts with mechanochemical methods from semiconductors such as titanium dioxide. These mechanochemical methods are simple and environmentally friendly, because no solvents are used; in addition, they are fast and easily reproducible. It is about finding an effective and stable formulation in hydrogen production and the best preparation parameters (mechanochemical energy, preparation time, etc.). The work includes the preparation of photocatalysts and their testing in a laboratory photoreactor. The best formulation will be characterized by different techniques.

3. Literature Survey

Hydrogen production with photocatalysts prepared by mechanochemical methods is the main objective of this thesis. The existing literature on hydrogen production via photocatalysis is in fact extensive. In this section, relevant research on the topic focused in the use of different photocatalysts is analysed.

Hydrogen is not only known as the most abundant gas in the universe, but also is the lightest. Moreover, it has the maximum energy content of conventional fuels per unit of weight, e.g. energy content of hydrogen is about three times of that of gasoline [6]. However, free hydrogen on the Earth is almost inexistent. Fortunately, there are different pathways to obtain it, e.g. through electrolysis, i.e. renewable assisted water splitting, thermochemical conversion of fossil fuels, or biological processes among others.

3.1. Hydrogen production

A significant part of the hydrogen produced today is not CO₂-free, it comes from oil, coal or gas. Therefore, producing hydrogen from natural gas does not help to solve energy-related problems because not only to the limitations of fossil fuels supply, but also to the process to obtain hydrogen produces massive amounts of carbon dioxide; a main contributor to global warming. However, if it is produced from renewable power via electrolysis, then hydrogen is fully renewable and CO₂-free.

Renewable hydrogen has the potential to decarbonize a large range of applications, from power to transport, among others. Figure 3 demonstrates the potential of producing hydrogen from renewable sources instead of using fossil fuels.

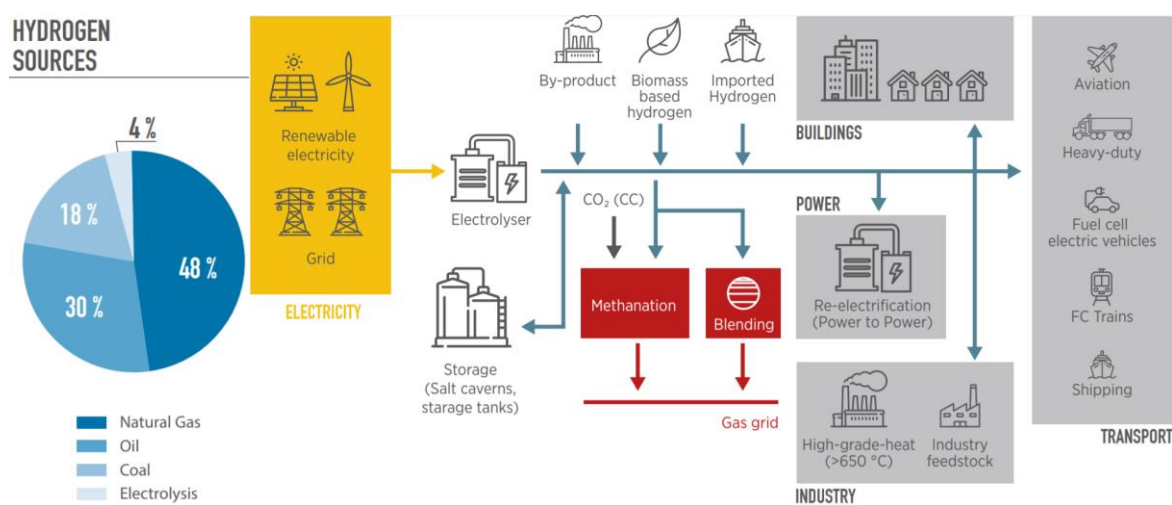


Figure 3. Hydrogen sources and integration of renewable sources into end uses by means of hydrogen adapted from [8].

Hydrogen (H₂) is considered one of the most suitable form of energy for the next years because its combustion is non-polluting. When hydrogen is combined with oxygen from the air produces just water vapor as the combustion product. Thus, through renewable assisted water splitting, thermochemical conversion of fossil fuels, and biological processes, hydrogen can be obtained. The most straightforward pathway is water splitting but has not been traditionally favoured as a result of its high energy demand [6]. Moreover, the storage possibilities of hydrogen make it an ideal candidate to replace natural gas, since it can be stored as a pressurized gas or liquid, or distributed over gas pipelines [8].

Table 1 summarizes hydrogen generation pathways, including their source of energy, hydrogen source, process, reaction kinetics adapted from the information [6].

Source of process energy	Hydrogen source	Approach	Process	Reactions
Fossil fuels Biomass Waste Biofuels	Fossil	Thermochemical	Reforming	$C_nH_m + nH_2O \rightleftharpoons (n + \frac{m}{2})H_2 + nCO$
	Biomass		Pyrolysis	$C_nH_m \rightarrow nC + \frac{m}{2}H_2$
	Waste Biofuels		Gasification	-
Bacteria Bacteria and light	Hydrocarbons	Biological	Dark fermentation Photofermentation	-
Light	Water	Photocatalysis	Photoelectrochemical	$2H_2O + light \rightleftharpoons 2H_2 + O_2$
Electricity	Wind energy Geothermal Hydroelectric Nuclear	Electrolysis	Electricity based	$2H_2O + electricity \rightleftharpoons 2H_2 + O_2$
	Solar energy Nuclear	Electrolysis Thermal cycles	Photochemical Thermoelectrical	$2H_2O \rightleftharpoons 2H_2 + O_2$ $2H_2O + heat \rightleftharpoons 2H_2 + O_2$

Table 1. Hydrogen generation sources adapted from [6].

Hydrogen generation via solar water splitting represents a promising solution to these needs, as H₂ can be stored, transported and consumed without generating polluting by-products. Even though, the cost of H₂ produced by electrolysis is still higher than that produced by fossil fuels [9].

3.1.1. Reforming and gasification processes

Currently, reforming processes account the 95 % of H₂ production. This technology includes different techniques, as steam reforming (SR), partial oxidation (PO), complete oxidation (combustion), water gas shift reaction (WGSR), dry reforming (DR) and autothermal reforming (ATR). Each of these reactions are defined below (Table 2). Moreover, these reforming techniques provide CO₂, which is used for different technologies of CO₂ capture.

Process	Reactions	Reactant	
Steam reforming (SR)	Natural Gas reforming: $CH_4 + H_2O \rightleftharpoons CO + 3H_2$	H_2O	Endothermic reaction $\Delta H^\circ > 0$
	$CH_4 + 2H_2O \rightleftharpoons CO_2 + 4H_2$	H_2O	
Partial oxidation (PO)	$CH_4 + O_2 \rightleftharpoons CO_2 + 2H_2$ $CH_4 + \frac{1}{2}O_2 \rightleftharpoons CO + 2H_2$	Air and O_2	Exothermic reaction $\Delta H^\circ < 0$
Combustion	$C_nH_m \rightarrow nC + \frac{m}{2}H_2$	excess of O_2	Exothermic reaction $\Delta H^\circ < 0$
Water gas shift reaction (WGSR)	Natural Gas reforming: $CO + H_2O \rightleftharpoons CO_2 + H_2$	H_2O	Exothermic reaction $\Delta H^\circ < 0$
Dry reforming (DR)	$CH_4 + CO_2 \rightleftharpoons 2CO + 2H_2$	CO_2	Endothermic reaction $\Delta H^\circ \gg 0$
Autothermal reforming (ATR)	$PO + SR$	$O_2 + H_2O$	$\Delta H^\circ \sim 0$

Table 2. Comparative of the techniques.

From all these techniques expose, SR is the most complete endothermic catalytic process for the generation of hydrogen-rich syngas from light hydrocarbons [6]. Thus, SR is one of the most extensive and at the same time least expensive processes for hydrogen production [10] due to its advantages, e.g. its efficiency or that just requires modest temperatures (around 180 °C).

Figure 4 illustrates an example of natural gas reforming scheme, where the incoming natural gas is burned to provide the necessary energy for the reaction. Then, high-pressure steam is included, which reacts with the methane. The synthesis gas contains a mixture of H_2 , CO_2 , CO , as well as unreacted CH_4 and H_2O , which goes through into the cooler shift reactor. Then, in the output of the shift reactor is obtained about three quarters of H_2 . Finally, in the pressure surge adsorption unit (PSA), the impurities are removed, and recycled back through the burner, giving more than 99.9% pure hydrogen.

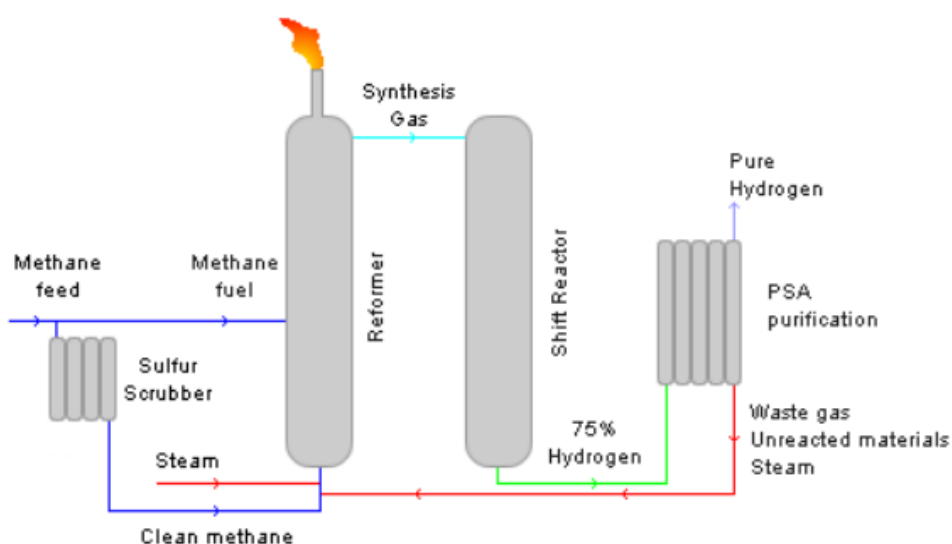


Figure 4. Scheme of steam reforming of natural gas. [11]

As it is defined in Table 2, ATR combines steam reforming (endothermic process) and partial oxidation (exothermic) reactions. As it is exposed, SR is an endothermic process, i.e. it is energy demanding. Thus, since this energy required has to be transferred into the system from the outside, ATR represents a significant over SR process due to that characteristic and because it can be shut down and started very rapidly [10].

Gasification is a very developed process, defined as a process whereby liquid or solid fuels such as coal, oil, waste and biomass are partially oxidised with oxygen and steam under high temperature and pressure in a gasifier reactor to form syngas (PO reactions). The reaction of coal with steam produces synthesis gas composed of a mixture of H₂ with CH₄, CO₂, CO and other compounds depending on the gasification temperature. When the temperature increases considerably, the proportion of H₂ and CO increases. Moreover, CO can react again with H₂O, producing more hydrogen, which is the case of WGSR.

The gasification process commonly has low thermal efficiency since biomass contained moisture that must also be vaporized. Furthermore, it can be completed with or without a catalyst and in a fixed-bed or fluidized-bed reactor, with the latter reactor having typically better performance[10].

Biomass can be considered a potential alternative fuel source, since it can be found from a wide range of sources such as crops, wood, industrial residue, animal waste, municipal solid waste, sawdust, aquatic plants and algae, waste paper, and many others. That's why it is expected that biomass could fill the energy demand by more than 25% by the year 2050. The CO₂ emissions from biomass are recycled from the air through plant photosynthesis, establishing a carbon neutral cycle, unlike fossil fuels [6]. Thus, reforming with renewable fuels is defined in Figure 5.

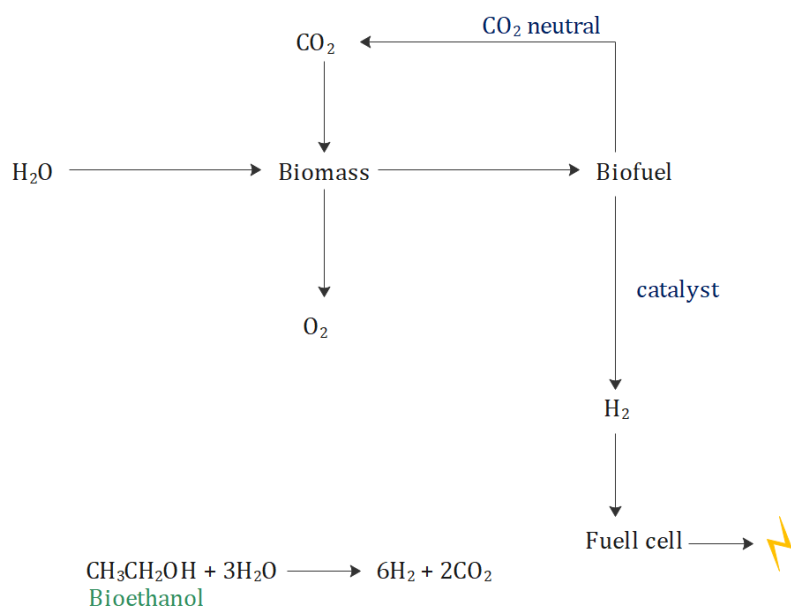


Figure 5. Scheme of the process of hydrogen production with biomass or biofuels.

In addition, thermochemical conversion of biomass is very similar to that of fossil fuels using gasification or pyrolysis, as it is illustrated in Figure 5 with bioethanol as combustion product. Both processes produce CO₂, CO or CH₄, which can be processed for excess hydrogen production through SR and WGSR [6].

3.1.2. Biological process

The biological processes are being widely considered because they do not deliver of carbon to the atmosphere, since this method uses the ability of microorganisms to produce hydrogen through the consumption of carbon dioxide, i.e. these methods offer carbon-neutral hydrogen production.

Therefore, fermentation is an ideal method to produce hydrogen, as it is used waste materials, being this production cheaper with concurrent waste treatment [6]. Dark fermentation is a relatively simple technique because of any light sources is needed, thus it can produce hydrogen at any time. In contrast, photofermentation requires solar energy to be able to produce some hydrogen.

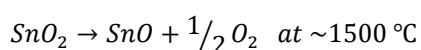
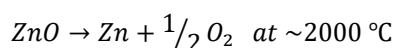
3.1.3. Thermal cycles

Thermal processes are those which require high temperature to be reached for the reaction to begin. That's why it can be utilized solar or nuclear energy to generate heat, causing that the steam dissociates into H₂ and O₂. Since, high temperature heat and water are required to start the process, H₂ and O₂ are obtained, one drawback of this process comes from the need of an effective technique to separate H₂ and O₂ to avoid ending up with an explosive mixture [10].

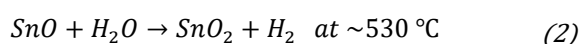
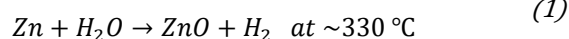
Moreover, at high-temperature conditions, the reaction kinetics of the electrolyser increase and, as a result, electrical losses in a fuel cell decrease [6]. Thus, high efficiency is obtained due to the high temperatures reached.

Solar thermal energy can be used as an energy source to produce hydrogen by thermochemical processes, regarding current studies, the two-step metal oxide reactions are the most investigated, i.e. thermal reduction and re-oxidation, for instance zinc-oxide cycle (ZnO) illustrated in Equation (1) and SnO₂/SnO based cycle (2) adapted from [6] are some of these reactions.

Dissociation:



Hydrolysis:



Therefore, as it is illustrated with Equations (1) and (2), the thermal cycles combine more than one reaction to obtain H₂ from H₂O.

3.1.4. Electrolysis

Electrolysis is an established technology, which consists of the decomposition of water into its constituent elements, hydrogen and oxygen, by means of electricity at room temperature (Figure 6). From two molecules of water there are obtained two molecules of hydrogen which will be used as fuel and one molecule of oxygen which is released to the ambient.

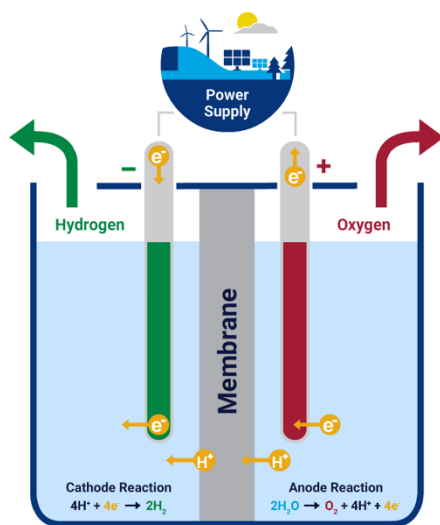


Figure 6. Scheme of hydrogen production through electrolysis. [12]

Depending on the source used as power supply is not profitable to use the hydrogen obtained to produce electricity, because of it would be obtained a smaller amount of electricity. Thus, for this process to be viable, the electricity initially required must come from renewable sources.

The energetic efficiency of the electrolysis of water in practice reaches 50-70 % [10]. There are three main commercial technologies electrolysis, as it is illustrated in Figure 7. The most commercial electrolysis technology is alkaline-based (AEC) but proton exchange membrane (PEM) and solid oxide electrolysis cells (SOEC) have been developed. Regarding that, SOEC has the highest potential for efficiency gains among commercial configurations, i.e. this electrolyzers are the most electrically efficient but the least developed [6][10].

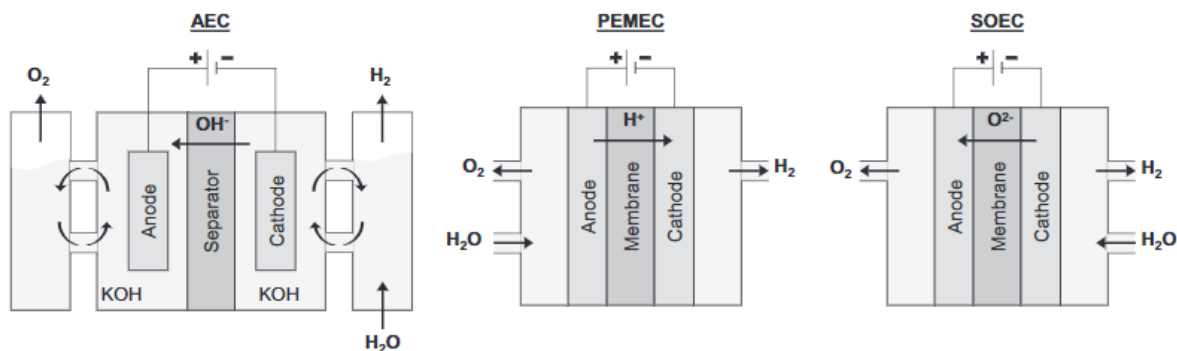


Figure 7. Scheme of the three main technologies used for the electrolysis process [13].

Summarizing, in water electrolysis, the electricity is the only energy source, and it is distinguished from the different sources used to begin the reaction, e.g. photocatalysis the water dissociation reaction by light. According to various papers, photocatalysis, with its potential to use sunlight to generate hydrogen, represents one of the promising technologies to produce clean and environmentally friendly hydrogen [6]. Furthermore, it provides a way to use sunlight or UV light to generate hydrogen as a renewable fuel.

3.2. Photocatalysis

In recent years solar energy has become an alternative and suitable for energy generation. As the installed capacity of photovoltaics (PVs) continues to grow, cost-effective technologies for solar energy will be required to satisfy the energy demand [9].

Photocatalysis is a photoelectrochemical systems, which utilizes UV radiation to power the water electrolysis process, making the obtaining of hydrogen viable. A semiconductor photo-electrode produced enough electricity to split water, when it is exposed to sunlight [14].

This process involves different requisites [6]:

1. The energy rating of the semiconductor materials should overlap the energy levels of the oxygen and hydrogen reduction reactions.
2. The semiconductor system ought to be stable under electrolysis circumstances.
3. The charge removed from the semiconductor surface has to be fast enough to avoid corrosion issues, which helps to reduce energy loss.

Figure 8 exemplifies the overall water-splitting reaction, where the photocatalytic water-splitting process photon energy is converted into chemical energy via the photocatalyst, i.e. the semiconductor material. Semiconductors have a void region, where there are not any energy levels available which is called band gap (E_g). This region as it is illustrated, is placed between the valence band (VB), the highest occupied energy band, and the conduction band (CB) defined as the lowest empty band [15].

When the energy of an irradiated photon is larger than E_g , electrons (e^-) can be excited from the VB into the CB, leaving holes (h^+) in the VB [15]. Water-splitting reaction is determined by the electronic band structure of the photocatalyst.

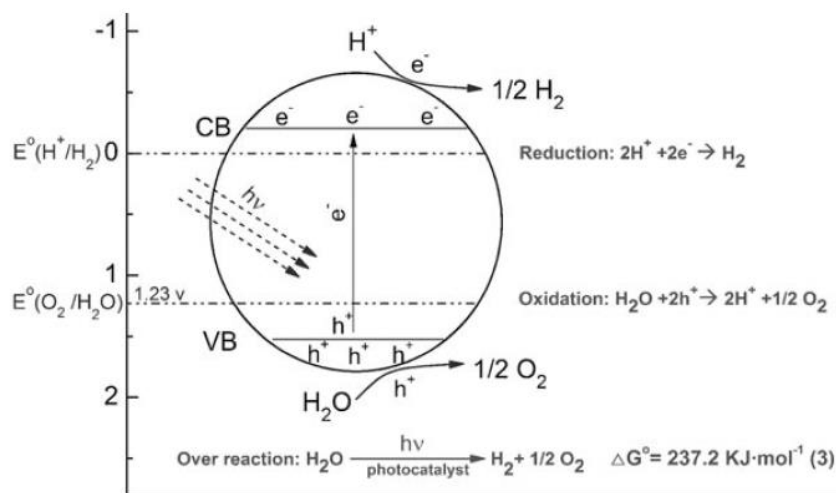


Figure 8. Scheme of the basic principle of the overall water-splitting reaction on a semiconductor photocatalyst adapted from [15].

Thus, when photons have an energy greater than that of the band gap, electron-hole pairs (e^- / h^+) are produced. These electron-hole pairs (e^- / h^+) generate free radicals capable of inducing secondary reactions (photocatalysis), or these pairs are capable of splitting the water molecule (electrolysis). The energy required for this reaction to take place depends on the band gap of the semiconductor that is desired to be used to achieve the separation of water, higher than 1.23 eV, however to use visible light it is necessary that this value be < 3.0 eV.

Therefore, it is based on the dissociation of water by means of solar radiation acting on some semiconductors, called photocatalysts, with a relatively wide band gap. Some semiconductors obtain more suitable results than others when they are used for photocatalysis, such as titanium dioxide (TiO_2), because of its wide band gap.

In addition, water properly separated into its components by photocatalysis will depend on the relative positions of the energy levels of the CB and the VB of the semiconductor used with respect to the redox potentials of hydrogen and oxygen. Thus, the energy level of the conduction band must be more negative than the level of hydrogen production, as it is demonstrated in Equation (3) while the energy level of the valence band must be more positive than the level of oxidation of water to produce oxygen, Equation (4) [16].

$$CB < E(H^+/H_2) \quad (3)$$

$$VB > E(O_2/H_2O) \quad (4)$$

Currently the photocatalysis is the least-cost and most-efficient method of producing renewable hydrogen. The production technology is still in the experimental stage but has already shown a promising efficiency and hydrogen generation costs [6].

3.2.1. Semiconductor materials

Semiconductor materials come from different groups in the periodic table, which share certain similarities, e.g. the combination of elements of column III and V or IV and IV form very important semiconductors. Thus, the properties of a semiconductor are related to their atomic characteristics and change from group to group. The most important parameters to consider of a semiconductor material for solar cell operation are:

- » The band gap.
- » The number of free carriers (electrons or holes) available for conduction.
- » The recombination of free carriers (electrons or holes) in response to light shining on the material.

That's why, researchers take advantage of these differences to improve the design and choose the optimal material for a PV application.

Common photocatalysts (semiconductor materials) studied are TiO₂, ZnO, WO₃, ZnS, CdS, CuO, SnO₂ [15], [17]–[27]. Thus, taking as primary photocatalyst TiO₂, the feasibility of mixing this photocatalyst with other semiconductors is analysed, considering the information of the existing studies.

Moreover, there are many studies on TiO₂ coupled with other semiconductors. In Table 3 are defined the semiconductor materials used in the production of hydrogen that satisfies the conditions of the band gap required to produce hydrogen. Due to the COVID-19 pandemic, it was not viable to study more semiconductors for this thesis.

Material		Mohs	CB energy [eV]	VB energy [eV]	Band gap energy [eV]	Ref
TiO ₂	Titanium dioxide	6 ¼	- 0.29	2.91	3.20	[15], [28], [29]
SnO ₂	Tin (IV) oxide	6.7	0	3.50	3.50	[15], [30], [31]
ZnO	Zinc oxide	4.0	- 0.31	2.89	3.20	[15], [28], [32]
CuO	Copper (II) oxide	3.5	- 0.20	1.50	1.70	[15], [30], [33]
ZnS	Zinc sulphide	3 ¾	- 0.85	2.75	3.60	[29], [34], [35]
CdS	Cadmium sulphide	3.0	- 0.52	1.88	2.40	[15], [30]

Table 3. Physical characteristics of the semiconductors used in this work.

Coupling TiO₂ with other semiconductors that possess different redox energy levels, for their corresponding conduction and valence bands is investigated in this thesis. In addition, one effective technique for improving TiO₂ photoactivity is coupling it with other semiconductors that generally have lower band gap energy [17].

Regarding the information of [15] when TiO₂ and the semiconductor are activated by UV light simultaneously, photoinduced e⁻ would be injected from the semiconductor with a more negative CB level to the positive one, while h⁺ would be transferred from the semiconductor with a more positive VB level to the negative one. Thus, a wide separation of photoinduced charges is achieved, which consequently enhances their lifetime as well as the efficiency of the charge transfer to water[15].

Considering this information, the relative position of the CB and VB, by the different photocatalysts from Figure 42 can be divided into these equations (5), (6) and (7) adapted from the information of [15]. For example, Equation (5) describes when e⁻ injects from SC to TiO₂ and h⁺ injects from TiO₂ to SC.

$$\left. \begin{array}{l} CB_{SC} < CB_{TiO_2} \\ VB_{SC} < VB_{TiO_2} \end{array} \right\} \begin{array}{l} e^-: SC \rightarrow TiO_2 \\ h^+: TiO_2 \rightarrow SC \end{array} \quad (5)$$

$$\left. \begin{array}{l} CB_{SC} > CB_{TiO_2} \\ VB_{SC} > VB_{TiO_2} \end{array} \right\} \begin{array}{l} e^-: TiO_2 \rightarrow SC \\ h^+: SC \rightarrow TiO_2 \end{array} \quad (6)$$

$$\left. \begin{array}{l} CB_{SC} > CB_{TiO_2} \\ VB_{SC} < VB_{TiO_2} \end{array} \right\} \begin{array}{l} e^-: TiO_2 \rightarrow SC \\ h^+: TiO_2 \rightarrow SC \end{array} \quad (7)$$

Therefore, with the data of Table 3, different papers are consulted for the different photocatalysts prepared by ball milling studied in the thesis.

Regarding [21], [27], TiO₂ and SnO₂ is coupled highly due to ball milling, forming the SnO₂/TiO₂ photocatalyst. The increased photocatalytic activity of the photocatalyst formed by SnO₂/TiO₂ is attributed to the enhance charge separation efficiency and extend the wavelength range of photoexcitation. Thus, in this research has demonstrated that without ball milling, TiO₂ and SnO₂ the coupled photocatalysts is not formed, and each photocatalyst works independently, but after ball milling, SnO₂ and TiO₂ form coupled SnO₂/TiO₂ photocatalysts, improving the results obtained for each element separately, i.e. the light absorption intensity and photocatalytic activity are improved.

Considering [19] which analyses the viability of the combination of TiO₂ and ZnO semiconductor, pure TiO₂ powder photocatalyst, without p-ZnO present in the photocatalyst, photoreduction activity is lower. The p-n junction p-ZnO/TiO₂ photocatalyst in this research was prepared by ball milling of TiO₂ in H₂O solution doped with p-ZnO.

Concerning the information of that paper, the ball milling time also influences the photocatalytic activity strongly, increasing the ball milling time the specific surface area of the photocatalyst increases. As the formation of p-n junction p-ZnO/TiO₂ photocatalyst and p-type ZnO species can trap the hole, the photogenerated electron-hole pairs are separated by the inner electric field, and the photocatalytic reduction activity is enhanced significantly [19].

According to the studies [18], [22]–[26], [36] which analyses the photocatalyst formed by CuO and TiO₂, explains the photocatalytic process of these two compounds. As it is defined once the sample is exposed to light irradiation, electrons from the VB of TiO₂ are excited to the CB and then directly transferred to CuO.

The results obtained in [20], [24] show an improvement on the rate of H₂ production of CuO/TiO₂, for instance the H₂ production of the compound of CuO/TiO₂ is 15 times more than the photocatalyst of just TiO₂. In addition, regarding [25], by using the effect of temperature on a suitable photocatalyst compound (CuO/TiO₂), the rate of H₂ generation is increased by 5-7 times at 90 °C compared to room temperature.

In addition, the papers [22], [23] prove the synthesis of an efficient photocatalyst, CuO/TiO₂ heterojunction, for selective aerobic photo-oxidation of methanol to methyl formation and for photoelectrochemical reduction of CO₂ into methanol under visible light irradiation.

Therefore, several advantages regarding the compound of CuO/TiO₂ are demonstrated, not only for hydrogen production, but also for other products and reactions, as it was exposed in the previous studies.

Concerning [37], the CdS semiconductor, is selected as photocatalyst for the conversion of solar energy into chemical energy under UV light irradiation, because CdS has a narrow band gap (as it was illustrated in Table 3). Moreover, the potential of its CB is more negative than the reduction potential of hydrogen proton (H⁺/H₂), thus it is more suitable for the H₂ generation. However, the photocatalytic activity of CdS itself toward water reduction is very low due to high-rate charge recombination of photogenerated electron. In order to suppress this recombination, it was designed the photocatalyst formed by TiO₂ and CdS improves the photocatalytic activity.

Moreover, according to [15] paper, TiO₂ coupled, CdS, ZnO and CuO, have the potential to evolve hydrogen from water because the e⁻ occupied CB level is more negative than TiO₂. Their capabilities have been verified by results reported on CdS/TiO₂, and CuO/TiO₂ [15].

Finally, all these combinations of semiconductors to obtain a photocatalyst more efficient are prepared by ball milling method, a technique widely studied [21], [38]–[41].

Ball milling is a simple, fast, cost-effective green technology with enormous potential [41], is defined a mechanical technique widely used to grind powders into fine heterogenous particles. Depending on the application, there are different type of ball milling, which can be used for synthesis of nanomaterials in which balls impact upon the powder charge. Figure 9 illustrates a scheme of the ball milling technique used to develop this thesis, which consists of a grinding bowl performing vertically oscillating movements with 900 – 3,000 oscillations per minute at 9 mm amplitude, with 1 grinding ball of 15 mm or 3 grinding balls of 10 mm.

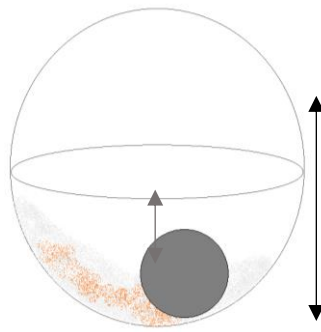


Figure 9. Schematic representation of a ball mill with two powder material to grind.

Thus, the efficiency of the final compound prepared by ball milling depends on the duration and the type of this method. One of the main advantages of this method is the possibility to combine it with different materials, thus allowing obtaining the desired products with minimal effort.

The importance of ball milling technique in order to form photocatalysts by different semiconductors is proven in the papers [21], [27], [42], as it was previously exposed.

4. Experimental setup and conditions

The purpose of this project was to study the process of photoproduction of hydrogen in a tubular photoreactor from catalysts dispersed in cellulose supports. These analyses were done with the help of a micro gas chromatograph (Micro GC) Agilent 490 [43], where the composition of the gases coming from the photoreactor are analysed.

The equipment used to determine the hydrogen production by different photocatalysts is formed by different elements, as it is illustrated in Figure 10. A current of argon initiates the reaction of the circuit used. Then, it can be found a Drechsel gas scrubber bottle with a water-ethanol mixture through in which this stream of argon is passed. The next element of the circuit is a two-piece tubular glass photoreactor, to which a UV source is attached. Finally, the micro gas chromatograph Agilent 490 (Micro GC), which analyses the composition of the gases coming from the photoreactor.

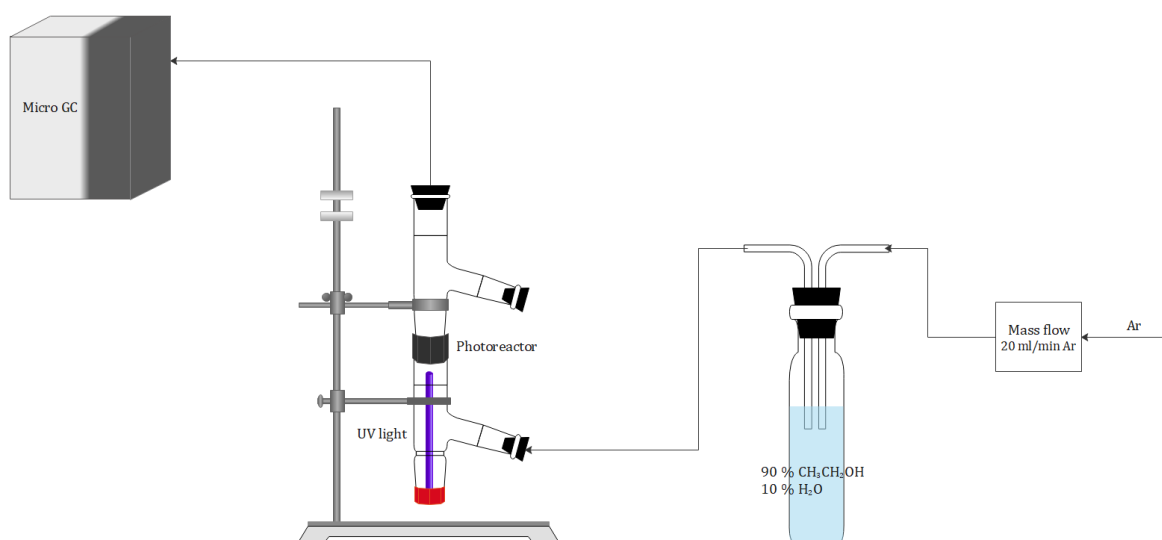


Figure 10. Scheme of the system used to develop the thesis.

Hydrogen production tests were realized with different photocatalysts prepared by the mechanochemical method of ball milling with different configurations (one ball of 15 mm or 3 balls of 10 mm) and proportions of semiconductors.

In order to be able to determine the efficiency of the photocatalyst formed of two different semiconductors, first of all it is analysed the efficiency of a sample with only titanium dioxide (TiO₂). As previously explained, TiO₂ is the most studied transition oxide semiconductor for photochemical and photoelectrochemical applications. Thus, research is intended for a semiconductor that possess the same stability and versatility of TiO₂. That's why in this research TiO₂ is combined with another semiconductor to obtain a photocatalyst more active and/or economic.

Each sample of photocatalyst is prepared under the same conditions. First, it is prepared the photocatalyst that consist only of TiO_2 to be able to compare its efficiency with the photocatalysts made by different compounds. These samples are formed by a 90 % weight of TiO_2 and a 10 % weight of one of the compounds mentioned in the [Chapter 3.2.1](#). The weight of a sample is approximately of 300 mg. Thus, it is formed by 270 mg of TiO_2 and 30 mg of the semiconductor selected.

4.1. Preparation of the photocatalyst

The recipient of stainless-steel that will be used for the ball milling device, a FRITSCH PULVERISETTE 23 [44], is selected, considering the number of balls and size (1 of 15 mm or 3 of 10 mm), as it is illustrated in Figure 11.



Figure 11. Type of recipient to do ball milling.

Once it is selected, it is tared in the laboratory balance to obtain a sample of 300 mg of photocatalyst, as it was mentioned above. Figure 12 exemplifies the preparation of a sample, which consists of one stainless-steel ball of 15 mm, 270 mg approximately of TiO_2 and 30 mg approximately of CdS.



Figure 12. Preparation of one sample in the laboratory balance.

At that point, once it is weighted the sample, the stainless-steel container is closed to proceed to place it in the ball milling device. This device is kept at 50 Hz for 10 minutes, as it is shown in Figure 13. It has to be checked that it is well attached due to the frequency chosen.



Figure 13. Preparation of one sample for ball milling.

The next step is to prepare the support with the catalyst to be placed in the photoreactor. into that end, an Eppendorf is filled with 2 mg of the catalyst and suspended in 0.15 mL of absolute ethanol. The mixture is sonicated for about 10 minutes in a ultrasonic bath, Fisher Scientific [45]. Then, circles are cut with a diameter of approximately 2.5 cm, which corresponds to the outer diameter of the glass connection where the support will be placed. Once cut, a circle must be marked with a pencil following the inner perimeter of the black ring, as it will be the area exposed to the UV source. The filter is placed in a glass petri dish and with an Easy 40+ micropipette 10 μ l of the suspension are added inside the marked inner circle. Finally, the samples are dried in the oven at 80 $^{\circ}$ C for 8 minutes. These lasts steps are illustrated in Figure 14.



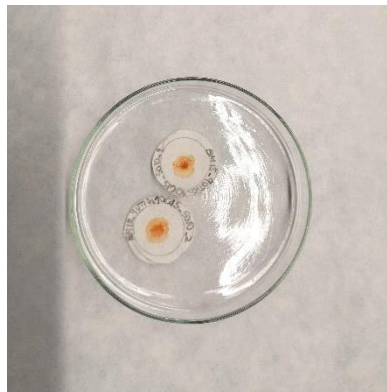


Figure 14. Last steps in the preparation of the sample for the photochemical reactor

4.2. Photocatalytic system

The photocatalytic system is divided into three parts:

1. A Drechsel gas scrubber bottle with a water-ethanol mixture through which a stream of argon is passed.
2. A two-piece tubular glass photoreactor, to which a UV source is attached.
3. A micro gas chromatograph Agilent 490 (Micro GC), which analyses the composition of the gases coming from the photoreactor.

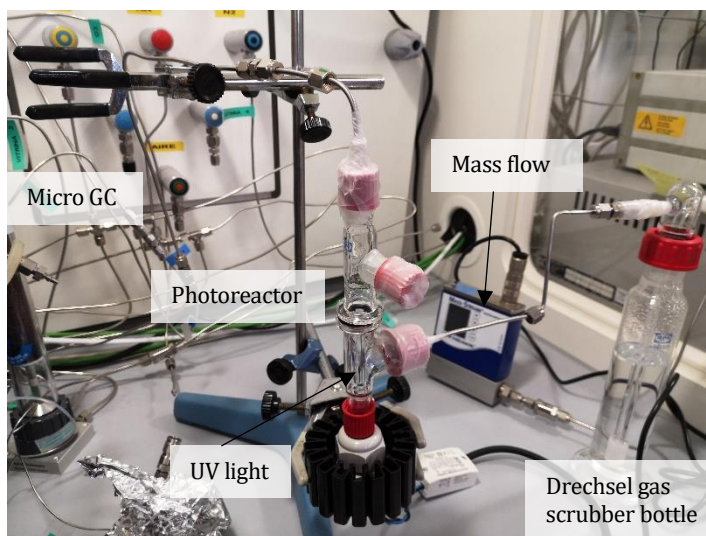


Figure 15. Photocatalytic system.

4.2.1. Photoreactor

A photoreactor is a device in which photons, photocatalyst and reactants come into contact, additionally, this device must collect the reaction products to be able to analyse them in order to determine which products are formed.

The reaction that occurs inside a photoreactor is known as photochemical reaction, which is a chemical reaction originated by the absorption of energy in the form of light, in our case UV light. In addition, the power of the UV light is measured, before starting the experiments, obtaining a value of 107 mW/cm² in order to verify that the equipment works properly.

The design of this device is a two-piece tubular glass photoreactor, one of them is fitted with a UV source. Inside the photoreactor, between the two tubular glasses, the sample with the catalyst is placed, as it is illustrated in Figure 16.

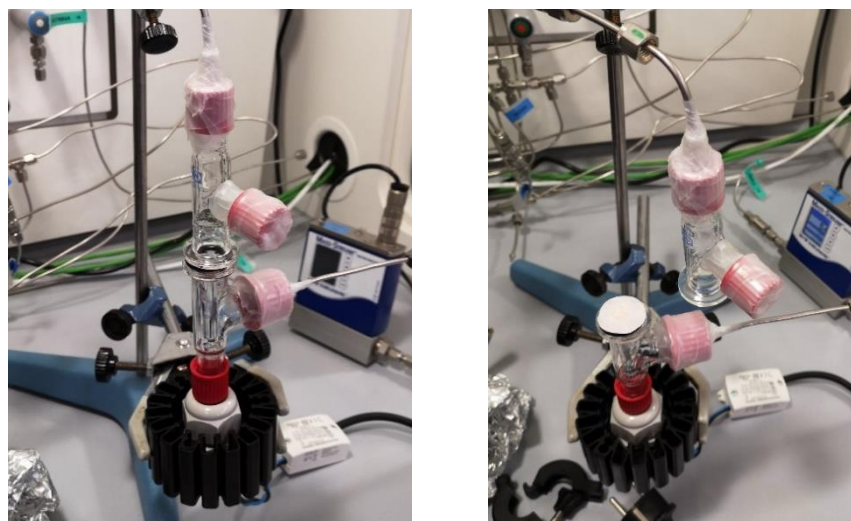


Figure 16. Tubular photoreactor without the sample (left) and with the sample (right).

4.2.2. Micro Gas Chromatograph

Gas chromatography (GC) is a common type of laboratory technique for the separation of a mixture used in analytical chemistry. Typical uses of GC include testing the purity of a particular substance, or separating the different components of a mixture. In the situation to study, GC will help in identifying the products formed, such as the presence of hydrogen.

In gas chromatography it is used a carrier gas, usually an inert gas such as helium or an unreactive gas such as nitrogen. Therefore, for the Micro GC these gas clean filters are recommended to remove any traces of moisture and oxygen. Since a specific carrier gas is required, the Micro GC used, Agilent 490, is configured for He and Ar [43]. The device used for this project uses an argon stream as carrier gas.

The 490 Micro GC can be equipped with one to four independent column channels. Each column channel is a complete, miniaturized GC with electronic carrier gas control, micro-machined injector, narrow-bore analytical column and micro thermal conductivity detector (μ TCD) [43]. The equipment used is equipped with three channels. Channel 1 detects the presence of H₂, O₂, N₂, Methane (CH₄), Carbon Monoxide (CO). Channel 2 distinguishes between CH₄, Carbon Dioxide (CO₂), and H₂O. Finally, Channel 3 detects Acetaldehyde (CH₃CHO), Acetone (C₃H₆O), Methanol (CH₃OH), Ethanol (CH₃CH₂OH) and H₂O.

Even though Micro GC has data in three channels, only two of them will be analysed in depth, Channel 1 and Channel 3. Both channels give information about obtaining hydrogen from the samples analysed.

4.2.3. Experimental plan and method

As it was mentioned previously, the circuit must be checked to avoid any possible leaks. Thus, the joints should be wrapped tightly with Parafilm to prevent leaks or oxygen inlets into the system.

For the tubular glass photoreactor, where it will be connected the UV source to the bottom of the photoreactor, also it has to be cover with Parafilm to prevent leaks both in this part and in the side entrance where the argon current reaches, which is settled a current of 20 ml/min. Thus, if it is opened the argon valve, it can be observed how the gas is bubbling in the bottle. In this side entrance it is very important that the internal joint is well located in the central and wider part of the thread. This will prevent leaks. Moreover, the upper tube of the photoreactor must also be sealed correctly with Parafilm (with several layers) at both the side outlet (blocked with a plug) and the outlet leading to the gas chromatograph.

Furthermore, at this point it can be checked if the system has leaks. It is locked the two glass tubes, black ring included, it is covered with Parafilm (2-3 pieces) and the black clamp. Thus, it is measured the gas flow with a stopwatch by connecting the Micro GC outlet tube to a burette containing soap (Figure 17). If there are no leaks, the bubble should take 3 s to make its way between the 0 to 1 marks. If the time it takes is longer, all connections should be checked to locate the leak before proceeding.



Figure 17. Micro GC and burette of flow measurement. [46]

4.3. Realization of the experiments

First, the Micro GC is conditioned to work properly. Then the cellulose membrane containing the photocatalyst dispersed is placed between the two glass tubes of the photoreactor. The black ring is placed centered above the lower tube, which is where the UV source is located, and the membrane with the photocatalyst is placed looking down above this ring. The two glass tubes are joined to close the system and, keeping the whole set straight, the two glass tubes are covered again with two or three pieces of Parafilm. Finally, it is closed with a black clamp. Figure 18 illustrates this process.

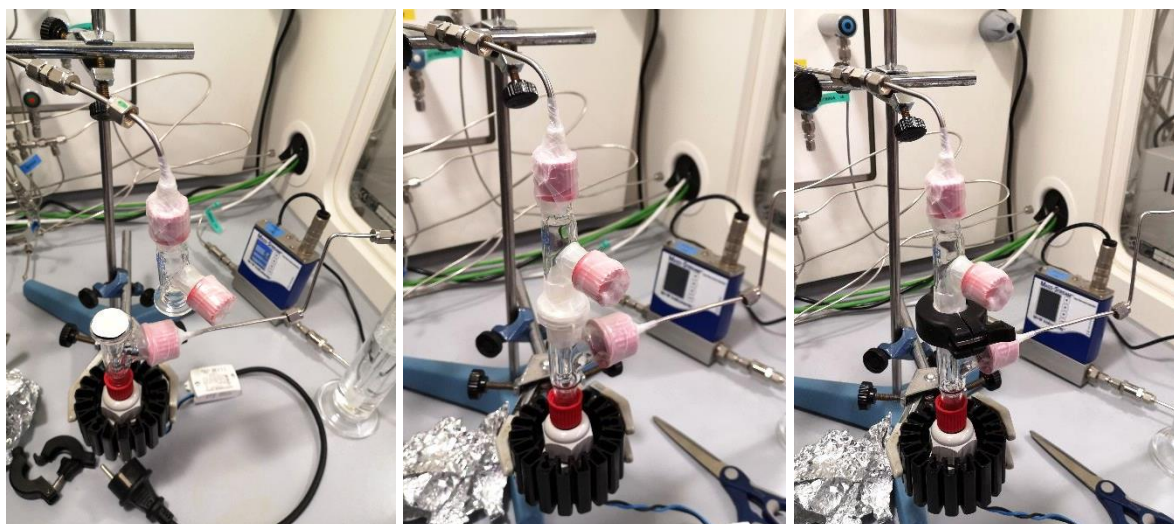


Figure 18. Placing the sample in the photoreactor.

Again, it is checked if the system has any leaks by measuring the time it takes a bubble to make the distance from 0 to 1, as it was previously mentioned. If there is a leak, it has to be tried either to close the black clamp harder or to put more parafilm or disassemble this part and check that

the cellulose membrane had not bent. The system has to be turned off again and check for leaks, and when the conditions of the Micro GC are the optimum, the analysis can start.

Regarding the Micro GC, it will analyse the content of the gases. It has to be controlled from when the oxygen content is below 0.01%, which is the maximum tolerance accepted (approximately 10-15 repetitions). Once the oxygen content is below 0.01%, the photoreactor is covered with aluminium foil to protect from radiation. Then the UV source is turned on.

The first measurement with the source turned on is the next step, taking notes when it is turned on and what is the first measurement with the UV source.

Furthermore, until it is observed that the amount of hydrogen measured is approximately constant, the measurements must continue. Every certain number of measures, it is necessary to control that there are no leaks. Therefore, it is required to measure how long the soap bubble takes as indicated above. Finally, when the amount of hydrogen measured decays or has been constant for a significant number of repetitions, the UV source is unplugged (it must be registered the number of the repetition) and it has to continue to take about three or four more repetitions to check how the hydrogen content decreases to zero.

4.3.1. Data collection of the photocatalysts

In this section, it is collected the data of the photocatalysts prepared following the process previously exposed, i.e. their composition and the conditions of the Micro GC. This information is exposed in Table 4. As it can be observed several repetitions were planned for statistical reasons, but most of them could not be tested due to the COVID-19 situation.

Element 1 TiO ₂	Element 2 2 nd Semiconductor	Ball milling conditions	Mass of TiO ₂ [mg]	Mass of 2 nd SC [mg]	Total mass [mg]	Experiment	Mass of the catalyst [mg]	Num. repetition UV on	Num. repetition UV off
100 %TiO ₂	-	-	-	-	-	E1	2.3	-	-
100 %TiO ₂	-	1x15 mm	300.3	-	300.3	E2	2.1	10	26
						E3	2.2	-	-
						E4	2.2	-	-
		3x10 mm	300.9	-	300.9	E5	2.4	-	-
						E6	2.1	-	-
90 % TiO ₂	10 % ZnO	1x15 mm	271.0	34.1	305.1	E7	2.2	Error	Error
						E8	2.2	13	30
						E9	2.1	-	-
		3x10 mm	270.6	30.0	300.6	E10	2.1	14	35
						E11	2.3	-	-
90 % TiO ₂	10 % CuO	1x15 mm	271.0	31.0	302.0	E12	2.0	16	31
						E13	2.2	-	-
		3x10 mm	270.0	33.6	303.6	E14	2.3	-	-
						E15	2.0	-	-

Element 1 TiO ₂	Element 2 2 nd Semiconductor	Ball milling conditions	Mass of TiO ₂ [mg]	Mass of 2 nd SC [mg]	Total mass [mg]	Experiment	Mass of the catalyst [mg]	Num. repetition UV on	Num. repetition UV off
90 % TiO ₂	10 % CdS	1x15 mm	270.1	31.9	302.0	E16	2.5	14	31
						E17	2.6	-	-
		3x10 mm	270.4	30.4	300.8	E18	2.0	-	-
						E19	2.3	-	-
90 % TiO ₂	10 % ZnS	1x15 mm	270.1	30.9	301.0	E20	2.1	18	34
						E21	2.0	-	-
		3x10 mm	270.1	31.4	301.5	E22	2.2	-	-
						E23	2.4	-	-
90 % TiO ₂	10 % SnO ₂	1x15 mm	270.4	31.0	301.4	E24	2.2	14	31
						E25	2.3	-	-
		3x10 mm	270.2	31.4	301.6	E26	2.1	20	40
						E27	2.1	-	-

Table 4. Experimental data.

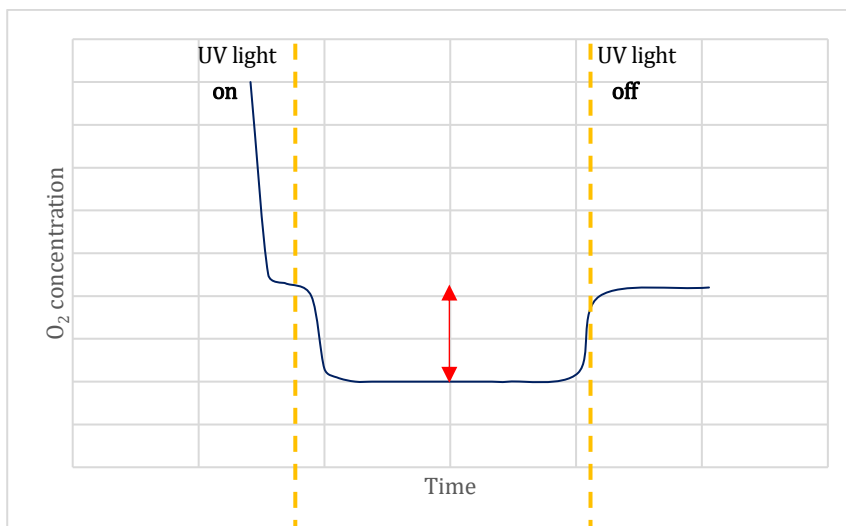


Figure 19. Evolution of the O_2 concentration during the experiment.

In addition, in Figure 20 is exposed a graph of what should be the result of the analysis in Channel 3, with the formation of CH_3CHO . As it mentioned before, this compound is used to verify the results of the analysis of H_2 production. When the UV light is tuned on, starts not only the production of H_2 from the photocatalyst, obtaining the curve of H_2 measured in the Micro GC in Channel 1, but also the CH_3CHO production.

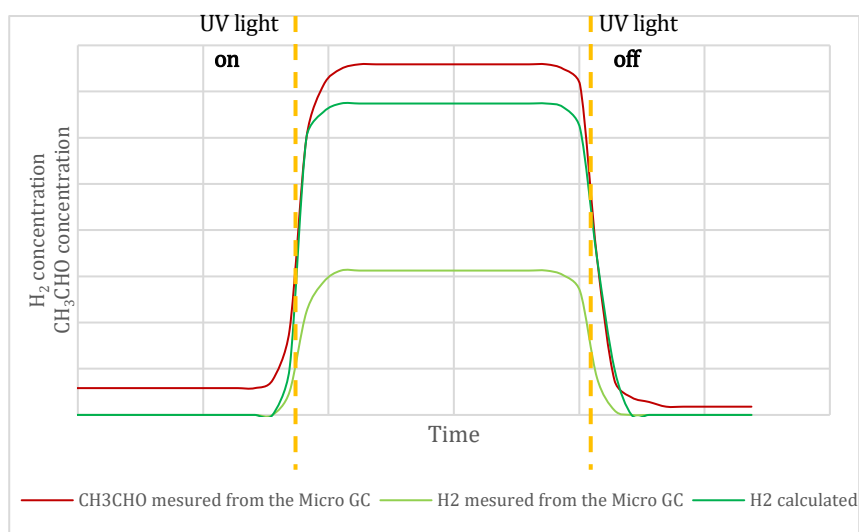


Figure 20. Evolution of H_2 concentration and CH_3CHO concentration during the experiment.

As a result of these analysis, the amount of H_2 produced is calculated from the sum of the H_2 obtain by Equations (8), H_2 measured by the Micro GC by the Channel 1, and (9), obtaining the curve shown in the graph. Thus, when the UV light is tuned off, both reactions are stopped due to this absence of light to activate the photocatalyst.

Moreover, the values of the analysis of the Micro GC are volumetric percentages. Thus, to graph the results obtained the units has to be $\mu\text{mol}/\text{min}\cdot\text{g}$ catalyst. The general ideal gas equation is applied (10).

$$PV = nRT \quad (10)$$

For Channel 3 with the reaction described in Equation (8), first it is obtained the ml/min of CH_3CHO considering volume of the current of Ar going through the system, as it is shown in (11). As it is known 1 mole of gas is equivalent to 22.4 l (Equation (12)), thus this is used to obtain the moles of gas. Finally, this result is divided by the mass of the photocatalyst used, obtaining the value in $\mu\text{mol}/\text{min}\cdot\text{g}$ catalyst as it is sum up in Equation (13).

$$x \% \text{ of } \text{CH}_3\text{CHO} \cdot 20 \text{ ml Ar}/\text{min} \text{ at } 1 \text{ atm and } 24^\circ\text{C} \quad (11)$$

$$\frac{1 \text{ mol gas}}{22.4 \text{ l}} \quad (12)$$

$$x \% \text{ of } \text{CH}_3\text{CHO} \cdot \frac{20 \text{ ml}}{\text{min}} \cdot \frac{1 \text{ l}}{10^3 \text{ ml}} \cdot \frac{1 \text{ mol}}{22.4 \text{ l}} \cdot \frac{1}{x \text{ g ctalayst}} \quad (13)$$

Regarding Channel 1, the procedure to obtain the results of H_2 production consists of two parts. On one hand, it is calculated the O_2 consumed when it is turned on the UV light, as it was mentioned with Figure 19, with the results of Channel 1 of oxygen. Then this value obtained is multiplied by 2 (Equation (14)), because of the number of moles of H_2 regarding the number of moles of O_2 described in Equation (9). This value is added to the one obtained directly from Channel 1 with the analysis done by the Micro GC. Once is obtained the total amount of H_2 in %, the procedure described in Equation (13) is repeated, with the amount of H_2 , as it is mentioned below (Equation (15)).

$$x \% \text{ of } \text{H}_{2\text{measured}} + 2 \cdot x \% \text{ of } \text{O}_{2\text{consumed}} = \% \text{ of } \text{H}_{2\text{TOTAL}} \quad (14)$$

$$x \% \text{ of } \text{H}_{2\text{TOTAL}} \cdot \frac{20 \text{ ml}}{\text{min}} \cdot \frac{1 \text{ l}}{10^3 \text{ ml}} \cdot \frac{1 \text{ mol}}{22.4 \text{ l}} \cdot \frac{1}{x \text{ g ctalayst}} \quad (15)$$

5.2. Results

In this section the results of the different tests done are exposed and discussed.

Therefore, the analysis of these results is divided in the following subsections:

- » Influence of the compounds of the photocatalyst prepared.
- » Verification of the H_2 obtained with the amount of CH_3CHO produced.
- » Comparison of the results between preparing the photocatalyst with different conditions of ball milling.

5.2.1. Influence of the compounds of the photocatalyst prepared.

In this first analysis, the aim is to determine the hydrogen produced as a first verification step, i.e. detect if with the catalyst used has been obtained some hydrogen, as it was illustrated in Figure 19. The 8 samples which were analysed in the Micro GC as it was shown in Table 4, are studied to determine which compound obtain better results.

Below, different graphs are exposed with the results obtained from the Micro GC and from the difference on the amount of O_2 used to calculate the amount of H_2 obtained by the reaction reflected in Equation (9) when the UV light is turned on. Thus, each graph includes not only this O_2 evolution obtained directly from the Micro GC during the exposure to UV light, but also the response to this exposure with the H_2 produced

Figure 21 shows the results obtained for the reference photocatalyst, i.e. the catalyst is formed just with titanium dioxide (TiO_2). It can be noticed how the amount of oxygen decrease when the UV light is turned on, because of the hydrogen being produced.

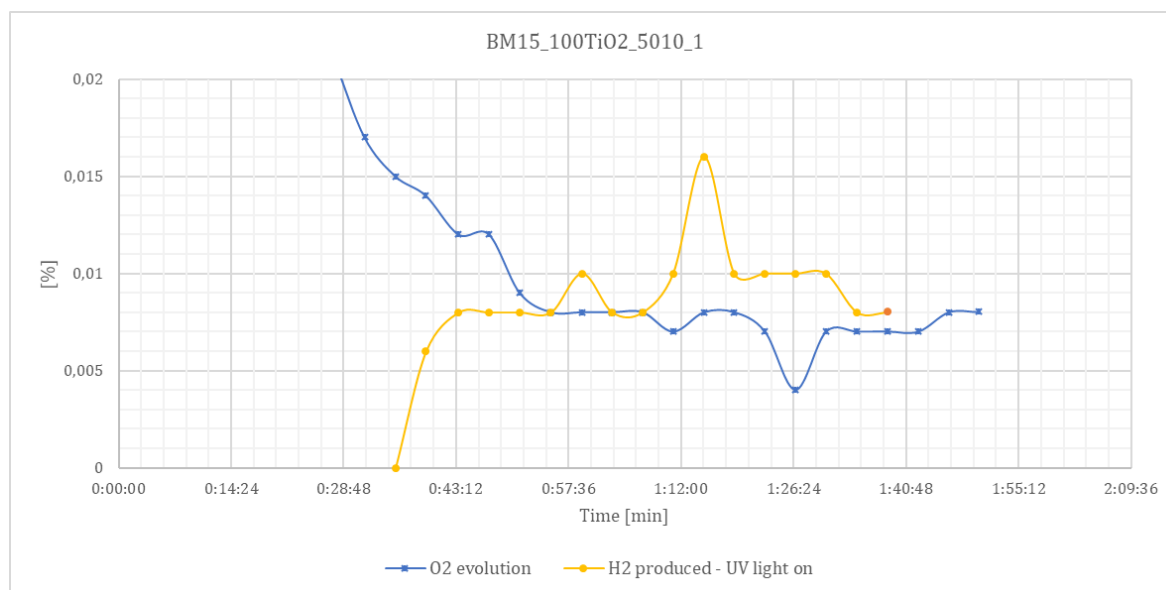


Figure 21. Evolution of the O_2 concentration and the H_2 produced for a catalyst of 100 % TiO_2 .

The next sample analysed, is formed by 90 % TiO_2 and 10 % ZnO , it can be observed in Figure 22 how barely the catalyst reacts to the UV light. Thus, this sample does not improve the results obtained with the an only TiO_2 catalyst, because the analysis done with the Micro GC demonstrates that hardly any hydrogen is produced.

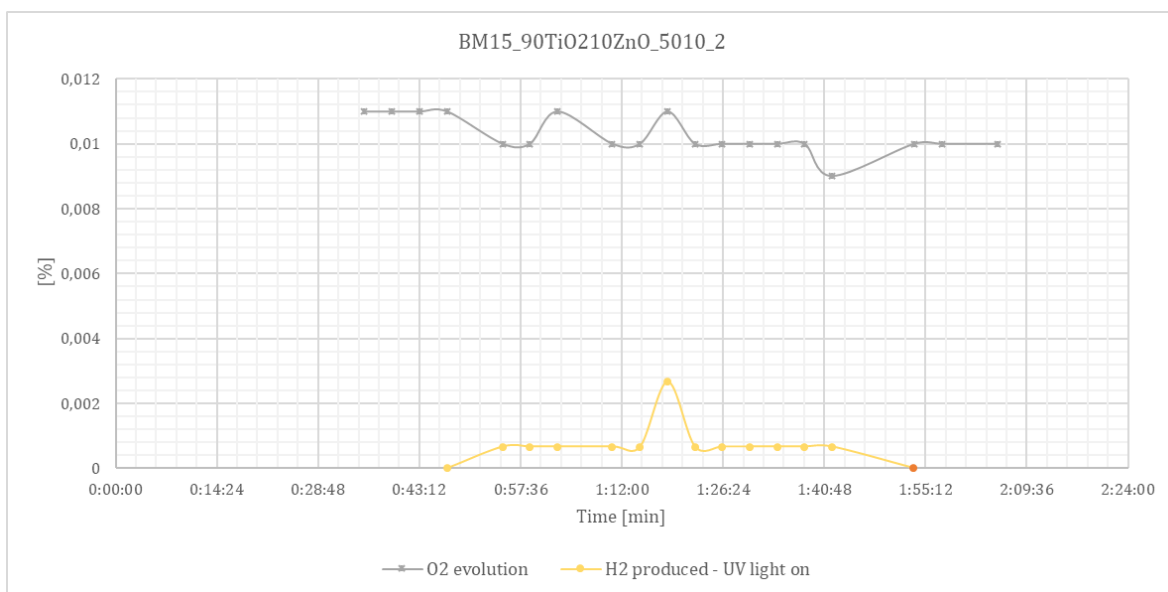


Figure 22. Evolution of the O_2 concentration and the H_2 produced for a catalyst of 90 % TiO_2 10 % ZnO .

The catalyst prepared with 3 balls of 10 mm instead of 1 of 15 mm by 90 % TiO_2 and 10 % ZnO , obtains inconclusive results. Figure 23 shows how the sample reacts with the UV light, which seems that the reaction is relatively instable. This result obtained could be due to some error in the analysis on the Micro GC or because this mixture does not work properly.

Considering the results obtained with the same compound, but prepared with 1 ball of 15 mm instead of 3 of 10 mm, it can be supposed that the combination of these two semiconductors, TiO_2 and ZnO is not suitable while obtaining H_2 .

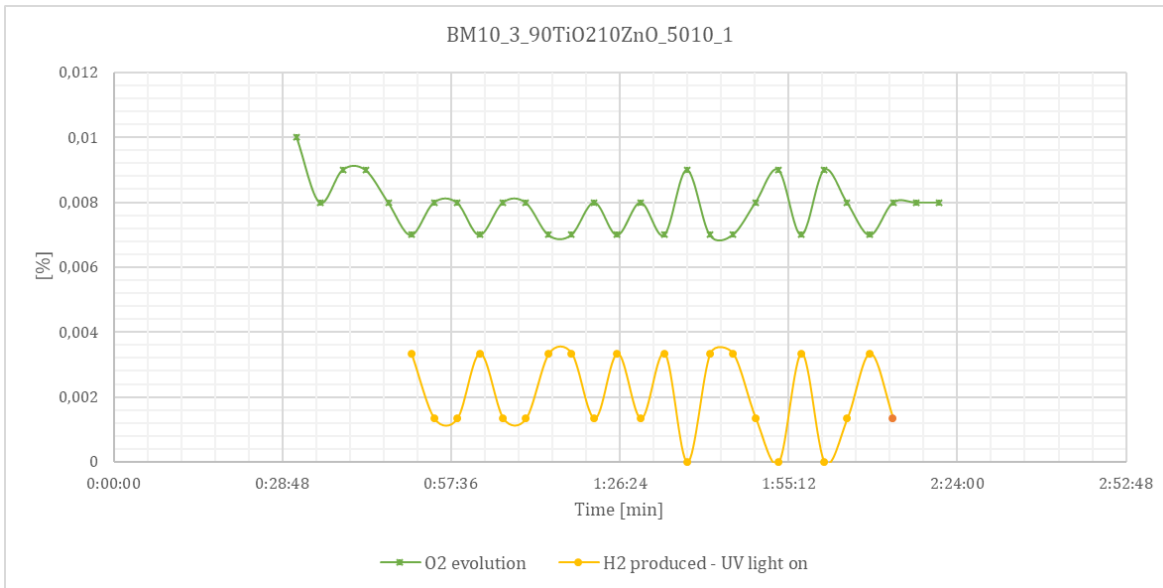


Figure 23. Evolution of the O_2 concentration and the H_2 produced for a catalyst of 90 % TiO_2 10 % ZnO .

In contrast the catalyst formed by 90 % TiO_2 and 10 % CuO obtains better results, not only compared with 90 % TiO_2 10 % ZnO catalyst, but also compared with 100 % TiO_2 . While the sample with ZnO hardly react when the UV light was turned on, the catalyst with CuO displays notable improvement in hydrogen production, as it is illustrated in Figure 24.

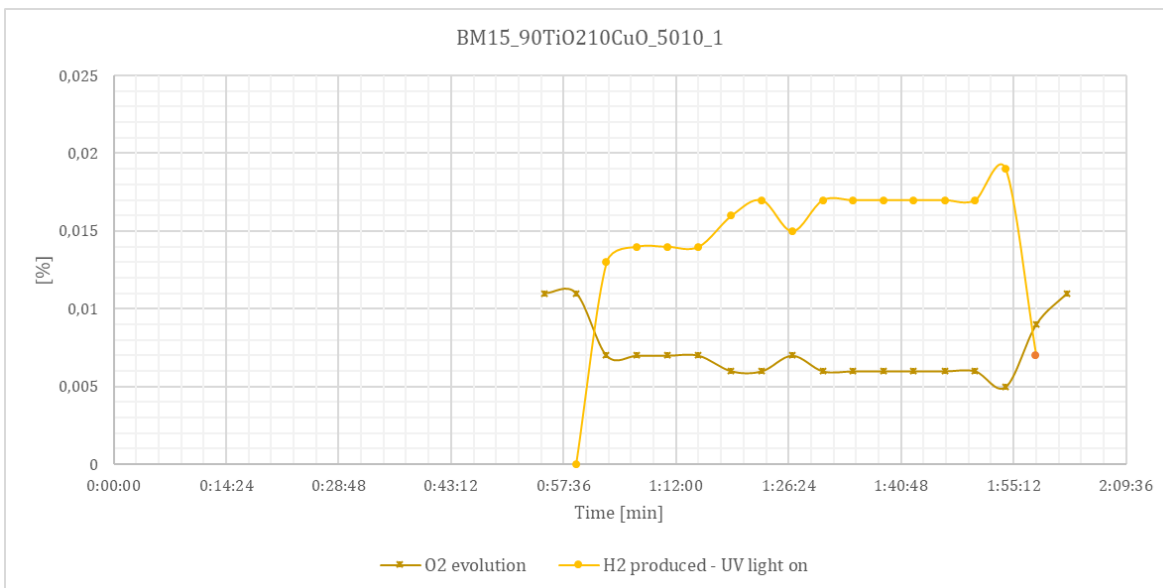


Figure 24. Evolution of the O_2 concentration and the H_2 produced for a catalyst of 90 % TiO_2 10 % CuO .

For the sample of 90 % TiO_2 10 % CdS is obtained a fairly constant H_2 production, contrary to the sample with ZnO , but not as good as the results with CuO . Even though, this compound reacts to the UV light, nonetheless not improving the results obtained from the reference sample (TiO_2).

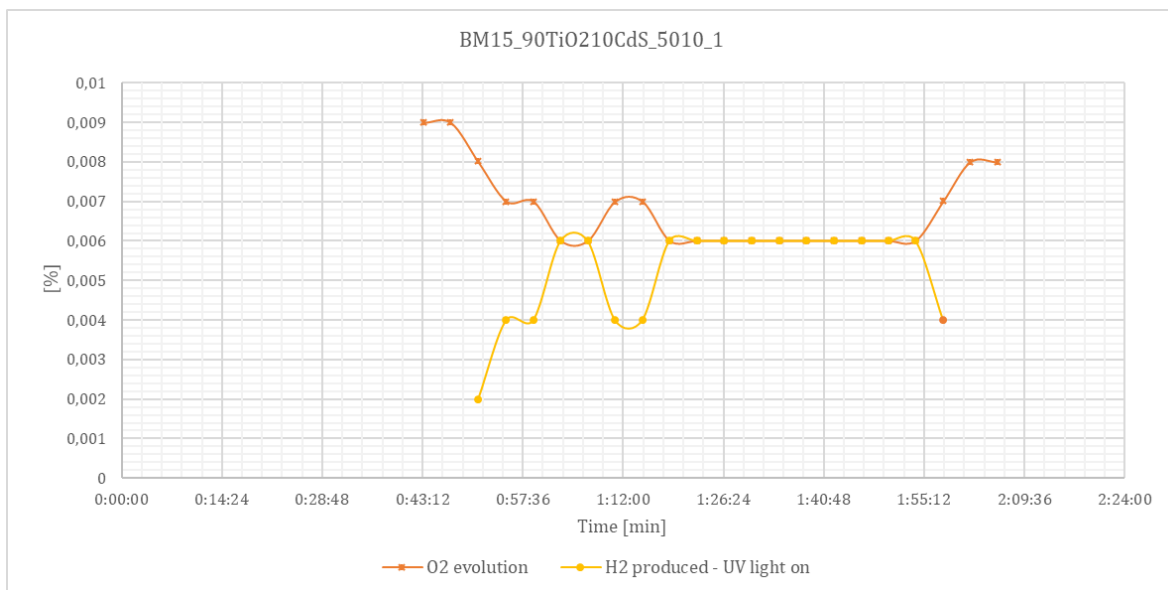


Figure 25. Evolution of the O₂ concentration and the H₂ produced for a catalyst of 90 % TiO₂ 10 % CdS.

Figure 26 illustrates the evolution of the O₂ concentration and the H₂ produced for a catalyst of 90 % TiO₂ 10 % CdS when the UV light is tuned on. As it was observed with the samples with ZnO, the hydrogen production for this compound is also instable. Thus, the assumption that has been made previously with the ZnO mixture catalyst is reinforced, and may be due to the presence of Zn, because the 3 catalysts which contains Zn had comparable results.

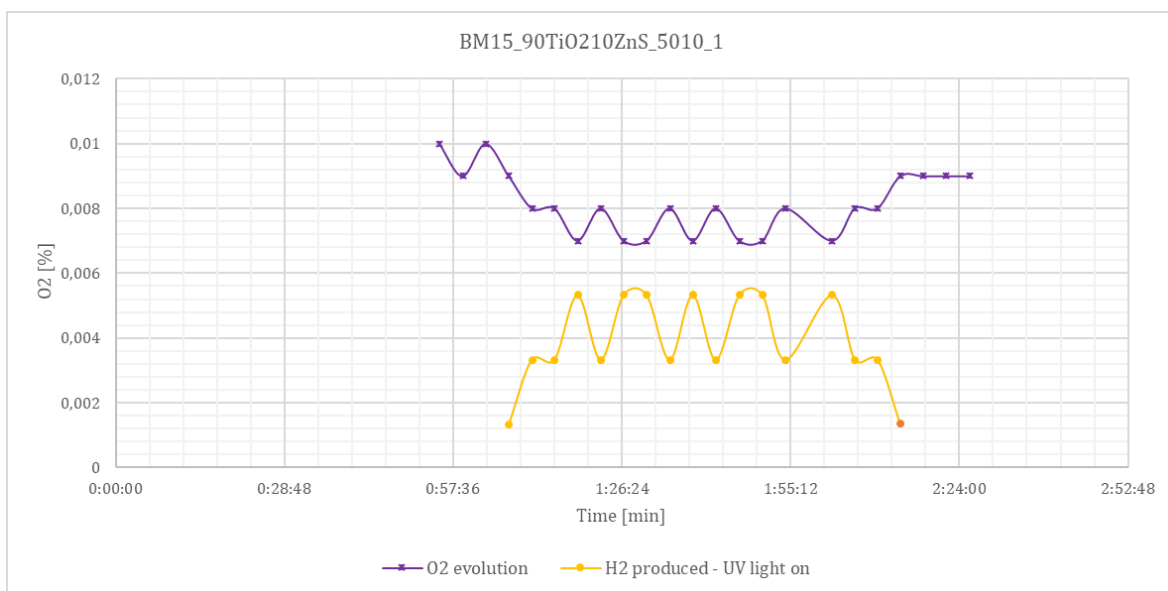


Figure 26. Evolution of the O₂ concentration and the H₂ produced for a catalyst of 90 % TiO₂ 10 % ZnS.

The results obtained for the photocatalyst formed by TiO₂ and SnO₂ are similar to the obtained with CuO. Thus, this sample is also suitable for hydrogen production. Figure 27 demonstrates how the hydrogen production starts when the UV light is switched on, i.e. hydrogen production rises significantly when UV light is turned on.

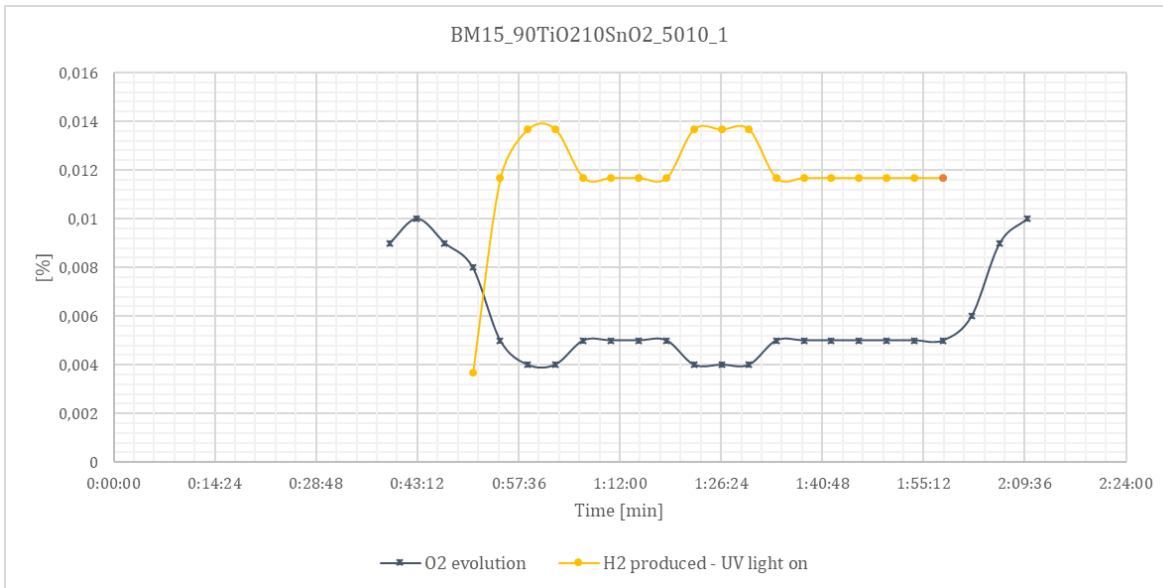


Figure 27. Evolution of the O₂ concentration and the H₂ produced for a catalyst of 90 % TiO₂ 10 % SnO₂.

In addition, the catalyst prepared with 3 balls of 10 mm instead of 1 of 15 mm by 90 % TiO₂ and 10 % SnO₂, obtains notable results as well. Figure 28 illustrates how the sample reacts with the UV light, obtaining a constant hydrogen production, nonetheless the results found for the same compound prepared with 1 ball of 15 mm are better.

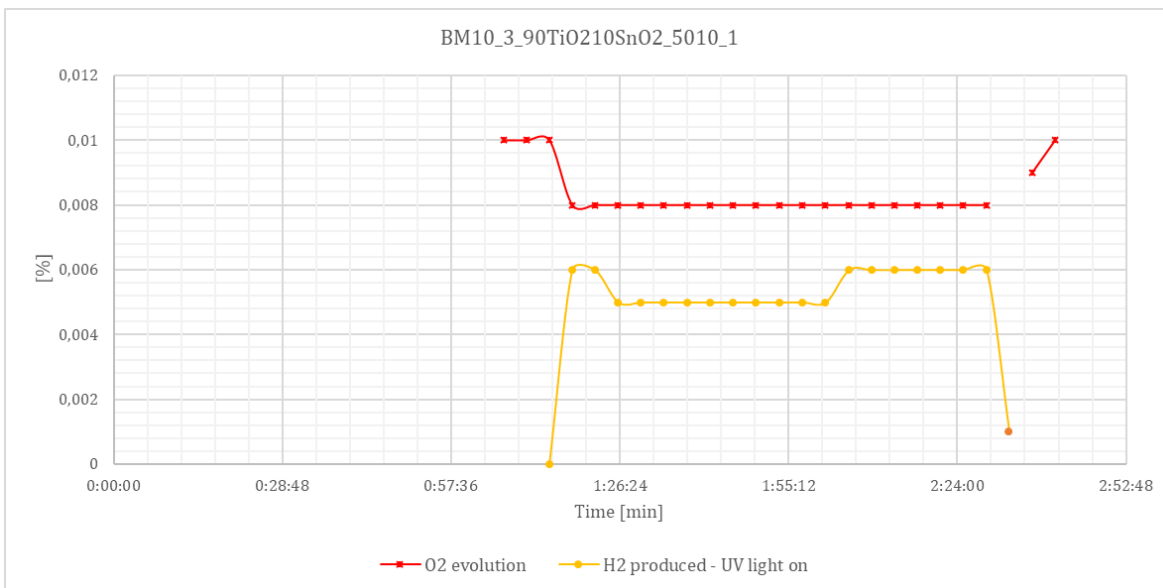


Figure 28. Evolution of the O₂ concentration and the H₂ produced for a catalyst of 90 % TiO₂ 10 % SnO₂.

5.2.2. Verification of the H₂ obtained with the amount of CH₃CHO produced.

In this analysis, the aim is to validate that the results regarding hydrogen detected are reliable, as it was exposed above, in Figure 20. The 8 samples which were analysed in the Micro GC as it was shown in Table 4, are studied to determine the reliability of the results. Thus, the comparison with the graphs of the H₂ and the CH₃CHO produced has to have similar.

First, for the reference sample, 100 % of TiO₂, Figure 29 illustrates how the two results obtained have similar forms. Therefore, for this result it is assumed that the information is correct, being produced $620.75 \mu\text{mol}/\text{min} \cdot \text{g catalyst}$ of H₂ and $581.63 \mu\text{mol}/\text{min} \cdot \text{g catalyst}$ of CH₃CHO.

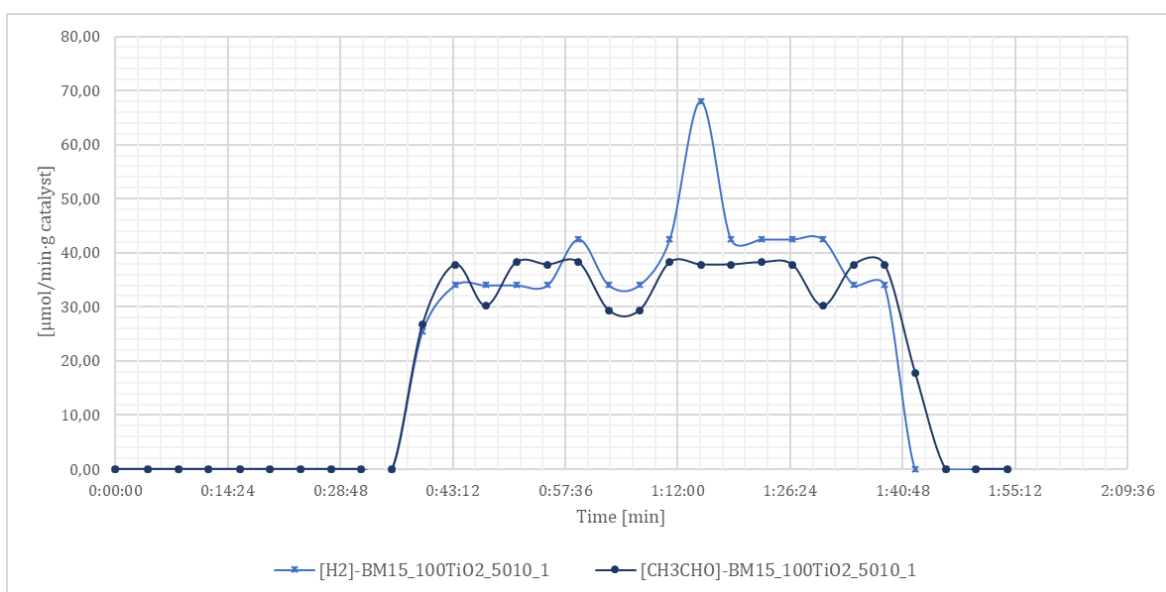


Figure 29. Comparison between the H₂ and the CH₃CHO produced for 100 % TiO₂.

Figure 30 shows more stability result of H₂ produced than CH₃CHO which has some instabilities that might be caused by leaks in the circuit. As it was mentioned in the previous section, for this catalyst the results when obtaining H₂ are low compared with the other samples. Being produced $29.76 \mu\text{mol}/\text{min} \cdot \text{g catalyst}$ of H₂ and $120.94 \mu\text{mol}/\text{min} \cdot \text{g catalyst}$ of CH₃CHO, values significantly lower than those obtained with the reference sample.

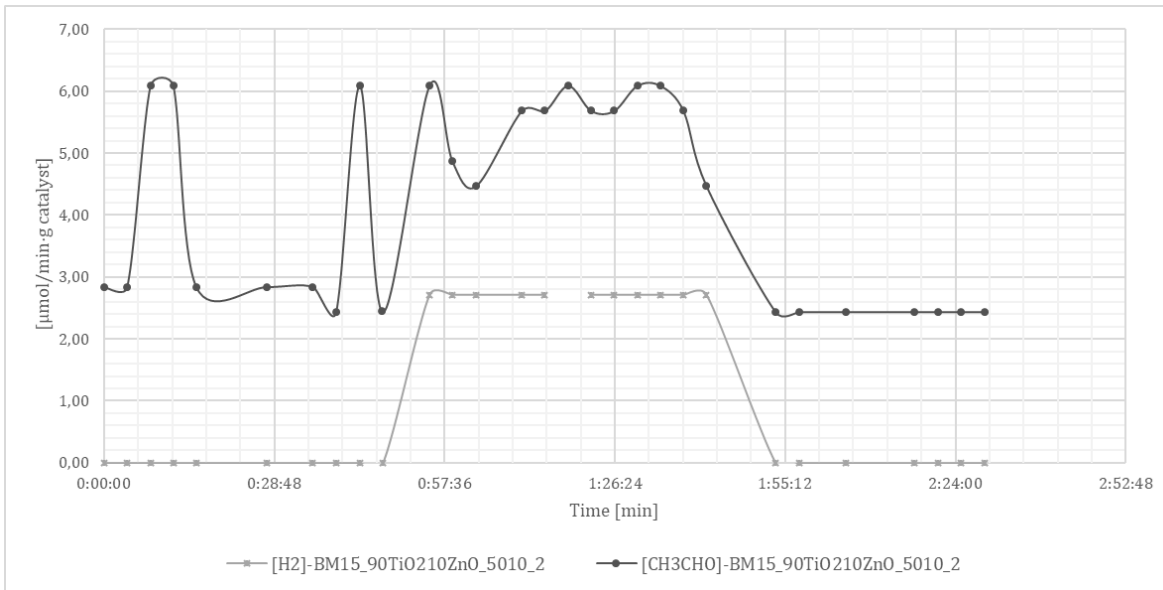


Figure 30. Comparison between the H_2 and the CH_3CHO produced for 90 % TiO_2 10 % ZnO .

In addition, the results from the catalyst prepared with 3 balls of 10 mm instead of 1 of 15 mm by 90 % TiO_2 and 10 % ZnO , obtains unstable results. Figure 31 shows how the H_2 production is pretty discontinuous. This result obtained might be due to some error in the analysis on the Micro GC or because this mixture does not work properly. Nevertheless, the results obtained are $192.74 \mu mol/min \cdot g catalyst$ for H_2 and $59.52 \mu mol/min \cdot g catalyst$ for CH_3CHO .

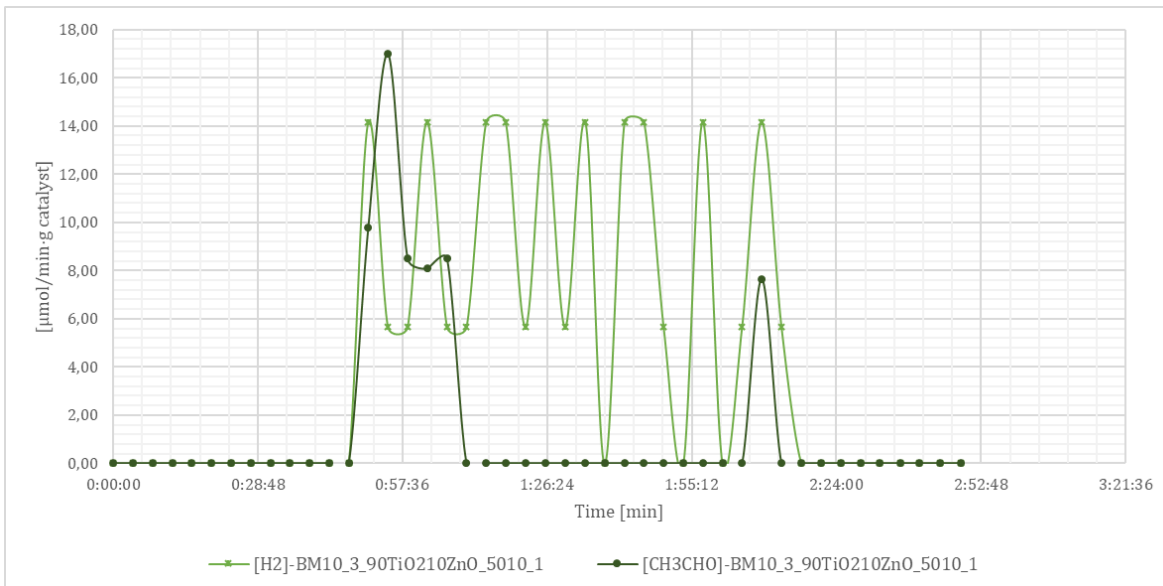


Figure 31. Comparison between the H_2 and the CH_3CHO produced for 90 % TiO_2 10 % ZnO .

The results for the mixture with CuO, as it was expected, are the best, since the H₂ produced is higher for this sample than for the reference sample formed just by TiO₂. These values are $1,031.25 \mu\text{mol}/\text{min} \cdot \text{g catalyst}$ for H₂ produced and $1,069.20 \mu\text{mol}/\text{min} \cdot \text{g catalyst}$ for CH₃CHO. Moreover, the H₂ and CH₃CHO produced have similar behaviour (Figure 32), thus it can be assumed that the results from this test are correct.

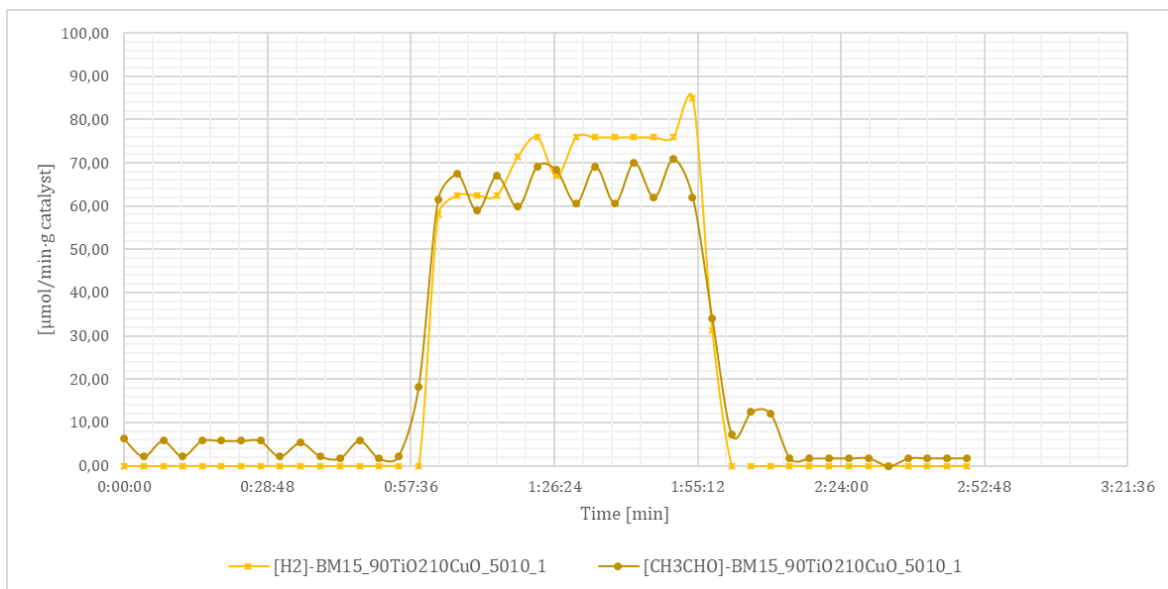


Figure 32. Comparison between the H₂ and the CH₃CHO produced for 90 % TiO₂ 10 % CuO.

The next sample analysed is formed by TiO₂ and CdS, as it was observed in Figure 25, around the hour and 10 minutes of the experiment apparently some oxygen went through the circuit, thus these peaks that are also detected in the figure below, Figure 33 are linked to the leaks of the system. Regarding the H₂ produced, with this compound is obtained approximately half compared to the base sample, being these values are $335.71 \mu\text{mol}/\text{min} \cdot \text{g catalyst}$ for H₂ produced and $320.36 \mu\text{mol}/\text{min} \cdot \text{g catalyst}$ for CH₃CHO.

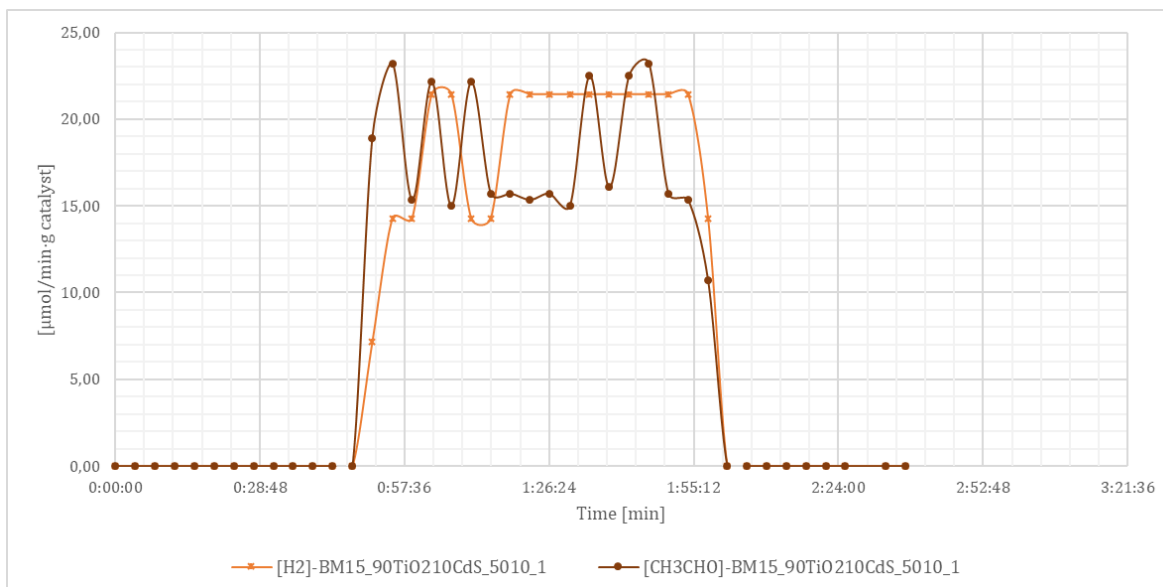


Figure 33. Comparison between the H_2 and the CH_3CHO produced for 90 % TiO_2 10 % CdS .

As it was mentioned in the previous section the compounds which contain Zn have fairly unstable results. Although, the results on H_2 production are not as bad as the ones obtained from the TiO_2 and ZnO mixture. Thus, for this compound the amount of H_2 produced is similar to the case studied above (TiO_2 with CdS), being these values are $283.45 \mu mol / min \cdot g catalyst$ for H_2 produced and $334.61 \mu mol / min \cdot g catalyst$ for CH_3CHO .

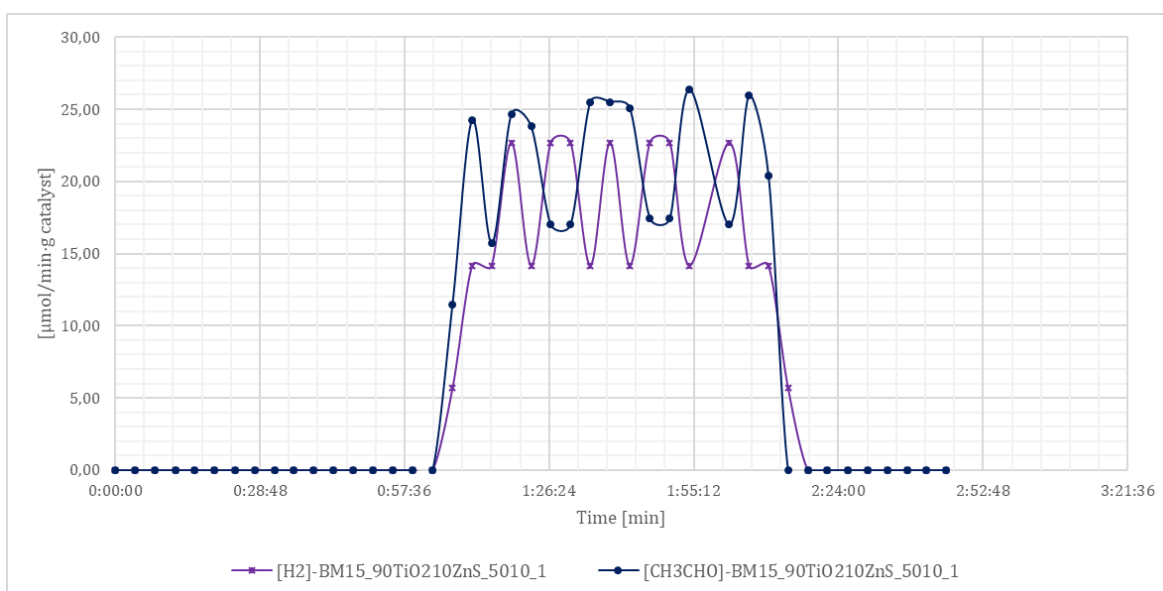


Figure 34. Comparison between the H_2 and the CH_3CHO produced for 90 % TiO_2 10 % ZnS .

Finally, the samples formed by TiO_2 and SnO_2 are analysed. As it was indicated in the previous section, the results are similar to the obtained with CuO . Figure 35 illustrates how stable this compound is, having the H_2 and CH_3CHO similar behaviour. Thus, for this compound the amount of H_2 produced is between the best case studied above (TiO_2 with CuO) and the reference sample (TiO_2 catalyst), being these values are $860.39 \mu\text{mol}/\text{min} \cdot \text{g catalyst}$ for H_2 produced and $1,053.57 \mu\text{mol}/\text{min} \cdot \text{g catalyst}$ for CH_3CHO .

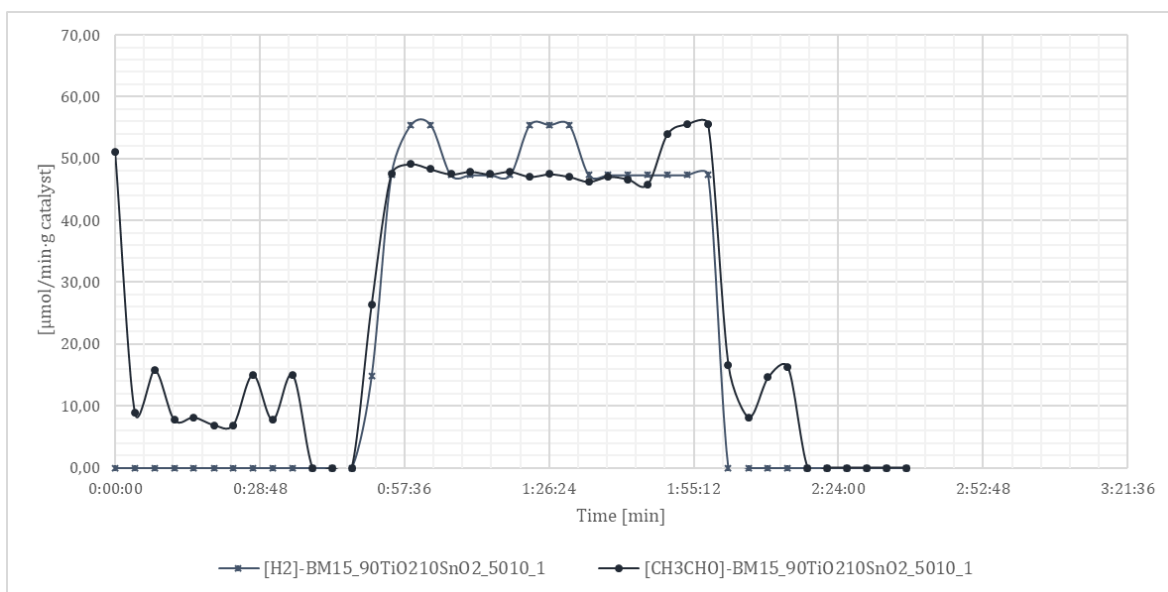


Figure 35. Comparison between the H_2 and the CH_3CHO produced for 90 % TiO_2 10 % SnO_2 .

In contrast, the results obtained for the catalyst prepared with 3 balls of 10 mm instead of 1 of 15 mm formed by TiO_2 and SnO_2 indicates, on one hand that until the UV light is turned on (around 1 hour of experiment), the concentration of oxygen in the circuit was higher than in the other cases.

On the other hand, the compound obtains notable results, but the case previously studied has produced the double amount of H_2 , as it can be observed in Figure 36. The values obtained for this case are $446.43 \mu\text{mol}/\text{min} \cdot \text{g catalyst}$ for H_2 produced and $889.46 \mu\text{mol}/\text{min} \cdot \text{g catalyst}$ for CH_3CHO .

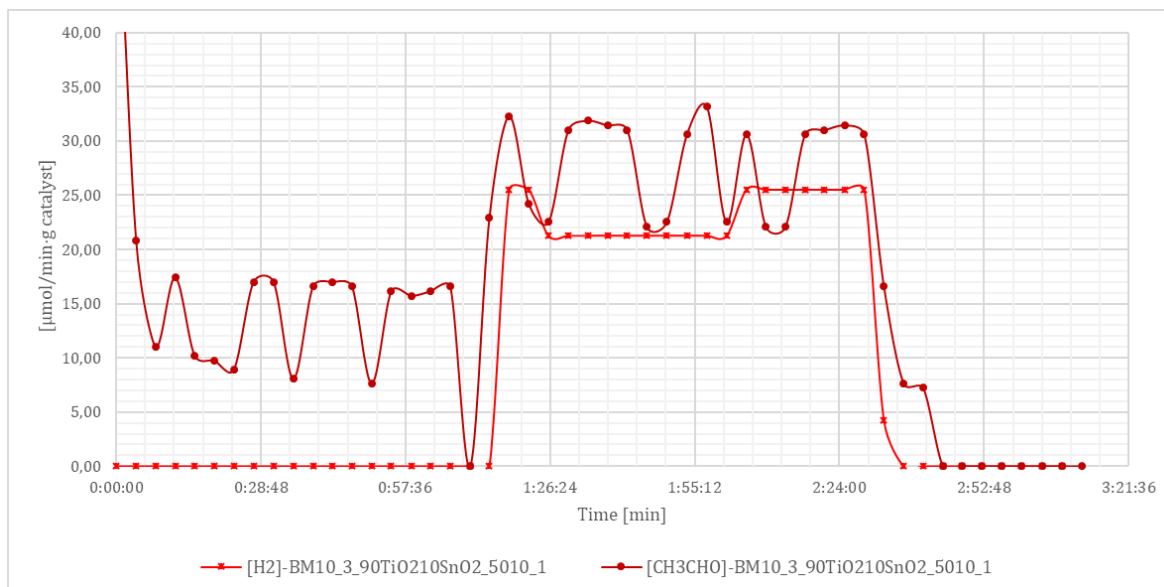


Figure 36. Comparison between the H_2 and the CH_3CHO produced for 90 % TiO_2 10 % SnO_2 .

5.2.3. Comparison of the results between preparing the photocatalyst with different conditions of ball milling.

In this section it is analysed how the conditions while preparing the sample can affect to the results of the efficiency of the photocatalyst. As it was previously mentioned, due to the pandemic, it was not possible to realise many tests.

Therefore, two catalysts prepared with 3 balls of 10 mm and 1 ball of 15 mm have been studied. These two compounds are the formed by 90% TiO_2 10 % ZnO and 90 % TiO_2 10 % SnO_2 .

5.2.3.1. 90 % TiO_2 10 % ZnO catalyst

The first samples analysed are the mixtures of TiO_2 and ZnO . Figure 37 illustrates similar behaviour between the two samples, both shows unstable performance without being possible to detect when the UV light is turned on. Unless it cannot be noticed the drop of oxygen due to the H_2 production, the sample prepared with 3 balls of 10 mm has a lower percentage of oxygen than the sample prepared with 1 ball of 15 mm. Thus, it can be assumed that it will be produced more hydrogen with the sample prepared with 3 balls of 10 mm.

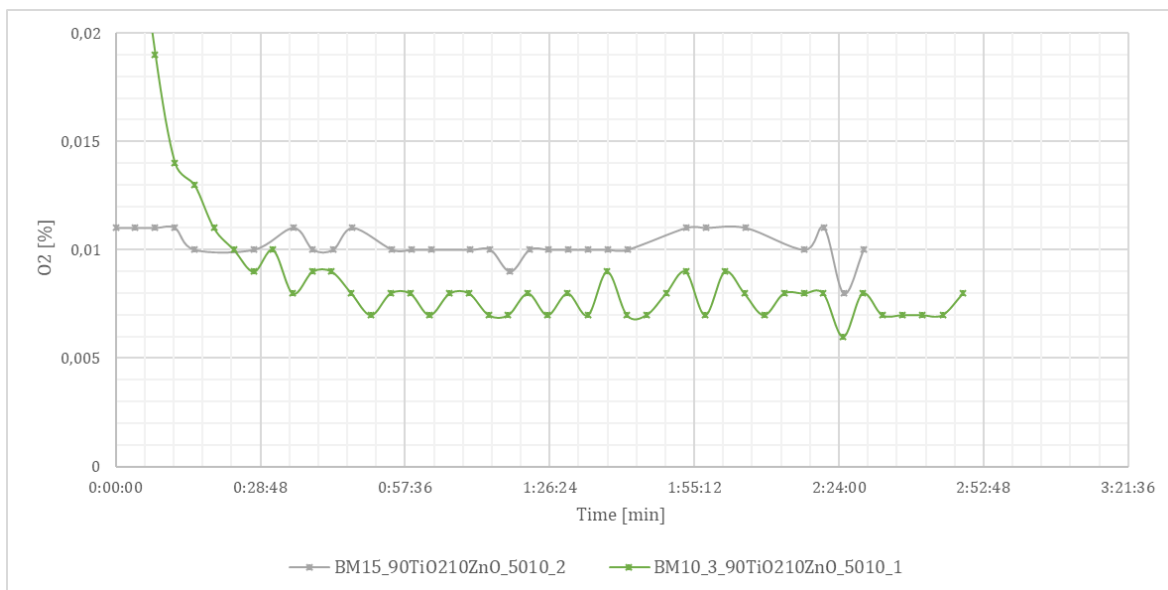


Figure 37. Comparison between the evolution of O₂ concentration of the ZnO compound.

In contrast, regarding the H₂ production, Figure 38 shows a noticeable difference in the H₂ produced. Thus, while in the first figure, the behaviour was quite similar, does not occur the same when it is analysed the H₂ production. Moreover, as it was assumed the sample prepared with 3 balls of 10 mm obtained better results, although these results display an irregular behaviour. As it was mentioned before, this behaviour might be due to some leaks in the circuit during it was performed the analysis into the Micro GC.

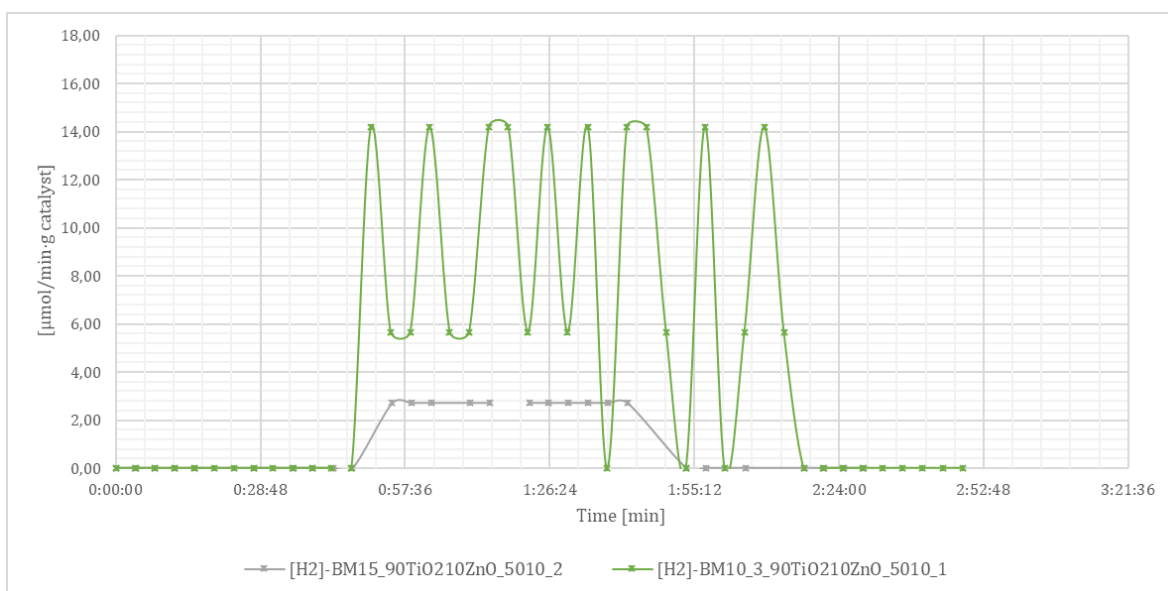


Figure 38. Comparison between the amount of H₂ produced of ZnO compound.

5.2.3.2. 90 % TiO₂ 10 % SnO₂ catalyst

The next samples analysed are the compounds of TiO₂ and SnO₂. Figure 39 illustrates the difference in the oxygen concentration between the two samples when the UV light is turned on due to obtaining H₂. In this case, the sample prepared with 1 ball of 15 mm obtains better results than the sample prepared with 3 balls of 10 mm. Thus, it could be expected that the compound prepared with 1x15 mm is obtaining more H₂.

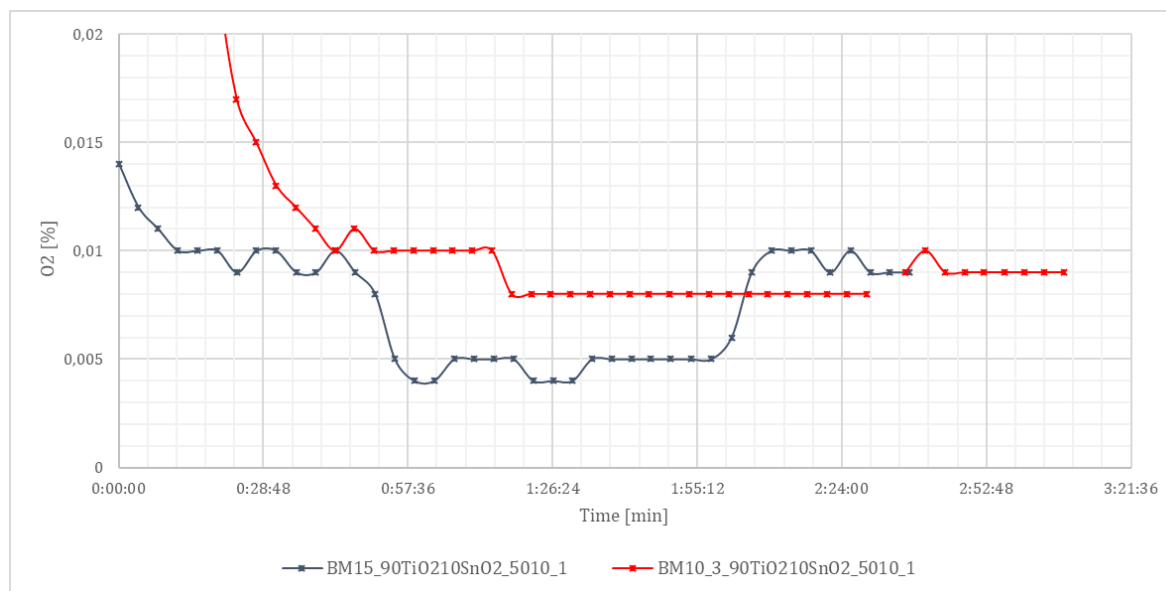


Figure 39. Comparison between the evolution of O₂ concentration of the SnO₂ compound.

Finally, Figure 40 shows a remarkable difference in the H₂ produced, even though both samples have a constant behaviour while obtaining H₂. Thus, the sample prepared with 1x15 mm obtained better results, doubling the results obtained by 3x10 mm.

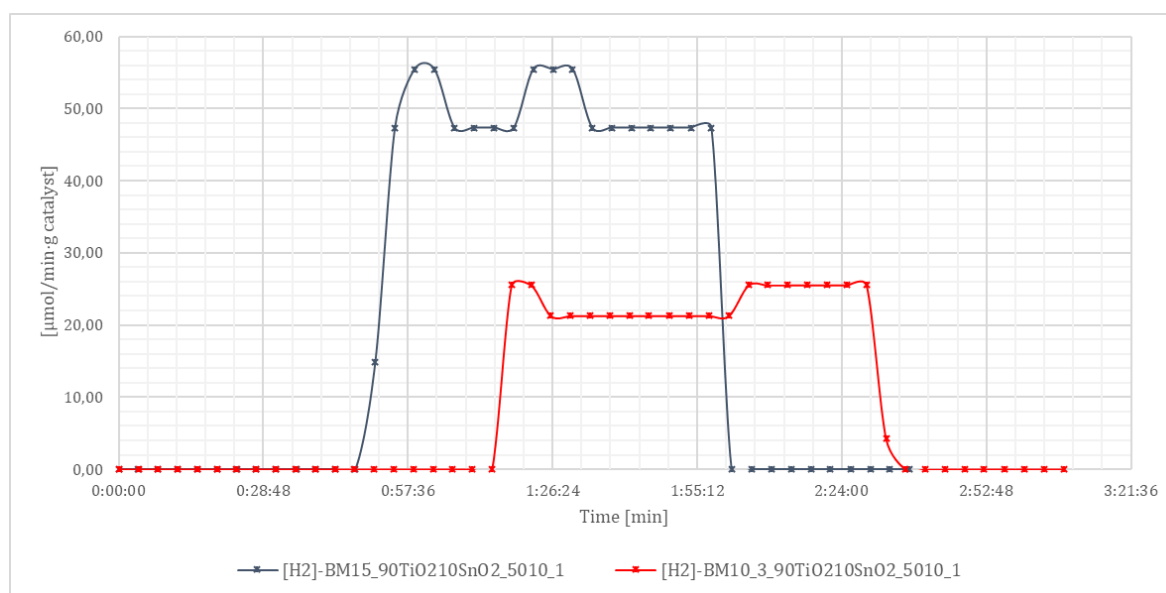


Figure 40. Comparison between the amount of H₂ produced of SnO₂ compound.

5.2.4. Analysis of the results

To sum up, as it is explained in the previous sections, the photocatalyst that shows better results is the one formed by TiO_2 and CuO .

From the firsts experiments analysed in [Section 5.2.1](#), it can be mentioned that there are two samples that obtain notable better results. The photocatalysts formed by TiO_2 and CuO , and TiO_2 and SnO_2 are those that improve the results of the catalyst with only TiO_2 , while the photocatalysts which contain Zn are not good. In Table 5 the different catalysts with their H_2 production and characteristics can be observed.

Element 1 TiO_2	Element 2 2 nd Semiconductor	Ball milling conditions	Sample Name	H_2 produced [$\mu\text{mol}/\text{min}\cdot\text{g}$ catalyst]
100 % TiO_2	-	1x15 mm	BM15_100TiO2_5010_1	621
90 % TiO_2	10 % ZnO	1x15 mm	BM15_90TiO210ZnO_5010_2	30
		3x10 mm	BM10_3_90TiO210ZnO_5010_1	193
90 % TiO_2	10 % CuO	1x15 mm	BM15_90TiO210CuO_5010_1	1031
90 % TiO_2	10 % CdS	1x15 mm	BM15_90TiO210CdS_5010_1	336
90 % TiO_2	10 % ZnS	1x15 mm	BM15_90TiO210ZnS_5010_1	284
90 % TiO_2	10 % SnO_2	1x15 mm	BM15_90TiO210SnO2_5010_1	860
		3x10 mm	BM10_3_90TiO210SnO2_5010_1	446

Table 5. Comparison between all the catalysts analysed regarding H_2 production.

Moreover, Figure 41 illustrates the results of the H_2 produced by each catalyst. Thus, it can be observed how the mixture of TiO_2 and CuO has the most suitable results, and with the sample with SnO_2 obtaining better results than the reference sample, while the other compounds are below the values of hydrogen obtained with the photocatalyst of 100 % TiO_2 .

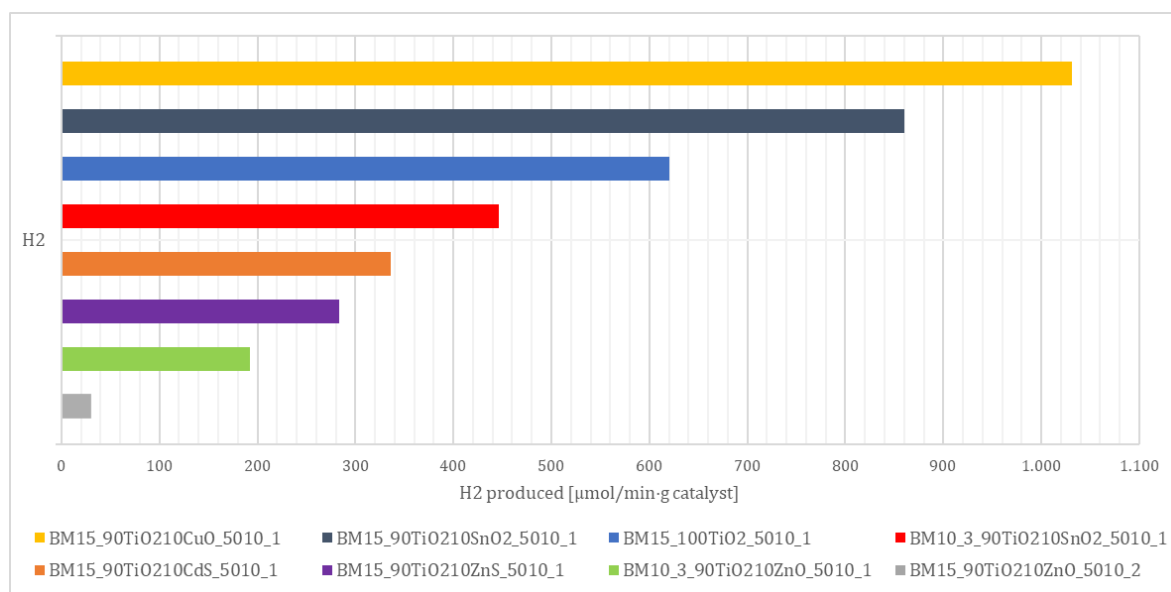


Figure 41. Comparison between all the catalysts analysed regarding H_2 production.

Regarding the relation of these results to the characteristics of the compounds, it does not seem that there is a clear relation with the hardness of the material regarding the data collected in Table 3, since CuO which is the material that displays better results has a similar hardness than the material that has the worst results, ZnO.

However, it is verified the relation with the band gap, CB and VB energy. As it was mentioned in the [Section 3.2.1](#), coupling TiO₂ with other semiconductors that generally have lower band gap energy improves its photoactivity. This statement is proven except for the results for the compound with SnO₂, since CuO has the lower band gap. Figure 42 demonstrates the different band energies related with the information of the semiconductors of Table 3.

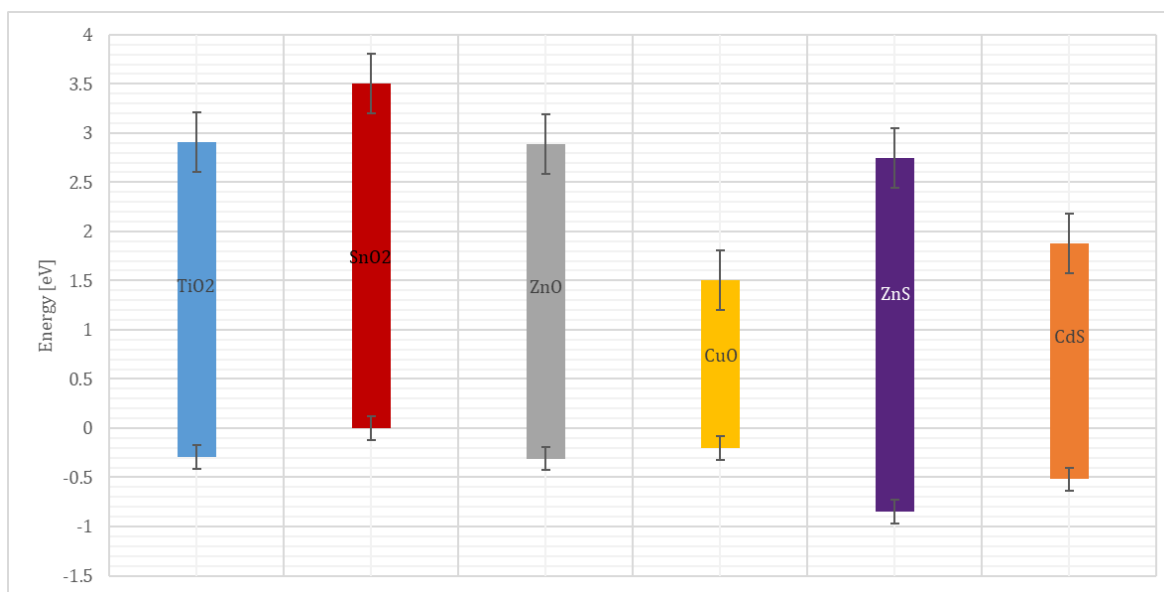


Figure 42. Band energies of the photocatalysts consider in the thesis with respect to TiO₂.

In addition, with the information of Figure 42 and from the equations (5)(6)(7), an order is clearly established regarding which compounds work better based on the information of the CB and VB. When $CB_{SC} > CB_{TiO_2}$ and $VB_{SC} < VB_{TiO_2}$ (7), which is the case of the compound 90 % TiO₂ 10 % CuO, the results obtained regarding the hydrogen production are significantly higher than in the other cases analysed. The next conditions that obtain favourable results are $CB_{SC} > CB_{TiO_2}$ and $VB_{SC} > VB_{TiO_2}$ (6), which is the case of 90 % TiO₂ 10 % SnO₂. Finally, the compounds where $CB_{SC} < CB_{TiO_2}$ and $VB_{SC} < VB_{TiO_2}$ (5) are those which obtain worse results, corresponding to the mixtures of CdS, ZnS and ZnO.

Furthermore, as it was exposed in the [Section 3.1.3](#), the semiconductor of ZnO is used for hydrogen production by thermal cycles. Thus, this element might obtain better results with this process instead of by photocatalysis, because it is not reached high temperatures.

The comparison done in between the H₂ obtained and the amount of CH₃CHO produced of the different samples support the assumptions exposed with the first section. The compounds

formed by ZnO and TiO₂, does not obtain the results expected, because the H₂ produced does not improve the results obtained with just TiO₂, which is the reference sample. While the results found by the samples of CuO and SnO₂ improve the results obtained just with TiO₂.

For the analysis of how the sample is prepared could affect the efficiency of the photocatalyst, is observed different results for the mixture of ZnO and SnO₂. On one hand, for the sample of TiO₂ and ZnO prepared with 1 ball of 15 mm and 3 of 10 mm, it is noticed that the none of the compounds obtain optimum results, despite that the mixture prepared with 3x10 mm has better results.

On the other hand, even though for the compound formed by TiO₂ and SnO₂ both conditions of ball milling obtain notable results, the sample prepared with 1x15 mm obtains better results. These differences between the mixture of SnO₂ and ZnO could be due to the difference of hardness of the components used. While SnO₂ and TiO₂ have similar hardness, the resulting compound might not be properly fixed with 3 balls. In contrast TiO₂ and ZnO have quite different hardness values, thus with 3 balls instead of 1 could help both materials to be combined more uniform.

Finally, the positive synergy between TiO₂ and CuO could be ascribed to a better light use than in bare TiO₂, taking into account than the band gap of CuO (1.7 eV) is much smaller than that of TiO₂ (3.2 eV). In other words, CuO can act as an efficient photon antenna for TiO₂ (Figure 43). The ball milling method favours such interaction.

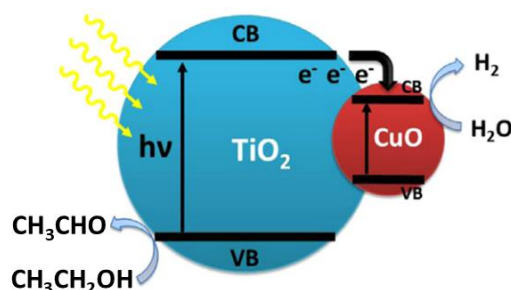


Figure 43. Schematic diagram of the photogeneration of H₂ on the TiO₂-CuO system. [47]

Conclusions

In this section the main results and conclusions are exposed.

The main focus of this thesis was to study the hydrogen production according to the preparation of photocatalysts with mechanochemical methods from combination of semiconductors such as TiO_2 , CuO , SnO_2 , CdS , ZnS , ZnO .

Photocatalysis is the technique used in this project, which utilizes UV radiation to power the water electrolysis process, making the obtaining of hydrogen viable, i.e. depending on the power source the electricity obtained by hydrogen production would be a smaller than the required to start the process.

The main advantage of producing hydrogen from renewable sources is the fact that is an unlimited resource and also the amounts of carbon dioxide that will be avoided, in contrast to fossil fuels the main contributors to global warming. However, if it is produced from renewable power via electrolysis, then hydrogen is fully renewable and CO_2 -free.

Therefore, different photocatalyst were analysed to determine its efficiency. The photocatalysts were prepared by ball milling which is considered a simple, fast, cost-effective green technology. Moreover, the main photocatalyst considered for the project is the titanium dioxide (TiO_2), since it is the most used semiconductor photocatalysts, because its relatively wide band gap. Thus, different compounds were formed with TiO_2 and one of these semiconductors; ZnO , CuO , CdS ZnS or SnO_2 .

The proportion chosen to carry out this analysis were 90 % TiO_2 and 10 % SC. The initial idea was to determine which of these mixtures obtained better results and then vary that proportion to find the most optimal. Nevertheless, due to the current situation due to COVID-19 this could not be done.

Regarding the results of the influence of the compounds analysed, the mixtures formed by TiO_2 and CuO , and TiO_2 and SnO_2 are those that improve the results of the catalyst with only TiO_2 , while the photocatalysts which contain Zn do not present optimum results.

Moreover, regarding the different samples of photocatalysts, it was demonstrated that coupling TiO_2 with other semiconductors that generally have lower band gap energy improves its photoactivity. This approach was proven for the samples analysed, since CuO has the lower band gap and it's the compound that obtains the best results.

Considering the results obtained, it was proven that the best combination of TiO_2 and another semiconductor is the one in which the VB of the semiconductor is smaller compared to the VB of

TiO₂ while the CB of the semiconductor is larger, i.e. when the band gap of the SC is within the band gap of the TiO₂ (Figure 42). This situation causes that both electrons and holes move from TiO₂ to SC. On the other hand, it is also obtained improved results when both CB and VB of the semiconductor are larger than the values for TiO₂, as it was proven with the results of the combination of TiO₂/SnO₂. Finally, it was demonstrated that when the CB and the VB of the SC is lower than the CB and VB of TiO₂, the results obtained for that mixture, regarding the hydrogen production, do not improve the production of using TiO₂ alone as photocatalyst. Which are the cases of ZnO, ZnS and CdS.

Furthermore, the hardness of the elements does not seem to have relation in the effectiveness between the different compounds, since CuO which is the material that displays better results has a similar hardness than the material that has the worst results, ZnO. Despite that, it was noticed an effect when the same compound is analysed, but with different ball milling conditions one prepared with 1 ball of 15 mm and the other prepared with 3 balls of 10 mm.

For the sample of TiO₂ and ZnO prepared with 1x15 mm and 3x10 mm, none of the compounds obtain optimum results, despite that the mixture prepared with 3x10 mm has better results. While SnO₂ and TiO₂ have similar hardness, the resulting compound might not be properly fixed with 3 balls. In contrast TiO₂ and ZnO have quite different hardness values, thus with 3 balls instead of 1 could help both materials to be combined more uniform.

To sum up, from this thesis, it can be verified that coupling by ball milling TiO₂ with a semiconductor with a lower energy band gap, where $CB_{SC} > CB_{TiO_2}$ and $VB_{SC} < VB_{TiO_2}$ (7), which is the case of the compound TiO₂/CuO, or $CB_{SC} > CB_{TiO_2}$ and $VB_{SC} > VB_{TiO_2}$ (6), which is the case of TiO₂/SnO₂ improve the results of using just TiO₂.

Future work

As it was observed in this project, investigation on photocatalysts preparation with mechanochemical methods for obtaining hydrogen is an important field of study. Therefore, it is required more investigation in this field.

Next steps can be done considering the information consulted for this research and the results obtained. Since the compound of CuO and TiO₂ obtained the best results, it could be interesting to explore more in detail this photocatalyst system and also, extend the study to other copper oxides, such as Cu₂O, in order to determine the efficiency of diverse compounds which includes. In addition, the photocatalyst formed by SnO₂ and TiO₂ also obtained promising results. Thus, it might be explored in more detail the TiO₂-SnO₂ system and to extend the study to other tin oxides, such as SnO. Thus, to characterize the TiO₂-CuO and TiO₂-SnO₂ systems by different physical-chemical tools and to compare the results with those of bare TiO₂, might be the next step of this project.

Therefore, further investigation is required to better understand the combination of semiconductors.

Temporal planning

In the current context in which we find, with a pandemic, the planning of this project was disrupted. Not only the planning was affected, but also the main idea and objective of it. Therefore, the thesis and initial plan had to be reassessed to adapt to the new circumstances. Figure 44 illustrates the final planning of this project.

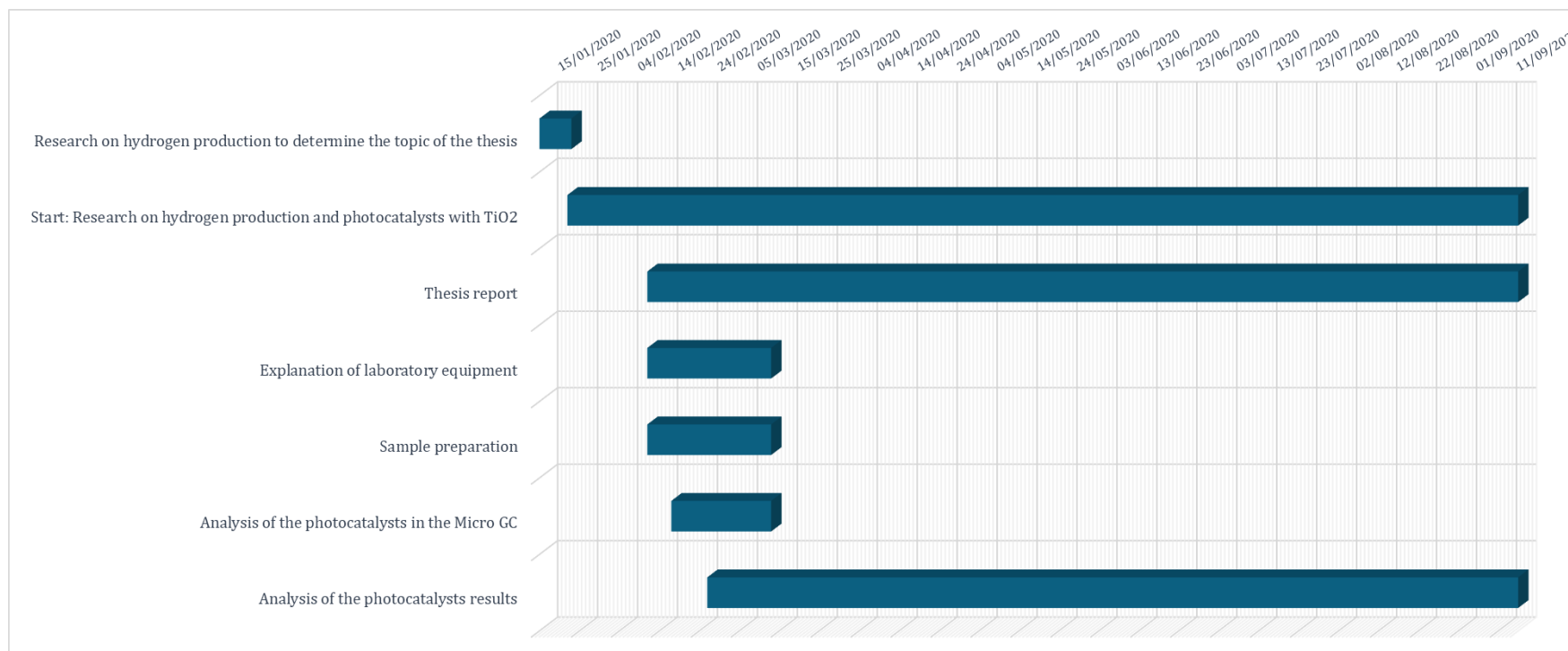


Figure 44. Gantt Diagram of the thesis.

Economic analysis

The thesis cost mainly depends on the semiconductor compounds used to analyse their efficiency as photocatalysts, the laboratory equipment used to analyse the samples and the material resources.

It is dedicated an amount of time equivalent to 900 hours of work approximately. This time is considering each of the activities that are completed through the thesis. From doing a deep research on photocatalysts to the laboratory work and subsequent writing. Thus, according to information on salaries of the “*Ministerio de Trabajo, Migraciones y Seguridad Social*” [48], for teachers and researchers, and research staff, this costs are exposed in Table 6.

Item	Quantity	Cost	Total cost
Teachers and Researchers	100 h	20.17 €	2,016.70 €
Research staff	800 h	12.34 €	9,874.06 €
			11,890.76 €

Table 6. Personnel costs associated to the thesis.

Regarding the laboratory equipment required for this project, consist of a micro gas chromatograph Agilent 490, a photoreactor, an UV light, an oven, an ultrasonic bath (Fisher Scientific), the ball milling equipment (FRITSCH PULVERISETTE 23), laboratory balance as it is illustrated in Table 7. Moreover, it was also required different material used to prepare the samples, such as the container with the compound, a spatula, beakers, Eppendorf’s tubes, micropipette, filter paper.

Item	Quantity	Cost	Total cost
Micro gas chromatograph Agilent 490 [43]	1	25,000.00 €	25,000.00 €
UV light	1	100.00 €	100.00 €
Oven	1	4,400.00 €	4,400.00 €
Fisher Scientific [45]	1	450.00 €	450.00 €
FRITSCH PULVERISETTE 23 [44]	1	3,000.00 €	3,000.00 €
Balance	1	500.00 €	500.00 €
			33,450.00 €

Table 7. Cost of the equipment associated to the thesis.

Considering that the amortization time of each equipment is approximately 5 years, and that the duration of this project has been approximately 3 months, until the start of the pandemic of COVID-19, the final cost of the equipment is the one shown in Table 8. Furthermore, the number of hours to complete the thesis has also been counted, with the information of Table 6.

Item	Total cost
Teachers and Researchers	2,016.70 €
Research staff	9,874.06 €
Micro gas chromatograph Agilent 490 [43]	1,250.00 €
UV light	5.00 €
Oven	220.00 €
Fisher Scientific [45]	22.50 €
FRITSCH PULVERISETTE 23 [44]	150.00 €
Balance	25.00 €
Laboratory material	300.00 €
Compounds	300.00 €
	14,163.26 €

Table 8. Economic budget associated to the thesis.

In Table 8 is summarized the approximately cost of the equipment required to realize this project, without considering the fees (IVA). Considering the governmental fees, the final cost is obtained in Table 9.

Item	Cost	IVA	Total cost
Thesis	14,163.26 €	21%	17,137.54 €

Table 9. Project final cost.

To conclude, the average cost of the project is calculated as 17,138 €, considering the all the costs, i.e. taking into account the cost of all the material used and the work of the laboratory technicians or the engineers, thus the time spend by researchers to complete this study.

Environmental impact

This project is focused on reducing the environmental impact when obtaining H₂ with photocatalysts prepared by mechanochemical methods.

Therefore, it is studied the ball milling method to obtain the photocatalyst, since it is a simple, fast, cost-effective green technology with enormous potential. Ball milling is a mechanical technique widely used in industry, because is an environmental-friendly, cost-effective technique. One of the main advantages of this method is the possibility to combine it with chemical treatments, thus allowing obtaining the desired products with minimal effort.

Thus, in this project it is thought the environmental impact, not only for the main purpose, but also for the techniques used to achieve this objective. Hydrogen, as it was mentioned in previous sections is mainly obtained from fossil fuels, that's why in this thesis it is considered and analyse the potential of hydrogen production through renewables energy, in this case, through photovoltaic energy.

In summary, the environmental impact associated to this thesis is minimum, because with project it is sought to decrease the impact of producing hydrogen, not only by using renewable energy, but also in the form of preparing the samples of photocatalysts used for each of the tests performed.

Nomenclature

AEC	Alkaline electrolysis cells
Ar	Argon
ATR	Autothermal reforming
C ₃ H ₆ O	Acetone
CB	Conduction band
CCUS	Carbon Capture Utilisation and Storage
CdS	Cadmium sulphide
CH ₃ CH ₂ OH	Ethanol
CH ₃ CHO	Acetaldehyde (Ethanal)
CH ₃ OH	Methanol
CH ₄	Methane
CO	Carbon Monoxide
CO ₂	Carbon Dioxide
CuO	Copper (II) oxide
DR	Dry reforming
H ₂	Hydrogen
H ₂ O	Water
He	Helium
N ₂	Nitrogen
O ₂	Oxygen
PEM	Proton exchange membrane fuel cell
PO	Partial oxidation
PV	Photovoltaics
SC	Semiconductor
SOEC	Solid oxide electrolysis cell
SnO ₂	Tin (IV) oxide
SR	Steam reforming
TiO ₂	Titanium dioxide
UV	Ultraviolet
VB	Balance band
WGSR	Water gas shift reaction
ZnO	Zinc oxide
ZnS	Zinc sulphide

Bibliography

- [1] United Nations Environment Programme (UNEP), "Facts about the Climate Emergency," *United Nations Environment Programme (UNEP)*, 2020. [Online]. Available: <https://www.unenvironment.org/explore-topics/climate-change/facts-about-climate-emergency>.
- [2] International Energy Agency (IEA), "Climate change – Topics," *International Energy Agency (IEA)*, 2019. [Online]. Available: <https://www.iea.org/topics/climate-change>.
- [3] International Energy Agency (IEA), "Emissions – Global Energy & CO2 Status Report 2019 – Analysis," *International Energy Agency (IEA)*, 2019. [Online]. Available: <https://www.iea.org/reports/global-energy-co2-status-report-2019/emissions#abstract>.
- [4] M. Stone, "Carbon emissions are falling sharply due to coronavirus. But not for long.," *NATIONAL GEOGRAPHIC*, 2020.
- [5] International Energy Agency (IEA), "Global Energy Review 2020 – Analysis - The impacts of the Covid-19 crisis on global energy demand and CO2 emissions," *International Energy Agency (IEA)*, 2020. [Online]. Available: <https://www.iea.org/reports/global-energy-review-2020>.
- [6] Z. Abdin, A. Zafaranloo, A. Rafiee, W. Mérida, W. Lipiński, and K. R. Khalilpour, "Hydrogen as an energy vector," *Renew. Sustain. Energy Rev.*, vol. 120, no. December 2019, 2020.
- [7] International Energy Agency (IEA), "The Future of Hydrogen – Analysis," *International Energy Agency (IEA)*, 2019. [Online]. Available: <https://www.iea.org/reports/the-future-of-hydrogen>.
- [8] IRENA, "Hydrogen From Renewable Power: Technology outlook for the energy transition," 2018.
- [9] J. Jia *et al.*, "Solar water splitting by photovoltaic-electrolysis with a solar-to-hydrogen efficiency over 30%," *Nat. Commun.*, vol. 7, no. May, pp. 1–6, 2016.
- [10] C. M. Kalamaras, A. M. Efstathiou, Y. Al-Assaf, and A. Poullikkas, "Conference Paper Hydrogen Production Technologies: Current State and Future Developments," *Conf. Pap. Energy*, vol. 2013, 2013.
- [11] "Steam Reforming of Natural Gas." [Online]. Available: <http://www.digipac.ca/chemical/mtom/contents/chapter4/steamreform.htm>.
- [12] AleaSoft Energy Forecasting, "The green hydrogen is the fuel of the future," *AleaSoft Energy Forecasting*. [Online]. Available: <https://aleasoft.com/green-hydrogen-fuel-future/>.
- [13] O. Schmidt, A. Gambhir, I. Staffell, A. Hawkes, J. Nelson, and S. Few, "Future cost and performance of water electrolysis: An expert elicitation study," *Int. J. Hydrogen Energy*, vol. 42, no. 52, pp. 30470–30492, Dec. 2017.

-
- [14] C. A. Grimes, O. K. Varghese, and S. Ranjan, Eds., *Light, water, hydrogen: The solar generation of hydrogen by water photoelectrolysis*. Boston, MA: Springer US, 2008.
- [15] D. Y. C. Leung *et al.*, "Hydrogen production over titania-based photocatalysts," *ChemSusChem*, vol. 3, no. 6, pp. 681–694, 2010.
- [16] J. Li and N. Wu, "Semiconductor-based photocatalysts and photoelectrochemical cells for solar fuel generation: a review," *Catal. Sci. Technol.*, vol. 5, no. 3, pp. 1360–1384, 2015.
- [17] Z. Shayegan, C. S. Lee, and F. Haghghat, "TiO₂ photocatalyst for removal of volatile organic compounds in gas phase – A review," *Chem. Eng. J.*, vol. 334, no. August 2017, pp. 2408–2439, 2018.
- [18] T. H. Nguyen, T. L. Nguyen, T. D. T. Ung, and Q. L. Nguyen, "Synthesis and characterization of nano-CuO and CuO/TiO₂ photocatalysts," *Adv. Nat. Sci. Nanosci. Nanotechnol.*, vol. 4, no. 2, 2013.
- [19] S. Chen, W. Zhao, W. Liu, and S. Zhang, "Preparation, characterization and activity evaluation of p-n junction photocatalyst p-ZnO/n-TiO₂," *Appl. Surf. Sci.*, vol. 255, no. 5 PART 1, pp. 2478–2484, 2008.
- [20] K. Manjunath, V. S. Souza, T. Ramakrishnappa, G. Nagaraju, J. D. Scholten, and J. Dupont, "Heterojunction CuO-TiO₂ nanocomposite synthesis for significant photocatalytic hydrogen production," *Mater. Res. Express*, vol. 3, no. 11, p. 115904, Nov. 2016.
- [21] C. Shifu, C. Lei, G. Shen, and C. Gengyu, "The preparation of coupled SnO₂/TiO₂ photocatalyst by ball milling," *Mater. Chem. Phys.*, vol. 98, no. 1, pp. 116–120, 2006.
- [22] Q. Shi *et al.*, "CuO/TiO₂ heterojunction composites: An efficient photocatalyst for selective oxidation of methanol to methyl formate," *J. Mater. Chem. A*, vol. 7, no. 5, pp. 2253–2260, 2019.
- [23] K. R. Karim, M. Anak, P. Jebi, H. R. Ong, and H. Abdullah, "CuO-TiO₂ as a visible light responsive photocatalyst for the photoelectroreduction of CO₂ to methanol," *Natl. Conf. Postgrad. Res.*, no. December, pp. 103–111, 2018.
- [24] K. Manjunath, V. S. Souza, T. Ramakrishnappa, G. Nagaraju, J. D. Scholten, and J. Dupont, "Heterojunction CuO-TiO₂ nanocomposite synthesis for significant photocatalytic hydrogen production," *Mater. Res. Express*, vol. 3, no. 11, pp. 1–7, 2016.
- [25] C. K. Nuo Peh, X.-Q. Wang, and G. W. Ho, "Increased photocatalytic activity of CuO/TiO₂ through broadband solar absorption heating under natural sunlight," *Procedia Eng.*, vol. 215, pp. 171–179, 2017.
- [26] J. M. Kum, S. H. Yoo, G. Ali, and S. O. Cho, "Photocatalytic hydrogen production over CuO and TiO₂ nanoparticles mixture," *Int. J. Hydrogen Energy*, vol. 38, no. 31, pp. 13541–13546, 2013.
- [27] X. Cai, P. Zhang, and S. H. Wei, "Revisit of the band gaps of rutile SnO₂ and TiO₂: A

- first-principles study,” *J. Semicond.*, vol. 40, no. 9, 2019.
- [28] ENERGIA LIMPIA XXI, “Norway, Portugal and Costa Rica are 100% renewable energy using wind, solar, hydro and geothermal resources,” *ENERGIA LIMPIA XXI*, 2019. [Online]. Available: <https://energialimpiaparatodos.com/2019/03/23/climate-change-expansion-renovable-energia-limpia-xxi-cambio-matriz-renovable-hoy/>.
- [29] J. Solans Huguet and M. Domenech, “Naturaleza y significado de la dureza de los minerales,” in *Trabajos de geología*, vol. 10, no. 10, 1978, pp. 407–424.
- [30] P. Walker, W. H. Tarn, B. Raton, B. London, and N. Y. Washington, *HANDBOOK OF METAL ETCHANTS*. CRC Press, 1991.
- [31] A. M. Ganose and D. O. Scanlon, “Band gap and work function tailoring of SnO₂ for improved transparent conducting ability in photovoltaics,” *J. Mater. Chem. C*, vol. 4, no. 7, pp. 1467–1475, Feb. 2016.
- [32] A. Arif, O. Belahssen, S. Gareh, and S. Benramache, “The calculation of band gap energy in zinc oxide films,” *J. Semicond.*, vol. 36, no. 1, p. 013001, Jan. 2015.
- [33] J. S. Sagu, T. A. N. Peiris, and K. G. U. Wijayantha, “Rapid and simple potentiostatic deposition of copper (II) oxide thin films,” *Electrochem. commun.*, vol. 42, pp. 68–71, May 2014.
- [34] P. D’Amico, A. Calzolari, A. Ruini, and A. Catellani, “New energy with ZnS: Novel applications for a standard transparent compound,” *Sci. Rep.*, vol. 7, no. 1, pp. 1–9, Dec. 2017.
- [35] R. E. Brandt *et al.*, “Band offsets of n-type electron-selective contacts on cuprous oxide (Cu₂O) for photovoltaics,” *Appl. Phys. Lett.*, vol. 105, no. 26, p. 263901, Dec. 2014.
- [36] IRENA, *Hydrogen: a Renewable Energy Perspective*, no. September. 2019.
- [37] Q. X. Peng, D. Xue, S. Z. Zhan, and C. L. Ni, “Visible-light-driven photocatalytic system based on a nickel complex over CdS materials for hydrogen production from water,” *Appl. Catal. B Environ.*, vol. 219, pp. 353–361, 2017.
- [38] A. Gómez-Barea, P. Ollero, and R. Arjona, “Reaction-diffusion model of TGA gasification experiments for estimating diffusional effects,” *Fuel*, vol. 84, no. 12–13, pp. 1695–1704, 2005.
- [39] X. Fu, Y. Hu, Y. Yang, W. Liu, and S. Chen, “Ball milled h-BN: An efficient holes transfer promoter to enhance the photocatalytic performance of TiO₂,” *J. Hazard. Mater.*, vol. 244–245, pp. 102–110, 2013.
- [40] T. Prasad Yadav, R. Manohar Yadav, and D. Pratap Singh, “Mechanical Milling: a Top Down Approach for the Synthesis of Nanomaterials and Nanocomposites,” *Nanosci. Nanotechnol.*, vol. 2, no. 3, pp. 22–48, Aug. 2012.
- [41] C. C. Piras, S. Fernández-Prieto, and W. M. De Borggraeve, “Ball milling: A green technology for the preparation and functionalisation of nanocellulose derivatives,”

Nanoscale Adv., vol. 1, no. 3, pp. 937–947, 2019.

- [42] S. Yin, Q. Zhang, F. Saito, and T. Sato, "Preparation of visible light-activated titania photocatalyst by mechanochemical method," *Chem. Lett.*, vol. 32, no. 4, pp. 358–359, 2003.
- [43] Agilent Technologies, "Agilent Technologies Agilent 490 □ Micro Gas Chromatograph User Manual Notices," 2017.
- [44] FRITSCH, "Mini-Mill PULVERISETTE 23 / TECHNICAL DATA - fritsch.de." [Online]. Available: <https://www.fritsch-international.com/sample-preparation/milling/ball-mills/details/product/pulverisette-23/technical-details/>.
- [45] Fisher Scientific, "Ultrasound for the laboratory Fisher Scientific."
- [46] "Fotoproducció d'H₂ en un fotoreactor tubular utilitzant catalitzadors dispersats en membrana de cel·lulosa."
- [47] L. Zhu, M. Hong, and G. W. Ho, "Fabrication of wheat grain textured TiO₂/CuO composite nanofibers for enhanced solar H₂ generation and degradation performance," *Nano Energy*, vol. 11, pp. 28–37, Jan. 2015.
- [48] BOE, "Resolución de 27 de agosto de 2019, de la Dirección General de Trabajo, por la que se registra y publica el VIII Convenio colectivo nacional de universidades privadas, centros universitarios privados y centros de formación de postgraduados," «BOE» núm. 221, 2019. [Online]. Available: https://www.boe.es/diario_boe/txt.php?id=BOE-A-2019-13119.

A Excel calculations

In this appendix, it is attached the calculation realized in Excel to analyse the results obtained with the Micro GC. Therefore, it is divided in two tables between the data from Channel 1 (Table 10) and Channel 3 (Table 11), as it is shown below. Each column corresponds to a different parameter calculated or obtained from the Micro GC.

The name of the sample indicates first the characteristics of the ball milling container (1x15 mm or 3x10 mm), secondly the composition of the catalyst, i.e. 100TiO₂ corresponds to 100 % of TiO₂ which means that the photocatalyst is formed just with TiO₂, then it is specified the conditions of the ball milling 50 Hz 10 min, and finally the number of the sample. Moreover, it is marked when it was turned on and off the UV light. For each sample is selected with a yellow background (☀) the repetition when the UV light is turned on, on the other hand it is marked in orange (☹) when that UV light was switched off.

Table 10 illustrates the information involving Channel 1. The first line describes the information that each column will have. Those cells which said Channel 1 represents the information obtained directly from the data of the Micro GC, except the column of "O₂ consumed" where is calculated the O₂ consumed, thus the H₂ production as it was mentioned in the [Section 5.1](#). The lasts four columns show the data obtain by the calculations describe in the first line of the table to obtain the total amount of H₂ produced, thus each column corresponds to one step. Moreover, these calculations are those explained in the [Section 5.1](#), i.e. the column "H₂ + ½O₂ → H₂O" indicates the amount of hydrogen obtained by that equation. The last column indicates the total amount of H₂ obtained by the specific catalyst in a specific time.

Table 11 explains the information involving Channel 3. As it was previously explained, the first line describes the information that each column will have. The column which said Channel 3 represents the information obtained directly from the data of the Micro GC. The lasts three columns show the data obtain by the calculations describe in the first line of the table to obtain the total amount of CH₃CHO produced, thus each column corresponds to one stage. Furthermore, these calculations are those explained also in the [Section 5.1](#), i.e. the column "20 ml Ar/min" indicates the calculation described in Equation (11). The last column indicates the total amount of CH₃CHO obtained by the specific catalyst in a specific period.

Finally, some cells do not have any numeric value or it is indicated "0.000 BDL", which means that the Micro GC in that moment did not register any data or an error has appeared.

				CHANNEL 1	CHANNEL 1	CHANNEL 1	CHANNEL 1	H2 + ½O2 → H2O	20 ml Ar/min	1 mol gas = 22,4 l	
units	mg	-	min	%	%	%	%	%	ml/min	µmol/min	µmol/min· g catalyst
SAMPLE	CATALYST	REP	Time	H2	O2	N2	O2 consumed	H2 total	H2	H2	H2
BM15_100TiO2_5010_1	2.1	1	0:00:00	0	0.173	0.348		0.00000	0.00000	0.00000	0.00000
BM15_100TiO2_5010_1	2.1	2	0:04:13	0	0.081	0.149		0.00000	0.00000	0.00000	0.00000
BM15_100TiO2_5010_1	2.1	3	0:08:04	0	0.046	0.081		0.00000	0.00000	0.00000	0.00000
BM15_100TiO2_5010_1	2.1	4	0:11:58	0	0.03	0.048		0.00000	0.00000	0.00000	0.00000
BM15_100TiO2_5010_1	2.1	5	0:15:56	0	0.021	0.036		0.00000	0.00000	0.00000	0.00000
BM15_100TiO2_5010_1	2.1	6	0:19:50	0	0.017	0.029		0.00000	0.00000	0.00000	0.00000
BM15_100TiO2_5010_1	2.1	7	0:23:44	0	0.015	0.025		0.00000	0.00000	0.00000	0.00000
BM15_100TiO2_5010_1	2.1	8	0:27:39	0	0.014	0.024		0.00000	0.00000	0.00000	0.00000
BM15_100TiO2_5010_1	2.1	9	0:31:30	0	0.012	0.023	0.0120	0.00000	0.00000	0.00000	0.00000
BM15_100TiO2_5010_1	2.1	10	0:35:26	0	0.012	0.022	0.0000	0.00000	0.00000	0.00000	0.00000
BM15_100TiO2_5010_1	2.1	11	0:39:20	0	0.009	0.02	0.0030	0.00600	0.00120	0.05357	25.51020
BM15_100TiO2_5010_1	2.1	12	0:43:31	0	0.008	0.021	0.0040	0.00800	0.00160	0.07143	34.01361
BM15_100TiO2_5010_1	2.1	13	0:47:25	0	0.008	0.02	0.0040	0.00800	0.00160	0.07143	34.01361
BM15_100TiO2_5010_1	2.1	14	0:51:20	0	0.008	0.02	0.0040	0.00800	0.00160	0.07143	34.01361
BM15_100TiO2_5010_1	2.1	15	0:55:20	0	0.008	0.02	0.0040	0.00800	0.00160	0.07143	34.01361
BM15_100TiO2_5010_1	2.1	16	0:59:19	0	0.007	0.02	0.0050	0.01000	0.00200	0.08929	42.51701
BM15_100TiO2_5010_1	2.1	17	1:03:11	0	0.008	0.02	0.0040	0.00800	0.00160	0.07143	34.01361
BM15_100TiO2_5010_1	2.1	18	1:07:05	0	0.008	0.019	0.0040	0.00800	0.00160	0.07143	34.01361
BM15_100TiO2_5010_1	2.1	19	1:10:59	0	0.007	0.021	0.0050	0.01000	0.00200	0.08929	42.51701
BM15_100TiO2_5010_1	2.1	20	1:14:56	0	0.004	0.022	0.0080	0.01600	0.00320	0.14286	68.02721
BM15_100TiO2_5010_1	2.1	21	1:18:48	0	0.007	0.02	0.0050	0.01000	0.00200	0.08929	42.51701
BM15_100TiO2_5010_1	2.1	22	1:22:43	0	0.007	0.019	0.0050	0.01000	0.00200	0.08929	42.51701

				CHANNEL 1	CHANNEL 1	CHANNEL 1	CHANNEL 1	H2 + ½O2 → H2O	20 ml Ar/min	1 mol gas = 22,4 l	
units	mg	-	min	%	%	%	%	%	ml/min	µmol/min	µmol/min· g catalyst
SAMPLE	CATALYST	REP	Time	H2	O2	N2	O2 consumed	H2 total	H2	H2	H2
BM15_100TiO2_5010_1	2.1	23	1:26:38	0	0.007	0.021	0.0050	0.01000	0.00200	0.08929	42.51701
BM15_100TiO2_5010_1	2.1	24	1:30:33	0	0.007	0.021	0.0050	0.01000	0.00200	0.08929	42.51701
BM15_100TiO2_5010_1	2.1	25	1:34:33	0	0.008	0.021	0.0040	0.00800	0.00160	0.07143	34.01361
BM15_100TiO2_5010_1	2.1	26	1:38:27	0	0.008	0.023	0.0040	0.00800	0.00160	0.07143	34.01361
BM15_100TiO2_5010_1	2.1	27	1:42:22	0	0.01	0.02		0.00000	0.00000	0.00000	0.00000
BM15_100TiO2_5010_1	2.1	28	1:46:17	0	0.011	0.02		0.00000	0.00000	0.00000	0.00000
BM15_100TiO2_5010_1	2.1	29	1:50:12	0	0.011	0.02		0.00000	0.00000	0.00000	0.00000
BM15_100TiO2_5010_1	2.1	30	1:54:12	0	0.011	0.019		0.00000	0.00000	0.00000	0.00000
BM15_90TiO210ZnO_5010_1	2.2	1	0:00:00	0	0.04	0.08		0.00000	0.00000	0.00000	0.00000
BM15_90TiO210ZnO_5010_1	2.2	2	0:03:52					0.00000	0.00000	0.00000	0.00000
BM15_90TiO210ZnO_5010_1	2.2	3	0:07:45	0	0.019	0.033		0.00000	0.00000	0.00000	0.00000
BM15_90TiO210ZnO_5010_1	2.2	4	0:11:46	0	0.016	0.029		0.00000	0.00000	0.00000	0.00000
BM15_90TiO210ZnO_5010_1	2.2	5	0:15:38	0	0.015	0.027		0.00000	0.00000	0.00000	0.00000
BM15_90TiO210ZnO_5010_1	2.2	6	0:19:30	0	0.013	0.021		0.00000	0.00000	0.00000	0.00000
BM15_90TiO210ZnO_5010_1	2.2	7	0:23:24	0	0.014	0.024		0.00000	0.00000	0.00000	0.00000
BM15_90TiO210ZnO_5010_1	2.2	8	0:27:17	0	0.013	0.024		0.00000	0.00000	0.00000	0.00000
BM15_90TiO210ZnO_5010_1	2.2	9	0:31:11	0	0.013	0.023		0.00000	0.00000	0.00000	0.00000
BM15_90TiO210ZnO_5010_1	2.2	10	0:35:07	0	0.013	0.023		0.00000	0.00000	0.00000	0.00000
BM15_90TiO210ZnO_5010_1	2.2	11	0:39:06	0	0.012	0.021		0.00000	0.00000	0.00000	0.00000
BM15_90TiO210ZnO_5010_1	2.2	12	0:43:01	0	0.012	0.022		0.00000	0.00000	0.00000	0.00000
BM15_90TiO210ZnO_5010_1	2.2	13	0:47:00	0	0.012	0.022		0.00000	0.00000	0.00000	0.00000
BM15_90TiO210ZnO_5010_1	2.2	14	0:50:54					0.00000	0.00000	0.00000	0.00000
BM15_90TiO210ZnO_5010_1	2.2	15	0:54:51	0	0.012	0.022		0.00000	0.00000	0.00000	0.00000

				CHANNEL 1	CHANNEL 1	CHANNEL 1	CHANNEL 1	H2 + ½O2 → H2O	20 ml Ar/min	1 mol gas = 22,4 l	
units	mg	-	min	%	%	%	%	%	ml/min	µmol/min	µmol/min· g catalyst
SAMPLE	CATALYST	REP	Time	H2	O2	N2	O2 consumed	H2 total	H2	H2	H2
BM15_90TiO210ZnO_5010_1	2.2	16	0:58:44	0	0.013	0.016		0.00000	0.00000	0.00000	0.00000
BM15_90TiO210ZnO_5010_1	2.2	17	1:02:38	0	0.012	0.024		0.00000	0.00000	0.00000	0.00000
BM15_90TiO210ZnO_5010_1	2.2	18	1:06:33	0	0.012	0.022		0.00000	0.00000	0.00000	0.00000
BM15_90TiO210ZnO_5010_2	2.2	1	0:00:00	0	0.011	0.017		0.00000	0.00000	0.00000	0.00000
BM15_90TiO210ZnO_5010_2	2.2	2	0:03:53	0	0.011	0.014		0.00000	0.00000	0.00000	0.00000
BM15_90TiO210ZnO_5010_2	2.2	3	0:07:50	0	0.011	0.015		0.00000	0.00000	0.00000	0.00000
BM15_90TiO210ZnO_5010_2	2.2	4	0:11:41	0	0.011	0.014		0.00000	0.00000	0.00000	0.00000
BM15_90TiO210ZnO_5010_2	2.2	5	0:15:35	0	0.01	0.013		0.00000	0.00000	0.00000	0.00000
BM15_90TiO210ZnO_5010_2	2.2	8	0:27:27	0	0.01	0.015		0.00000	0.00000	0.00000	0.00000
BM15_90TiO210ZnO_5010_2	2.2	10	0:35:19	0	0.011	0.014		0.00000	0.00000	0.00000	0.00000
BM15_90TiO210ZnO_5010_2	2.2	11	0:39:13	0	0.01	0.014		0.00000	0.00000	0.00000	0.00000
BM15_90TiO210ZnO_5010_2	2.2	12	0:43:13	0	0.01	0.015	0.0103	0.00000	0.00000	0.00000	0.00000
BM15_90TiO210ZnO_5010_2	2.2	13	0:47:08	0	0.011	0.013	0.0000	0.00000	0.00000	0.00000	0.00000
BM15_90TiO210ZnO_5010_2	2.2	15	0:55:01	0	0.01	0.014	0.0003	0.00067	0.00013	0.00595	2.70563
BM15_90TiO210ZnO_5010_2	2.2	16	0:58:53	0	0.01	0.014	0.0003	0.00067	0.00013	0.00595	2.70563
BM15_90TiO210ZnO_5010_2	2.2	17	1:02:51	0	0.01	0.013	0.0003	0.00067	0.00013	0.00595	2.70563
BM15_90TiO210ZnO_5010_2	2.2	19	1:10:38	0	0.01	0.013	0.0003	0.00067	0.00013	0.00595	2.70563
BM15_90TiO210ZnO_5010_2	2.2	20	1:14:33	0	0.01	0.014	0.0003	0.00067	0.00013	0.00595	2.70563
BM15_90TiO210ZnO_5010_2	2.2	21	1:18:29	0	0.009	0.012	0.0013	0.00267	0.00053	0.02381	
BM15_90TiO210ZnO_5010_2	2.2	22	1:22:22	0	0.01	0.014	0.0003	0.00067	0.00013	0.00595	2.70563
BM15_90TiO210ZnO_5010_2	2.2	23	1:26:15	0	0.01	0.015	0.0003	0.00067	0.00013	0.00595	2.70563
BM15_90TiO210ZnO_5010_2	2.2	24	1:30:10	0	0.01	0.013	0.0003	0.00067	0.00013	0.00595	2.70563
BM15_90TiO210ZnO_5010_2	2.2	25	1:34:04	0	0.01	0.014	0.0003	0.00067	0.00013	0.00595	2.70563

				CHANNEL 1	CHANNEL 1	CHANNEL 1	CHANNEL 1	H2 + ½O2 → H2O	20 ml Ar/min	1 mol gas = 22,4 l	
units	mg	-	min	%	%	%	%	%	ml/min	µmol/min	µmol/min· g catalyst
SAMPLE	CATALYST	REP	Time	H2	O2	N2	O2 consumed	H2 total	H2	H2	H2
BM15_90TiO210ZnO_5010_2	2.2	26	1:37:58	0	0.01	0.013	0.0003	0.00067	0.00013	0.00595	2.70563
BM15_90TiO210ZnO_5010_2	2.2	27	1:41:52	0	0.01	0.015	0.0003	0.00067	0.00013	0.00595	2.70563
BM15_90TiO210ZnO_5010_2	2.2	30	1:53:34	0	0.011	0.013	0.0000	0.00000	0.00000	0.00000	0.00000
BM15_90TiO210ZnO_5010_2	2.2	31	1:57:34	0	0.011	0.015		0.00000	0.00000	0.00000	0.00000
BM15_90TiO210ZnO_5010_2	2.2	33	2:05:25	0	0.011	0		0.00000	0.00000	0.00000	0.00000
BM15_90TiO210ZnO_5010_2	2.2	36	2:17:05	0	0.01	0.014		0.00000	0.00000	0.00000	0.00000
BM15_90TiO210ZnO_5010_2	2.2	37	2:21:00	0	0.011	0.013		0.00000	0.00000	0.00000	0.00000
BM15_90TiO210ZnO_5010_2	2.2	38	2:24:55	0	0.008	0.012		0.00000	0.00000	0.00000	0.00000
BM15_90TiO210ZnO_5010_2	2.2	39	2:28:54	0	0.01	0.014		0.00000	0.00000	0.00000	0.00000
BM15_90TiO210CuO_5010_1	2.0	1	0:00:00	0	0.014	0.022		0.00000	0.00000	0.00000	0.00000
BM15_90TiO210CuO_5010_1	2.0	2	0:03:53	0	0.012	0.018		0.00000	0.00000	0.00000	0.00000
BM15_90TiO210CuO_5010_1	2.0	3	0:07:48	0	0.011	0.017		0.00000	0.00000	0.00000	0.00000
BM15_90TiO210CuO_5010_1	2.0	4	0:11:44	0	0.011	0.018		0.00000	0.00000	0.00000	0.00000
BM15_90TiO210CuO_5010_1	2.0	5	0:15:36	0	0.011	0.018		0.00000	0.00000	0.00000	0.00000
BM15_90TiO210CuO_5010_1	2.0	6	0:19:31	0	0.011	0.017		0.00000	0.00000	0.00000	0.00000
BM15_90TiO210CuO_5010_1	2.0	7	0:23:27	0	0.011	0.018		0.00000	0.00000	0.00000	0.00000
BM15_90TiO210CuO_5010_1	2.0	8	0:27:20	0	0.011	0.015		0.00000	0.00000	0.00000	0.00000
BM15_90TiO210CuO_5010_1	2.0	9	0:31:14	0	0.01	0.017		0.00000	0.00000	0.00000	0.00000
BM15_90TiO210CuO_5010_1	2.0	10	0:35:23	0	0.011	0.000 BDL		0.00000	0.00000	0.00000	0.00000
BM15_90TiO210CuO_5010_1	2.0	11	0:39:22					0.00000	0.00000	0.00000	0.00000
BM15_90TiO210CuO_5010_1	2.0	12	0:43:21	0	0.011	0.015		0.00000	0.00000	0.00000	0.00000
BM15_90TiO210CuO_5010_1	2.0	13	0:47:16	0	0.011	0.015		0.00000	0.00000	0.00000	0.00000
BM15_90TiO210CuO_5010_1	2.0	14	0:51:10	0	0.011	0.017		0.00000	0.00000	0.00000	0.00000

				CHANNEL 1	CHANNEL 1	CHANNEL 1	CHANNEL 1	H2 + ½O2 → H2O	20 ml Ar/min	1 mol gas = 22,4 l	
units	mg	-	min	%	%	%	%	%	ml/min	µmol/min	µmol/min· g catalyst
SAMPLE	CATALYST	REP	Time	H2	O2	N2	O2 consumed	H2 total	H2	H2	H2
BM15_90TiO210CuO_5010_1	2.0	15	0:55:05	0	0.011	0.018	0.0110	0.00000	0.00000	0.00000	0.00000
BM15_90TiO210CuO_5010_1	2.0	16	0:59:09	0	0.011	0.009	0.0000	0.00000	0.00000	0.00000	0.00000
BM15_90TiO210CuO_5010_1	2.0	17	1:03:03	0.005	0.007	0.015	0.0040	0.01300	0.00260	0.11607	58.03571
BM15_90TiO210CuO_5010_1	2.0	18	1:06:56	0.006	0.007	0.016	0.0040	0.01400	0.00280	0.12500	62.50000
BM15_90TiO210CuO_5010_1	2.0	19	1:10:52	0.006	0.007	0.016	0.0040	0.01400	0.00280	0.12500	62.50000
BM15_90TiO210CuO_5010_1	2.0	20	1:14:51	0.006	0.007	0.015	0.0040	0.01400	0.00280	0.12500	62.50000
BM15_90TiO210CuO_5010_1	2.0	21	1:19:03	0.006	0.006	0.014	0.0050	0.01600	0.00320	0.14286	71.42857
BM15_90TiO210CuO_5010_1	2.0	22	1:22:56	0.007	0.006	0.000 BDL	0.0050	0.01700	0.00340	0.15179	75.89286
BM15_90TiO210CuO_5010_1	2.0	23	1:26:50	0.007	0.007	0.017	0.0040	0.01500	0.00300	0.13393	66.96429
BM15_90TiO210CuO_5010_1	2.0	24	1:30:45	0.007	0.006	0.015	0.0050	0.01700	0.00340	0.15179	75.89286
BM15_90TiO210CuO_5010_1	2.0	25	1:34:38	0.007	0.006	0.015	0.0050	0.01700	0.00340	0.15179	75.89286
BM15_90TiO210CuO_5010_1	2.0	26	1:38:32	0.007	0.006	0.016	0.0050	0.01700	0.00340	0.15179	75.89286
BM15_90TiO210CuO_5010_1	2.0	27	1:42:25	0.007	0.006	0.016	0.0050	0.01700	0.00340	0.15179	75.89286
BM15_90TiO210CuO_5010_1	2.0	28	1:46:25	0.007	0.006	0.016	0.0050	0.01700	0.00340	0.15179	75.89286
BM15_90TiO210CuO_5010_1	2.0	29	1:50:17	0.007	0.006	0.015	0.0050	0.01700	0.00340	0.15179	75.89286
BM15_90TiO210CuO_5010_1	2.0	30	1:54:11	0.007	0.005	0.018	0.0060	0.01900	0.00380	0.16964	84.82143
BM15_90TiO210CuO_5010_1	2.0	31	1:58:06	0.003	0.009	0.014	0.0020	0.00700	0.00140	0.06250	31.25000
BM15_90TiO210CuO_5010_1	2.0	32	2:02:02	0	0.011	0.016		0.00000	0.00000	0.00000	0.00000
BM15_90TiO210CuO_5010_1	2.0	33	2:05:56	0	0.01	0.016		0.00000	0.00000	0.00000	0.00000
BM15_90TiO210CuO_5010_1	2.0	34	2:09:48	0	0.011	0.015		0.00000	0.00000	0.00000	0.00000
BM15_90TiO210CuO_5010_1	2.0	35	2:13:42	0	0.011	0.016		0.00000	0.00000	0.00000	0.00000
BM15_90TiO210CuO_5010_1	2.0	36	2:17:42	0	0.012	0.019		0.00000	0.00000	0.00000	0.00000
BM15_90TiO210CuO_5010_1	2.0	37	2:21:38	0	0.011	0.016		0.00000	0.00000	0.00000	0.00000

				CHANNEL 1	CHANNEL 1	CHANNEL 1	CHANNEL 1	H2 + ½O2 → H2O	20 ml Ar/min	1 mol gas = 22,4 l	
units	mg	-	min	%	%	%	%	%	ml/min	µmol/min	µmol/min· g catalyst
SAMPLE	CATALYST	REP	Time	H2	O2	N2	O2 consumed	H2 total	H2	H2	H2
BM15_90TiO210CuO_5010_1	2.0	38	2:25:40	0	0.011	0.015		0.00000	0.00000	0.00000	0.00000
BM15_90TiO210CuO_5010_1	2.0	39	2:29:36	0	0.011	0.014		0.00000	0.00000	0.00000	0.00000
BM15_90TiO210CuO_5010_1	2.0	40	2:33:33	0	0.011	0.015		0.00000	0.00000	0.00000	0.00000
BM15_90TiO210CuO_5010_1	2.0	41	2:37:27	0	0.011	0.015		0.00000	0.00000	0.00000	0.00000
BM15_90TiO210CuO_5010_1	2.0	42	2:41:22	0	0.01	0.000 BDL		0.00000	0.00000	0.00000	0.00000
BM15_90TiO210CuO_5010_1	2.0	43	2:45:17	0	0.011	0.017		0.00000	0.00000	0.00000	0.00000
BM15_90TiO210CuO_5010_1	2.0	44	2:49:11	0	0.011	0.017		0.00000	0.00000	0.00000	0.00000
BM10_3_90TiO210ZnO_5010_1	2.1	1	0:00:00	0	0.042	0.068		0.00000	0.00000	0.00000	0.00000
BM10_3_90TiO210ZnO_5010_1	2.1	2	0:03:57	0	0.027	0.04		0.00000	0.00000	0.00000	0.00000
BM10_3_90TiO210ZnO_5010_1	2.1	3	0:07:51	0	0.019	0.028		0.00000	0.00000	0.00000	0.00000
BM10_3_90TiO210ZnO_5010_1	2.1	4	0:11:47	0	0.014	0.02		0.00000	0.00000	0.00000	0.00000
BM10_3_90TiO210ZnO_5010_1	2.1	5	0:15:39	0	0.013	0.014		0.00000	0.00000	0.00000	0.00000
BM10_3_90TiO210ZnO_5010_1	2.1	6	0:19:32	0	0.011	0.015		0.00000	0.00000	0.00000	0.00000
BM10_3_90TiO210ZnO_5010_1	2.1	7	0:23:31	0	0.01	0.016		0.00000	0.00000	0.00000	0.00000
BM10_3_90TiO210ZnO_5010_1	2.1	8	0:27:26	0	0.009	0.000 BDL		0.00000	0.00000	0.00000	0.00000
BM10_3_90TiO210ZnO_5010_1	2.1	9	0:31:17	0	0.01	0.000 BDL		0.00000	0.00000	0.00000	0.00000
BM10_3_90TiO210ZnO_5010_1	2.1	10	0:35:12	0	0.008	0.000 BDL		0.00000	0.00000	0.00000	0.00000
BM10_3_90TiO210ZnO_5010_1	2.1	11	0:39:08	0	0.009	0.000 BDL		0.00000	0.00000	0.00000	0.00000
BM10_3_90TiO210ZnO_5010_1	2.1	12	0:42:59	0	0.009	0.000 BDL		0.00000	0.00000	0.00000	0.00000
BM10_3_90TiO210ZnO_5010_1	2.1	13	0:46:53	0	0.008	0.000 BDL	0.0087	0.00000	0.00000	0.00000	0.00000
BM10_3_90TiO210ZnO_5010_1	2.1	14	0:50:47	0	0.007	0.012	0.0017	0.00333	0.00067	0.02976	14.17234
BM10_3_90TiO210ZnO_5010_1	2.1	15	0:54:42	0	0.008	0	0.0007	0.00133	0.00027	0.01190	5.66893
BM10_3_90TiO210ZnO_5010_1	2.1	16	0:58:37	0	0.008	0.000 BDL	0.0007	0.00133	0.00027	0.01190	5.66893

				CHANNEL 1	CHANNEL 1	CHANNEL 1	CHANNEL 1	H2 + ½O2 → H2O	20 ml Ar/min	1 mol gas = 22,4 l	
units	mg	-	min	%	%	%	%	%	ml/min	µmol/min	µmol/min· g catalyst
SAMPLE	CATALYST	REP	Time	H2	O2	N2	O2 consumed	H2 total	H2	H2	H2
BM10_3_90TiO210ZnO_5010_1	2.1	17	1:02:29	0	0.007	0.008	0.0017	0.00333	0.00067	0.02976	14.17234
BM10_3_90TiO210ZnO_5010_1	2.1	18	1:06:28	0	0.008	0.009	0.0007	0.00133	0.00027	0.01190	5.66893
BM10_3_90TiO210ZnO_5010_1	2.1	19	1:10:21	0	0.008	0	0.0007	0.00133	0.00027	0.01190	5.66893
BM10_3_90TiO210ZnO_5010_1	2.1	20	1:14:15	0	0.007	0.000 BDL	0.0017	0.00333	0.00067	0.02976	14.17234
BM10_3_90TiO210ZnO_5010_1	2.1	21	1:18:09	0	0.007	0.000 BDL	0.0017	0.00333	0.00067	0.02976	14.17234
BM10_3_90TiO210ZnO_5010_1	2.1	22	1:22:04	0	0.008	0.000 BDL	0.0007	0.00133	0.00027	0.01190	5.66893
BM10_3_90TiO210ZnO_5010_1	2.1	23	1:25:58	0	0.007	0.000 BDL	0.0017	0.00333	0.00067	0.02976	14.17234
BM10_3_90TiO210ZnO_5010_1	2.1	24	1:29:58	0	0.008	0.008	0.0007	0.00133	0.00027	0.01190	5.66893
BM10_3_90TiO210ZnO_5010_1	2.1	25	1:34:00	0	0.007	0.000 BDL	0.0017	0.00333	0.00067	0.02976	14.17234
BM10_3_90TiO210ZnO_5010_1	2.1	26	1:37:52	0	0.009	0.009	0.0000	0.00000	0.00000	0.00000	0.00000
BM10_3_90TiO210ZnO_5010_1	2.1	27	1:41:47	0	0.007	0	0.0017	0.00333	0.00067	0.02976	14.17234
BM10_3_90TiO210ZnO_5010_1	2.1	28	1:45:41	0	0.007	0.001	0.0017	0.00333	0.00067	0.02976	14.17234
BM10_3_90TiO210ZnO_5010_1	2.1	29	1:49:35	0	0.008	0.000 BDL	0.0007	0.00133	0.00027	0.01190	5.66893
BM10_3_90TiO210ZnO_5010_1	2.1	30	1:53:30	0	0.009	0.000 BDL	0.0000	0.00000	0.00000	0.00000	0.00000
BM10_3_90TiO210ZnO_5010_1	2.1	31	1:57:23	0	0.007	0.000 BDL	0.0017	0.00333	0.00067	0.02976	14.17234
BM10_3_90TiO210ZnO_5010_1	2.1	32	2:01:18	0	0.009	0.000 BDL	0.0000	0.00000	0.00000	0.00000	0.00000
BM10_3_90TiO210ZnO_5010_1	2.1	33	2:05:12	0	0.008	0.000 BDL	0.0007	0.00133	0.00027	0.01190	5.66893
BM10_3_90TiO210ZnO_5010_1	2.1	34	2:09:06	0	0.007	0.000 BDL	0.0017	0.00333	0.00067	0.02976	14.17234
BM10_3_90TiO210ZnO_5010_1	2.1	35	2:13:03	0	0.008	0.000 BDL	0.0007	0.00133	0.00027	0.01190	5.66893
BM10_3_90TiO210ZnO_5010_1	2.1	36	2:17:00	0	0.008	0.01		0.00000	0.00000	0.00000	0.00000
BM10_3_90TiO210ZnO_5010_1	2.1	37	2:20:56	0	0.008	0.000 BDL		0.00000	0.00000	0.00000	0.00000
BM10_3_90TiO210ZnO_5010_1	2.1	38	2:24:53	0	0.006	0.000 BDL		0.00000	0.00000	0.00000	0.00000
BM10_3_90TiO210ZnO_5010_1	2.1	39	2:28:45	0	0.008	0.000 BDL		0.00000	0.00000	0.00000	0.00000

				CHANNEL 1	CHANNEL 1	CHANNEL 1	CHANNEL 1	H2 + ½O2 → H2O	20 ml Ar/min	1 mol gas = 22,4 l	
units	mg	-	min	%	%	%	%	%	ml/min	µmol/min	µmol/min· g catalyst
SAMPLE	CATALYST	REP	Time	H2	O2	N2	O2 consumed	H2 total	H2	H2	H2
BM10_3_90TiO210ZnO_5010_1	2.1	40	2:32:40	0	0.007	0.000 BDL		0.00000	0.00000	0.00000	0.00000
BM10_3_90TiO210ZnO_5010_1	2.1	41	2:36:39	0	0.007	0.000 BDL		0.00000	0.00000	0.00000	0.00000
BM10_3_90TiO210ZnO_5010_1	2.1	42	2:40:34	0	0.007	0.001		0.00000	0.00000	0.00000	0.00000
BM10_3_90TiO210ZnO_5010_1	2.1	43	2:44:41	0	0.007	0.000 BDL		0.00000	0.00000	0.00000	0.00000
BM10_3_90TiO210ZnO_5010_1	2.1	44	2:48:46	0	0.008	0.008		0.00000	0.00000	0.00000	0.00000
BM15_90TiO210CdS_5010_1	2.5	1	0:00:00	0	0.03	0.056		0.00000	0.00000	0.00000	0.00000
BM15_90TiO210CdS_5010_1	2.5	2	0:03:58	0	0.019	0.031		0.00000	0.00000	0.00000	0.00000
BM15_90TiO210CdS_5010_1	2.5	3	0:07:52	0	0.014	0.022		0.00000	0.00000	0.00000	0.00000
BM15_90TiO210CdS_5010_1	2.5	4	0:11:48	0	0.012	0.018		0.00000	0.00000	0.00000	0.00000
BM15_90TiO210CdS_5010_1	2.5	5	0:15:48	0	0.011	0.015		0.00000	0.00000	0.00000	0.00000
BM15_90TiO210CdS_5010_1	2.5	6	0:19:44	0	0.01	0.013		0.00000	0.00000	0.00000	0.00000
BM15_90TiO210CdS_5010_1	2.5	7	0:23:39	0	0.009	0.000 BDL		0.00000	0.00000	0.00000	0.00000
BM15_90TiO210CdS_5010_1	2.5	8	0:27:35	0	0.009	0.000 BDL		0.00000	0.00000	0.00000	0.00000
BM15_90TiO210CdS_5010_1	2.5	9	0:31:32	0	0.009	0.000 BDL		0.00000	0.00000	0.00000	0.00000
BM15_90TiO210CdS_5010_1	2.5	10	0:35:24	0	0.009	0.000 BDL		0.00000	0.00000	0.00000	0.00000
BM15_90TiO210CdS_5010_1	2.5	11	0:39:19	0	0.009	0.000 BDL		0.00000	0.00000	0.00000	0.00000
BM15_90TiO210CdS_5010_1	2.5	12	0:43:16	0	0.009	0.000 BDL		0.00000	0.00000	0.00000	0.00000
BM15_90TiO210CdS_5010_1	2.5	13	0:47:13	0	0.009	0.000 BDL	0.0090	0.00000	0.00000	0.00000	0.00000
BM15_90TiO210CdS_5010_1	2.5	14	0:51:10	0	0.008	0.000 BDL	0.0010	0.00200	0.00040	0.01786	7.14286
BM15_90TiO210CdS_5010_1	2.5	15	0:55:11	0	0.007	0.008	0.0020	0.00400	0.00080	0.03571	14.28571
BM15_90TiO210CdS_5010_1	2.5	16	0:59:05	0	0.007	0.000 BDL	0.0020	0.00400	0.00080	0.03571	14.28571
BM15_90TiO210CdS_5010_1	2.5	17	1:03:00	0	0.006	0.000 BDL	0.0030	0.00600	0.00120	0.05357	21.42857
BM15_90TiO210CdS_5010_1	2.5	18	1:06:54	0	0.006	0.000 BDL	0.0030	0.00600	0.00120	0.05357	21.42857

				CHANNEL 1	CHANNEL 1	CHANNEL 1	CHANNEL 1	H2 + ½O2 → H2O	20 ml Ar/min	1 mol gas = 22,4 l	
units	mg	-	min	%	%	%	%	%	ml/min	µmol/min	µmol/min· g catalyst
SAMPLE	CATALYST	REP	Time	H2	O2	N2	O2 consumed	H2 total	H2	H2	H2
BM15_90TiO210CdS_5010_1	2.5	19	1:10:50	0	0.007	0.000 BDL	0.0020	0.00400	0.00080	0.03571	14.28571
BM15_90TiO210CdS_5010_1	2.5	20	1:14:44	0	0.007	0.000 BDL	0.0020	0.00400	0.00080	0.03571	14.28571
BM15_90TiO210CdS_5010_1	2.5	21	1:18:38	0	0.006	0.000 BDL	0.0030	0.00600	0.00120	0.05357	21.42857
BM15_90TiO210CdS_5010_1	2.5	22	1:22:34	0	0.006	0.000 BDL	0.0030	0.00600	0.00120	0.05357	21.42857
BM15_90TiO210CdS_5010_1	2.5	23	1:26:29	0	0.006	0.000 BDL	0.0030	0.00600	0.00120	0.05357	21.42857
BM15_90TiO210CdS_5010_1	2.5	24	1:30:30	0	0.006	0.000 BDL	0.0030	0.00600	0.00120	0.05357	21.42857
BM15_90TiO210CdS_5010_1	2.5	25	1:34:25	0	0.006	0.000 BDL	0.0030	0.00600	0.00120	0.05357	21.42857
BM15_90TiO210CdS_5010_1	2.5	26	1:38:20	0	0.006	0.000 BDL	0.0030	0.00600	0.00120	0.05357	21.42857
BM15_90TiO210CdS_5010_1	2.5	27	1:42:15	0	0.006	0	0.0030	0.00600	0.00120	0.05357	21.42857
BM15_90TiO210CdS_5010_1	2.5	28	1:46:12	0	0.006	0.000 BDL	0.0030	0.00600	0.00120	0.05357	21.42857
BM15_90TiO210CdS_5010_1	2.5	29	1:50:05	0	0.006	0.001	0.0030	0.00600	0.00120	0.05357	21.42857
BM15_90TiO210CdS_5010_1	2.5	30	1:54:00	0	0.006	0.000 BDL	0.0030	0.00600	0.00120	0.05357	21.42857
BM15_90TiO210CdS_5010_1	2.5	31	1:57:58	0	0.007	0.000 BDL	0.0020	0.00400	0.00080	0.03571	14.28571
BM15_90TiO210CdS_5010_1	2.5	32	2:01:50	0	0.008	0.002		0.00000	0.00000	0.00000	0.00000
BM15_90TiO210CdS_5010_1	2.5	33	2:05:45	0	0.008	0.006		0.00000	0.00000	0.00000	0.00000
BM15_90TiO210CdS_5010_1	2.5	34	2:09:41	0	0.008	0.000 BDL		0.00000	0.00000	0.00000	0.00000
BM15_90TiO210CdS_5010_1	2.5	35	2:13:39	0	0.007	0.000 BDL		0.00000	0.00000	0.00000	0.00000
BM15_90TiO210CdS_5010_1	2.5	36	2:17:33	0	0.009	0.000 BDL		0.00000	0.00000	0.00000	0.00000
BM15_90TiO210CdS_5010_1	2.5	37	2:21:28	0	0.007	0.000 BDL		0.00000	0.00000	0.00000	0.00000
BM15_90TiO210CdS_5010_1	2.5	38	2:25:21	0	0.008	0.000 BDL		0.00000	0.00000	0.00000	0.00000
BM15_90TiO210CdS_5010_1	2.5	39	2:33:17	0	0.007	0.000 BDL		0.00000	0.00000	0.00000	0.00000
BM15_90TiO210CdS_5010_1	2.5	40	2:37:14	0	0.008	0.000 BDL		0.00000	0.00000	0.00000	0.00000
BM15_90TiO210ZnS_5010_1	2.1	1	0:00:00	0	0.018	0.022		0.00000	0.00000	0.00000	0.00000

				CHANNEL 1	CHANNEL 1	CHANNEL 1	CHANNEL 1	H2 + ½O2 → H2O	20 ml Ar/min	1 mol gas = 22,4 l	
units	mg	-	min	%	%	%	%	%	ml/min	µmol/min	µmol/min· g catalyst
SAMPLE	CATALYST	REP	Time	H2	O2	N2	O2 consumed	H2 total	H2	H2	H2
BM15_90TiO210ZnS_5010_1	2.1	2	0:03:59	0	0.014	0.023		0.00000	0.00000	0.00000	0.00000
BM15_90TiO210ZnS_5010_1	2.1	3	0:07:53	0	0.013	0.02		0.00000	0.00000	0.00000	0.00000
BM15_90TiO210ZnS_5010_1	2.1	4	0:11:55	0	0.011	0.021		0.00000	0.00000	0.00000	0.00000
BM15_90TiO210ZnS_5010_1	2.1	5	0:15:49	0	0.01	0.016		0.00000	0.00000	0.00000	0.00000
BM15_90TiO210ZnS_5010_1	2.1	6	0:19:44	0	0.011	0.014		0.00000	0.00000	0.00000	0.00000
BM15_90TiO210ZnS_5010_1	2.1	7	0:23:49	0	0.01	0.016		0.00000	0.00000	0.00000	0.00000
BM15_90TiO210ZnS_5010_1	2.1	8	0:27:46	0	0.01	0.015		0.00000	0.00000	0.00000	0.00000
BM15_90TiO210ZnS_5010_1	2.1	9	0:31:40	0	0.01	0.012		0.00000	0.00000	0.00000	0.00000
BM15_90TiO210ZnS_5010_1	2.1	10	0:35:34	0	0.01	0.012		0.00000	0.00000	0.00000	0.00000
BM15_90TiO210ZnS_5010_1	2.1	11	0:39:28	0	0.01	0.014		0.00000	0.00000	0.00000	0.00000
BM15_90TiO210ZnS_5010_1	2.1	12	0:43:24	0	0.01	0.011		0.00000	0.00000	0.00000	0.00000
BM15_90TiO210ZnS_5010_1	2.1	13	0:47:20	0	0.009	0.013		0.00000	0.00000	0.00000	0.00000
BM15_90TiO210ZnS_5010_1	2.1	14	0:51:16	0	0.01	0.011		0.00000	0.00000	0.00000	0.00000
BM15_90TiO210ZnS_5010_1	2.1	15	0:55:20	0	0.01	0.000 BDL		0.00000	0.00000	0.00000	0.00000
BM15_90TiO210ZnS_5010_1	2.1	16	0:59:16	0	0.009	0.012		0.00000	0.00000	0.00000	0.00000
BM15_90TiO210ZnS_5010_1	2.1	17	1:03:12	0	0.01	0.012	0.0097	0.00000	0.00000	0.00000	0.00000
BM15_90TiO210ZnS_5010_1	2.1	18	1:07:10	0	0.009	0.013	0.0007	0.00133	0.00027	0.01190	5.66893
BM15_90TiO210ZnS_5010_1	2.1	19	1:11:05	0	0.008	0.011	0.0017	0.00333	0.00067	0.02976	14.17234
BM15_90TiO210ZnS_5010_1	2.1	20	1:14:58	0	0.008	0.013	0.0017	0.00333	0.00067	0.02976	14.17234
BM15_90TiO210ZnS_5010_1	2.1	21	1:18:53	0	0.007	0.012	0.0027	0.00533	0.00107	0.04762	22.67574
BM15_90TiO210ZnS_5010_1	2.1	22	1:22:50	0	0.008	0.012	0.0017	0.00333	0.00067	0.02976	14.17234
BM15_90TiO210ZnS_5010_1	2.1	23	1:26:44	0	0.007	0.012	0.0027	0.00533	0.00107	0.04762	22.67574
BM15_90TiO210ZnS_5010_1	2.1	24	1:30:41	0	0.007	0.012	0.0027	0.00533	0.00107	0.04762	22.67574

				CHANNEL 1	CHANNEL 1	CHANNEL 1	CHANNEL 1	H2 + ½O2 → H2O	20 ml Ar/min	1 mol gas = 22,4 l	
units	mg	-	min	%	%	%	%	%	ml/min	µmol/min	µmol/min· g catalyst
SAMPLE	CATALYST	REP	Time	H2	O2	N2	O2 consumed	H2 total	H2	H2	H2
BM15_90TiO210ZnS_5010_1	2.1	25	1:34:36	0	0.008	0.01	0.0017	0.00333	0.00067	0.02976	14.17234
BM15_90TiO210ZnS_5010_1	2.1	26	1:38:32	0	0.007	0.012	0.0027	0.00533	0.00107	0.04762	22.67574
BM15_90TiO210ZnS_5010_1	2.1	27	1:42:28	0	0.008	0.012	0.0017	0.00333	0.00067	0.02976	14.17234
BM15_90TiO210ZnS_5010_1	2.1	28	1:46:28	0	0.007	0.000 BDL	0.0027	0.00533	0.00107	0.04762	22.67574
BM15_90TiO210ZnS_5010_1	2.1	29	1:50:26	0	0.007	0.000 BDL	0.0027	0.00533	0.00107	0.04762	22.67574
BM15_90TiO210ZnS_5010_1	2.1	30	1:54:22	0	0.008	0.011	0.0017	0.00333	0.00067	0.02976	14.17234
BM15_90TiO210ZnS_5010_1	2.1	31	2:02:16	0	0.007	0.01	0.0027	0.00533	0.00107	0.04762	22.67574
BM15_90TiO210ZnS_5010_1	2.1	32	2:06:13	0	0.008	0.013	0.0017	0.00333	0.00067	0.02976	14.17234
BM15_90TiO210ZnS_5010_1	2.1	33	2:10:05	0	0.008	0.011	0.0017	0.00333	0.00067	0.02976	14.17234
BM15_90TiO210ZnS_5010_1	2.1	34	2:13:59	0	0.009	0.012	0.0007	0.00133	0.00027	0.01190	5.66893
BM15_90TiO210ZnS_5010_1	2.1	35	2:17:55	0	0.009	0.012		0.00000	0.00000	0.00000	0.00000
BM15_90TiO210ZnS_5010_1	2.1	36	2:21:48	0	0.009	0.011		0.00000	0.00000	0.00000	0.00000
BM15_90TiO210ZnS_5010_1	2.1	37	2:25:52	0	0.009	0.013		0.00000	0.00000	0.00000	0.00000
BM15_90TiO210ZnS_5010_1	2.1	38	2:29:50	0	0.009	0.012		0.00000	0.00000	0.00000	0.00000
BM15_90TiO210ZnS_5010_1	2.1	39	2:33:42	0	0.009	0.000 BDL		0.00000	0.00000	0.00000	0.00000
BM15_90TiO210ZnS_5010_1	2.1	40	2:37:38	0	0.009	0.012		0.00000	0.00000	0.00000	0.00000
BM15_90TiO210ZnS_5010_1	2.1	41	2:41:34	0	0.009	0.012		0.00000	0.00000	0.00000	0.00000
BM15_90TiO210ZnS_5010_1	2.1	42	2:45:26	0	0.009	0.012		0.00000	0.00000	0.00000	0.00000
BM15_90TiO210SnO2_5010_1	2.2	1	0:00:00	0	0.014	0.021		0.00000	0.00000	0.00000	0.00000
BM15_90TiO210SnO2_5010_1	2.2	2	0:03:55	0	0.012	0.017		0.00000	0.00000	0.00000	0.00000
BM15_90TiO210SnO2_5010_1	2.2	3	0:07:50	0	0.011	0.015		0.00000	0.00000	0.00000	0.00000
BM15_90TiO210SnO2_5010_1	2.2	4	0:11:45	0	0.01	0.015		0.00000	0.00000	0.00000	0.00000
BM15_90TiO210SnO2_5010_1	2.2	5	0:15:40	0	0.01	0.015		0.00000	0.00000	0.00000	0.00000

				CHANNEL 1	CHANNEL 1	CHANNEL 1	CHANNEL 1	H2 + ½O2 → H2O	20 ml Ar/min	1 mol gas = 22,4 l	
units	mg	-	min	%	%	%	%	%	ml/min	µmol/min	µmol/min· g catalyst
SAMPLE	CATALYST	REP	Time	H2	O2	N2	O2 consumed	H2 total	H2	H2	H2
BM15_90TiO210SnO2_5010_1	2.2	6	0:19:37	0	0.01	0.013		0.00000	0.00000	0.00000	0.00000
BM15_90TiO210SnO2_5010_1	2.2	7	0:23:32	0	0.009	0.014		0.00000	0.00000	0.00000	0.00000
BM15_90TiO210SnO2_5010_1	2.2	8	0:27:24	0	0.01	0.013		0.00000	0.00000	0.00000	0.00000
BM15_90TiO210SnO2_5010_1	2.2	9	0:31:20	0	0.01	0.014		0.00000	0.00000	0.00000	0.00000
BM15_90TiO210SnO2_5010_1	2.2	10	0:35:21	0	0.009	0.015		0.00000	0.00000	0.00000	0.00000
BM15_90TiO210SnO2_5010_1	2.2	11	0:39:16	0	0.009	0.013		0.00000	0.00000	0.00000	0.00000
BM15_90TiO210SnO2_5010_1	2.2	12	0:43:09	0	0.01	0.012		0.00000	0.00000	0.00000	0.00000
BM15_90TiO210SnO2_5010_1	2.2	13	0:47:06	0	0.009	0.012	0.0093	0.00000	0.00000	0.00000	0.00000
BM15_90TiO210SnO2_5010_1	2.2	14	0:51:03	0.001	0.008	0.013	0.0013	0.00367	0.00073	0.03274	14.88095
BM15_90TiO210SnO2_5010_1	2.2	15	0:54:58	0.003	0.005	0.013	0.0043	0.01167	0.00233	0.10417	47.34848
BM15_90TiO210SnO2_5010_1	2.2	16	0:58:53	0.003	0.004	0.013	0.0053	0.01367	0.00273	0.12202	55.46537
BM15_90TiO210SnO2_5010_1	2.2	17	1:02:48	0.003	0.004	0.014	0.0053	0.01367	0.00273	0.12202	55.46537
BM15_90TiO210SnO2_5010_1	2.2	18	1:06:49	0.003	0.005	0.013	0.0043	0.01167	0.00233	0.10417	47.34848
BM15_90TiO210SnO2_5010_1	2.2	19	1:10:44	0.003	0.005	0.015	0.0043	0.01167	0.00233	0.10417	47.34848
BM15_90TiO210SnO2_5010_1	2.2	20	1:14:40	0.003	0.005	0.013	0.0043	0.01167	0.00233	0.10417	47.34848
BM15_90TiO210SnO2_5010_1	2.2	21	1:18:38	0.003	0.005	0.013	0.0043	0.01167	0.00233	0.10417	47.34848
BM15_90TiO210SnO2_5010_1	2.2	22	1:22:32	0.003	0.004	0.012	0.0053	0.01367	0.00273	0.12202	55.46537
BM15_90TiO210SnO2_5010_1	2.2	23	1:26:29	0.003	0.004	0.015	0.0053	0.01367	0.00273	0.12202	55.46537
BM15_90TiO210SnO2_5010_1	2.2	24	1:30:23	0.003	0.004	0.013	0.0053	0.01367	0.00273	0.12202	55.46537
BM15_90TiO210SnO2_5010_1	2.2	25	1:34:16	0.003	0.005	0.013	0.0043	0.01167	0.00233	0.10417	47.34848
BM15_90TiO210SnO2_5010_1	2.2	26	1:38:11	0.003	0.005	0.011	0.0043	0.01167	0.00233	0.10417	47.34848
BM15_90TiO210SnO2_5010_1	2.2	27	1:42:06	0.003	0.005	0.013	0.0043	0.01167	0.00233	0.10417	47.34848
BM15_90TiO210SnO2_5010_1	2.2	28	1:46:01	0.003	0.005	0.015	0.0043	0.01167	0.00233	0.10417	47.34848

				CHANNEL 1	CHANNEL 1	CHANNEL 1	CHANNEL 1	H2 + ½O2 → H2O	20 ml Ar/min	1 mol gas = 22,4 l	
units	mg	-	min	%	%	%	%	%	ml/min	µmol/min	µmol/min· g catalyst
SAMPLE	CATALYST	REP	Time	H2	O2	N2	O2 consumed	H2 total	H2	H2	H2
BM15_90TiO210SnO2_5010_1	2.2	29	1:49:56	0.003	0.005	0.013	0.0043	0.01167	0.00233	0.10417	47.34848
BM15_90TiO210SnO2_5010_1	2.2	30	1:53:56	0.003	0.005	0.012	0.0043	0.01167	0.00233	0.10417	47.34848
BM15_90TiO210SnO2_5010_1	2.2	31	1:58:01	0.003	0.005	0.014	0.0043	0.01167	0.00233	0.10417	47.34848
BM15_90TiO210SnO2_5010_1	2.2	32	2:02:03	0.001	0.006	0.013		0.00000	0.00000	0.00000	0.00000
BM15_90TiO210SnO2_5010_1	2.2	33	2:06:04	0	0.009	0.014		0.00000	0.00000	0.00000	0.00000
BM15_90TiO210SnO2_5010_1	2.2	34	2:09:59	0	0.01	0.013		0.00000	0.00000	0.00000	0.00000
BM15_90TiO210SnO2_5010_1	2.2	35	2:13:55	0	0.01	0.013		0.00000	0.00000	0.00000	0.00000
BM15_90TiO210SnO2_5010_1	2.2	36	2:17:50	0	0.01	0.013		0.00000	0.00000	0.00000	0.00000
BM15_90TiO210SnO2_5010_1	2.2	37	2:21:45	0	0.009	0.012		0.00000	0.00000	0.00000	0.00000
BM15_90TiO210SnO2_5010_1	2.2	38	2:25:44	0	0.01	0.013		0.00000	0.00000	0.00000	0.00000
BM15_90TiO210SnO2_5010_1	2.2	39	2:29:41	0	0.009	0.011		0.00000	0.00000	0.00000	0.00000
BM15_90TiO210SnO2_5010_1	2.2	40	2:33:35	0	0.009	0.013		0.00000	0.00000	0.00000	0.00000
BM15_90TiO210SnO2_5010_1	2.2	41	2:37:29	0	0.009	0.011		0.00000	0.00000	0.00000	0.00000
BM10_3_90TiO210SnO2_5010_1	2.1	1	0:00:00	0	0.651	1.556		0.00000	0.00000	0.00000	0.00000
BM10_3_90TiO210SnO2_5010_1	2.1	2	0:03:59	0	0.26	0.59		0.00000	0.00000	0.00000	0.00000
BM10_3_90TiO210SnO2_5010_1	2.1	3	0:07:50	0	0.115	0.245		0.00000	0.00000	0.00000	0.00000
BM10_3_90TiO210SnO2_5010_1	2.1	4	0:11:44	0	0.058	0.111		0.00000	0.00000	0.00000	0.00000
BM10_3_90TiO210SnO2_5010_1	2.1	5	0:15:38	0	0.034	0.059		0.00000	0.00000	0.00000	0.00000
BM10_3_90TiO210SnO2_5010_1	2.1	6	0:19:33	0	0.023	0.037		0.00000	0.00000	0.00000	0.00000
BM10_3_90TiO210SnO2_5010_1	2.1	7	0:23:26	0	0.017	0.025		0.00000	0.00000	0.00000	0.00000
BM10_3_90TiO210SnO2_5010_1	2.1	8	0:27:20	0	0.015	0.02		0.00000	0.00000	0.00000	0.00000
BM10_3_90TiO210SnO2_5010_1	2.1	9	0:31:21	0	0.013	0.023		0.00000	0.00000	0.00000	0.00000
BM10_3_90TiO210SnO2_5010_1	2.1	10	0:35:15	0	0.012	0.017		0.00000	0.00000	0.00000	0.00000

				CHANNEL 1	CHANNEL 1	CHANNEL 1	CHANNEL 1	H2 + ½O2 → H2O	20 ml Ar/min	1 mol gas = 22,4 l	
units	mg	-	min	%	%	%	%	%	ml/min	µmol/min	µmol/min· g catalyst
SAMPLE	CATALYST	REP	Time	H2	O2	N2	O2 consumed	H2 total	H2	H2	H2
BM10_3_90TiO210SnO2_5010_1	2.1	11	0:39:10	0	0.011	0.015		0.00000	0.00000	0.00000	0.00000
BM10_3_90TiO210SnO2_5010_1	2.1	12	0:43:03	0	0.01	0.014		0.00000	0.00000	0.00000	0.00000
BM10_3_90TiO210SnO2_5010_1	2.1	13	0:46:57	0	0.011	0.015		0.00000	0.00000	0.00000	0.00000
BM10_3_90TiO210SnO2_5010_1	2.1	14	0:50:51	0	0.01	0.014		0.00000	0.00000	0.00000	0.00000
BM10_3_90TiO210SnO2_5010_1	2.1	15	0:54:45	0	0.01	0.013		0.00000	0.00000	0.00000	0.00000
BM10_3_90TiO210SnO2_5010_1	2.1	16	0:58:43	0	0.01	0.014		0.00000	0.00000	0.00000	0.00000
BM10_3_90TiO210SnO2_5010_1	2.1	17	1:02:36	0	0.01	0.014		0.00000	0.00000	0.00000	0.00000
BM10_3_90TiO210SnO2_5010_1	2.1	18	1:06:31	0	0.01	0.013		0.00000	0.00000	0.00000	0.00000
BM10_3_90TiO210SnO2_5010_1	2.1	19	1:10:27	0	0.01	0.014	0.0100	0.00000	0.00000	0.00000	0.00000
BM10_3_90TiO210SnO2_5010_1	2.1	20	1:14:18	0	0.01	0.013	0.0000	0.00000	0.00000	0.00000	0.00000
BM10_3_90TiO210SnO2_5010_1	2.1	21	1:18:13	0.002	0.008	0.019	0.0020	0.00600	0.00120	0.05357	25.51020
BM10_3_90TiO210SnO2_5010_1	2.1	22	1:22:08	0.002	0.008	0.014	0.0020	0.00600	0.00120	0.05357	25.51020
BM10_3_90TiO210SnO2_5010_1	2.1	23	1:26:04	0.001	0.008	0.015	0.0020	0.00500	0.00100	0.04464	21.25850
BM10_3_90TiO210SnO2_5010_1	2.1	24	1:30:01	0.001	0.008	0.014	0.0020	0.00500	0.00100	0.04464	21.25850
BM10_3_90TiO210SnO2_5010_1	2.1	25	1:33:55	0.001	0.008	0.015	0.0020	0.00500	0.00100	0.04464	21.25850
BM10_3_90TiO210SnO2_5010_1	2.1	26	1:37:49	0.001	0.008	0.015	0.0020	0.00500	0.00100	0.04464	21.25850
BM10_3_90TiO210SnO2_5010_1	2.1	27	1:41:45	0.001	0.008	0.013	0.0020	0.00500	0.00100	0.04464	21.25850
BM10_3_90TiO210SnO2_5010_1	2.1	28	1:45:37	0.001	0.008	0.015	0.0020	0.00500	0.00100	0.04464	21.25850
BM10_3_90TiO210SnO2_5010_1	2.1	29	1:49:37	0.001	0.008	0.013	0.0020	0.00500	0.00100	0.04464	21.25850
BM10_3_90TiO210SnO2_5010_1	2.1	30	1:53:37	0.001	0.008	0.014	0.0020	0.00500	0.00100	0.04464	21.25850
BM10_3_90TiO210SnO2_5010_1	2.1	31	1:57:36	0.001	0.008	0.013	0.0020	0.00500	0.00100	0.04464	21.25850
BM10_3_90TiO210SnO2_5010_1	2.1	32	2:01:30	0.001	0.008	0.013	0.0020	0.00500	0.00100	0.04464	21.25850
BM10_3_90TiO210SnO2_5010_1	2.1	33	2:05:28	0.002	0.008	0.014	0.0020	0.00600	0.00120	0.05357	25.51020

				CHANNEL 1	CHANNEL 1	CHANNEL 1	CHANNEL 1	H2 + ½O2 → H2O	20 ml Ar/min	1 mol gas = 22,4 l	
units	mg	-	min	%	%	%	%	%	ml/min	µmol/min	µmol/min· g catalyst
SAMPLE	CATALYST	REP	Time	H2	O2	N2	O2 consumed	H2 total	H2	H2	H2
BM10_3_90TiO210SnO2_5010_1	2.1	34	2:09:19	0.002	0.008	0.013	0.0020	0.00600	0.00120	0.05357	25.51020
BM10_3_90TiO210SnO2_5010_1	2.1	35	2:13:15	0.002	0.008	0.013	0.0020	0.00600	0.00120	0.05357	25.51020
BM10_3_90TiO210SnO2_5010_1	2.1	36	2:17:07	0.002	0.008	0.014	0.0020	0.00600	0.00120	0.05357	25.51020
BM10_3_90TiO210SnO2_5010_1	2.1	37	2:21:01	0.002	0.008	0.014	0.0020	0.00600	0.00120	0.05357	25.51020
BM10_3_90TiO210SnO2_5010_1	2.1	38	2:25:01	0.002	0.008	0.013	0.0020	0.00600	0.00120	0.05357	25.51020
BM10_3_90TiO210SnO2_5010_1	2.1	39	2:28:56	0.002	0.008	0.013	0.0020	0.00600	0.00120	0.05357	25.51020
BM10_3_90TiO210SnO2_5010_1	2.1	40	2:32:50	0.001		0.013	0.0000	0.00100	0.00020	0.00893	4.25170
BM10_3_90TiO210SnO2_5010_1	2.1	41	2:36:45	0	0.009	0.014		0.00000	0.00000	0.00000	0.00000
BM10_3_90TiO210SnO2_5010_1	2.1	42	2:40:39	0	0.01	0.013		0.00000	0.00000	0.00000	0.00000
BM10_3_90TiO210SnO2_5010_1	2.1	43	2:44:35	0	0.009	0.014		0.00000	0.00000	0.00000	0.00000
BM10_3_90TiO210SnO2_5010_1	2.1	44	2:48:27	0	0.009	0.012		0.00000	0.00000	0.00000	0.00000
BM10_3_90TiO210SnO2_5010_1	2.1	45	2:52:21	0	0.009	0.014		0.00000	0.00000	0.00000	0.00000
BM10_3_90TiO210SnO2_5010_1	2.1	46	2:56:21	0	0.009	0.014		0.00000	0.00000	0.00000	0.00000
BM10_3_90TiO210SnO2_5010_1	2.1	47	3:00:16	0	0.009	0.014		0.00000	0.00000	0.00000	0.00000
BM10_3_90TiO210SnO2_5010_1	2.1	48	3:04:23	0	0.009	0.013		0.00000	0.00000	0.00000	0.00000
BM10_3_90TiO210SnO2_5010_1	2.1	49	3:08:18	0	0.009	0.013		0.00000	0.00000	0.00000	0.00000
BM10_3_90TiO210SnO2_5010_1	2.1	50	3:12:14	0	0.009	0.012		0.00000	0.00000	0.00000	0.00000

Table 10. Data from Channel 1.

				CHANNEL 3	20 ml Ar/min	1 mol gas = 22.4 l	
units	mg	-	min	%	ml/min	μmol/min	μmol/min·g catalyst
SAMPLE	CATALYST	REP	Time	Acetaldehyde (CH3CHO)	Acetaldehyde (CH3CHO)	Acetaldehyde (CH3CHO)	Acetaldehyde (CH3CHO)
BM15_100TiO2_5010_1	2.1	1	0:00:00	0.0000 BDL	0.00000	0.00000	0.00000
BM15_100TiO2_5010_1	2.1	2	0:04:13	0.0000 BDL	0.00000	0.00000	0.00000
BM15_100TiO2_5010_1	2.1	3	0:08:04	0.0000 BDL	0.00000	0.00000	0.00000
BM15_100TiO2_5010_1	2.1	4	0:11:58	0.0000 BDL	0.00000	0.00000	0.00000
BM15_100TiO2_5010_1	2.1	5	0:15:56	0.0000 BDL	0.00000	0.00000	0.00000
BM15_100TiO2_5010_1	2.1	6	0:19:50	0.0000 BDL	0.00000	0.00000	0.00000
BM15_100TiO2_5010_1	2.1	7	0:23:44	0.0000 BDL	0.00000	0.00000	0.00000
BM15_100TiO2_5010_1	2.1	8	0:27:39	0.0000 BDL	0.00000	0.00000	0.00000
BM15_100TiO2_5010_1	2.1	9	0:31:30	0.0000 BDL	0.00000	0.00000	0.00000
BM15_100TiO2_5010_1	2.1	10	0:35:26	0.0000 BDL	0.00000	0.00000	0.00000
BM15_100TiO2_5010_1	2.1	11	0:39:20	0.0063	0.00126	0.05625	26.78571
BM15_100TiO2_5010_1	2.1	12	0:43:31	0.0089	0.00178	0.07946	37.84014
BM15_100TiO2_5010_1	2.1	13	0:47:25	0.0071	0.00142	0.06339	30.18707
BM15_100TiO2_5010_1	2.1	14	0:51:20	0.009	0.00180	0.08036	38.26531
BM15_100TiO2_5010_1	2.1	15	0:55:20	0.0089	0.00178	0.07946	37.84014
BM15_100TiO2_5010_1	2.1	16	0:59:19	0.009	0.00180	0.08036	38.26531
BM15_100TiO2_5010_1	2.1	17	1:03:11	0.0069	0.00138	0.06161	29.33673
BM15_100TiO2_5010_1	2.1	18	1:07:05	0.0069	0.00138	0.06161	29.33673
BM15_100TiO2_5010_1	2.1	19	1:10:59	0.009	0.00180	0.08036	38.26531
BM15_100TiO2_5010_1	2.1	20	1:14:56	0.0089	0.00178	0.07946	37.84014
BM15_100TiO2_5010_1	2.1	21	1:18:48	0.0089	0.00178	0.07946	37.84014
BM15_100TiO2_5010_1	2.1	22	1:22:43	0.009	0.00180	0.08036	38.26531
BM15_100TiO2_5010_1	2.1	23	1:26:38	0.0089	0.00178	0.07946	37.84014
BM15_100TiO2_5010_1	2.1	24	1:30:33	0.0071	0.00142	0.06339	30.18707
BM15_100TiO2_5010_1	2.1	25	1:34:33	0.0089	0.00178	0.07946	37.84014

				CHANNEL 3	20 ml Ar/min	1 mol gas = 22.4 l	
units	mg	-	min	%	ml/min	μmol/min	μmol/min·g catalyst
SAMPLE	CATALYST	REP	Time	Acetaldehyde (CH3CHO)	Acetaldehyde (CH3CHO)	Acetaldehyde (CH3CHO)	Acetaldehyde (CH3CHO)
BM15_100TiO2_5010_1	2.1	26	1:38:27	0.0089	0.00178	0.07946	37.84014
BM15_100TiO2_5010_1	2.1	27	1:42:22	0.0042	0.00084	0.03750	17.85714
BM15_100TiO2_5010_1	2.1	28	1:46:17	0.0000 BDL	0.00000	0.00000	0.00000
BM15_100TiO2_5010_1	2.1	29	1:50:12	0.0000 BDL	0.00000	0.00000	0.00000
BM15_100TiO2_5010_1	2.1	30	1:54:12	0.0000 BDL	0.00000	0.00000	0.00000
BM15_90TiO210ZnO_5010_1	2.2	1	0:00:00	0.0000 BDL	0.00000	0.00000	0.00000
BM15_90TiO210ZnO_5010_1	2.2	2	0:03:52	0.0000 BDL	0.00000	0.00000	0.00000
BM15_90TiO210ZnO_5010_1	2.2	3	0:07:45	0.0000 BDL	0.00000	0.00000	0.00000
BM15_90TiO210ZnO_5010_1	2.2	4	0:11:46	0.0000 BDL	0.00000	0.00000	0.00000
BM15_90TiO210ZnO_5010_1	2.2	5	0:15:38	0.0000 BDL	0.00000	0.00000	0.00000
BM15_90TiO210ZnO_5010_1	2.2	6	0:19:30	0.0000 BDL	0.00000	0.00000	0.00000
BM15_90TiO210ZnO_5010_1	2.2	7	0:23:24	0.0000 BDL	0.00000	0.00000	0.00000
BM15_90TiO210ZnO_5010_1	2.2	8	0:27:17	0.0000 BDL	0.00000	0.00000	0.00000
BM15_90TiO210ZnO_5010_1	2.2	9	0:31:11	0.0000 BDL	0.00000	0.00000	0.00000
BM15_90TiO210ZnO_5010_1	2.2	10	0:35:07	0.0000 BDL	0.00000	0.00000	0.00000
BM15_90TiO210ZnO_5010_1	2.2	11	0:39:06	0.0000 BDL	0.00000	0.00000	0.00000
BM15_90TiO210ZnO_5010_1	2.2	12	0:43:01	0.0000 BDL	0.00000	0.00000	0.00000
BM15_90TiO210ZnO_5010_1	2.2	13	0:47:00	0.0000 BDL	0.00000	0.00000	0.00000
BM15_90TiO210ZnO_5010_1	2.2	14	0:50:54	0.0000 BDL	0.00000	0.00000	0.00000
BM15_90TiO210ZnO_5010_1	2.2	15	0:54:51	0.0000 BDL	0.00000	0.00000	0.00000
BM15_90TiO210ZnO_5010_1	2.2	16	0:58:44	0.0000 BDL	0.00000	0.00000	0.00000
BM15_90TiO210ZnO_5010_1	2.2	17	1:02:38	0.0000 BDL	0.00000	0.00000	0.00000
BM15_90TiO210ZnO_5010_1	2.2	18	1:06:33	0.0000 BDL	0.00000	0.00000	0.00000
BM15_90TiO210ZnO_5010_2	2.2	1	0:00:00	0.0007	0.00014	0.00625	2.84091
BM15_90TiO210ZnO_5010_2	2.2	2	0:03:53	0.0007	0.00014	0.00625	2.84091

				CHANNEL 3	20 ml Ar/min	1 mol gas = 22.4 l	
units	mg	-	min	%	ml/min	μmol/min	μmol/min·g catalyst
SAMPLE	CATALYST	REP	Time	Acetaldehyde (CH ₃ CHO)	Acetaldehyde (CH ₃ CHO)	Acetaldehyde (CH ₃ CHO)	Acetaldehyde (CH ₃ CHO)
BM15_90TiO ₂ 10ZnO_5010_2	2.2	3	0:07:50	0.0015	0.00030	0.01339	6.08766
BM15_90TiO ₂ 10ZnO_5010_2	2.2	4	0:11:41	0.0015	0.00030	0.01339	6.08766
BM15_90TiO ₂ 10ZnO_5010_2	2.2	5	0:15:35	0.0007	0.00014	0.00625	2.84091
BM15_90TiO ₂ 10ZnO_5010_2	2.2	8	0:27:27	0.0007	0.00014	0.00625	2.84091
BM15_90TiO ₂ 10ZnO_5010_2	2.2	10	0:35:19	0.0007	0.00014	0.00625	2.84091
BM15_90TiO ₂ 10ZnO_5010_2	2.2	11	0:39:13	0.0006	0.00012	0.00536	2.43506
BM15_90TiO ₂ 10ZnO_5010_2	2.2	12	0:43:13	0.0015	0.00030	0.01339	6.08766
BM15_90TiO ₂ 10ZnO_5010_2	2.2	13	0:47:08	0.0006	0.00012	0.00536	2.43506
BM15_90TiO ₂ 10ZnO_5010_2	2.2	15	0:55:01	0.0015	0.00030	0.01339	6.08766
BM15_90TiO ₂ 10ZnO_5010_2	2.2	16	0:58:53	0.0012	0.00024	0.01071	4.87013
BM15_90TiO ₂ 10ZnO_5010_2	2.2	17	1:02:51	0.0011	0.00022	0.00982	4.46429
BM15_90TiO ₂ 10ZnO_5010_2	2.2	19	1:10:38	0.0014	0.00028	0.01250	5.68182
BM15_90TiO ₂ 10ZnO_5010_2	2.2	20	1:14:33	0.0014	0.00028	0.01250	5.68182
BM15_90TiO ₂ 10ZnO_5010_2	2.2	21	1:18:29	0.0015	0.00030	0.01339	6.08766
BM15_90TiO ₂ 10ZnO_5010_2	2.2	22	1:22:22	0.0014	0.00028	0.01250	5.68182
BM15_90TiO ₂ 10ZnO_5010_2	2.2	23	1:26:15	0.0014	0.00028	0.01250	5.68182
BM15_90TiO ₂ 10ZnO_5010_2	2.2	24	1:30:10	0.0015	0.00030	0.01339	6.08766
BM15_90TiO ₂ 10ZnO_5010_2	2.2	25	1:34:04	0.0015	0.00030	0.01339	6.08766
BM15_90TiO ₂ 10ZnO_5010_2	2.2	26	1:37:58	0.0014	0.00028	0.01250	5.68182
BM15_90TiO ₂ 10ZnO_5010_2	2.2	27	1:41:52	0.0011	0.00022	0.00982	4.46429
BM15_90TiO ₂ 10ZnO_5010_2	2.2	30	1:53:34	0.0006	0.00012	0.00536	2.43506
BM15_90TiO ₂ 10ZnO_5010_2	2.2	31	1:57:34	0.0006	0.00012	0.00536	2.43506
BM15_90TiO ₂ 10ZnO_5010_2	2.2	33	2:05:25	0.0006	0.00012	0.00536	2.43506
BM15_90TiO ₂ 10ZnO_5010_2	2.2	36	2:17:05	0.0006	0.00012	0.00536	2.43506
BM15_90TiO ₂ 10ZnO_5010_2	2.2	37	2:21:00	0.0006	0.00012	0.00536	2.43506

				CHANNEL 3	20 ml Ar/min	1 mol gas = 22.4 l	
units	mg	-	min	%	ml/min	μmol/min	μmol/min·g catalyst
SAMPLE	CATALYST	REP	Time	Acetaldehyde (CH3CHO)	Acetaldehyde (CH3CHO)	Acetaldehyde (CH3CHO)	Acetaldehyde (CH3CHO)
BM15_90TiO210ZnO_5010_2	2.2	38	2:24:55	0.0006	0.00012	0.00536	2.43506
BM15_90TiO210ZnO_5010_2	2.2	39	2:28:54	0.0006	0.00012	0.00536	2.43506
BM15_90TiO210CuO_5010_1	2.0	1	0:00:00	0.0014	0.00028	0.01250	6.25000
BM15_90TiO210CuO_5010_1	2.0	2	0:03:53	0.0005	0.00010	0.00446	2.23214
BM15_90TiO210CuO_5010_1	2.0	3	0:07:48	0.0013	0.00026	0.01161	5.80357
BM15_90TiO210CuO_5010_1	2.0	4	0:11:44	0.0005	0.00010	0.00446	2.23214
BM15_90TiO210CuO_5010_1	2.0	5	0:15:36	0.0013	0.00026	0.01161	5.80357
BM15_90TiO210CuO_5010_1	2.0	6	0:19:31	0.0013	0.00026	0.01161	5.80357
BM15_90TiO210CuO_5010_1	2.0	7	0:23:27	0.0013	0.00026	0.01161	5.80357
BM15_90TiO210CuO_5010_1	2.0	8	0:27:20	0.0013	0.00026	0.01161	5.80357
BM15_90TiO210CuO_5010_1	2.0	9	0:31:14	0.0005	0.00010	0.00446	2.23214
BM15_90TiO210CuO_5010_1	2.0	10	0:35:23	0.0012	0.00024	0.01071	5.35714
BM15_90TiO210CuO_5010_1	2.0	11	0:39:22	0.0005	0.00010	0.00446	2.23214
BM15_90TiO210CuO_5010_1	2.0	12	0:43:21	0.0004	0.00008	0.00357	1.78571
BM15_90TiO210CuO_5010_1	2.0	13	0:47:16	0.0013	0.00026	0.01161	5.80357
BM15_90TiO210CuO_5010_1	2.0	14	0:51:10	0.0004	0.00008	0.00357	1.78571
BM15_90TiO210CuO_5010_1	2.0	15	0:55:05	0.0005	0.00010	0.00446	2.23214
BM15_90TiO210CuO_5010_1	2.0	16	0:59:09	0.0041	0.00082	0.03661	18.30357
BM15_90TiO210CuO_5010_1	2.0	17	1:03:03	0.0138	0.00276	0.12321	61.60714
BM15_90TiO210CuO_5010_1	2.0	18	1:06:56	0.0151	0.00302	0.13482	67.41071
BM15_90TiO210CuO_5010_1	2.0	19	1:10:52	0.0132	0.00264	0.11786	58.92857
BM15_90TiO210CuO_5010_1	2.0	20	1:14:51	0.015	0.00300	0.13393	66.96429
BM15_90TiO210CuO_5010_1	2.0	21	1:19:03	0.0134	0.00268	0.11964	59.82143
BM15_90TiO210CuO_5010_1	2.0	22	1:22:56	0.0155	0.00310	0.13839	69.19643
BM15_90TiO210CuO_5010_1	2.0	23	1:26:50	0.0153	0.00306	0.13661	68.30357

				CHANNEL 3	20 ml Ar/min	1 mol gas = 22.4 l	
units	mg	-	min	%	ml/min	μmol/min	μmol/min·g catalyst
SAMPLE	CATALYST	REP	Time	Acetaldehyde (CH ₃ CHO)	Acetaldehyde (CH ₃ CHO)	Acetaldehyde (CH ₃ CHO)	Acetaldehyde (CH ₃ CHO)
BM15_90TiO ₂ 10CuO_5010_1	2.0	24	1:30:45	0.0136	0.00272	0.12143	60.71429
BM15_90TiO ₂ 10CuO_5010_1	2.0	25	1:34:38	0.0155	0.00310	0.13839	69.19643
BM15_90TiO ₂ 10CuO_5010_1	2.0	26	1:38:32	0.0136	0.00272	0.12143	60.71429
BM15_90TiO ₂ 10CuO_5010_1	2.0	27	1:42:25	0.0157	0.00314	0.14018	70.08929
BM15_90TiO ₂ 10CuO_5010_1	2.0	28	1:46:25	0.0139	0.00278	0.12411	62.05357
BM15_90TiO ₂ 10CuO_5010_1	2.0	29	1:50:17	0.0159	0.00318	0.14196	70.98214
BM15_90TiO ₂ 10CuO_5010_1	2.0	30	1:54:11	0.0139	0.00278	0.12411	62.05357
BM15_90TiO ₂ 10CuO_5010_1	2.0	31	1:58:06	0.0076	0.00152	0.06786	33.92857
BM15_90TiO ₂ 10CuO_5010_1	2.0	32	2:02:02	0.0016	0.00032	0.01429	7.14286
BM15_90TiO ₂ 10CuO_5010_1	2.0	33	2:05:56	0.0028	0.00056	0.02500	12.50000
BM15_90TiO ₂ 10CuO_5010_1	2.0	34	2:09:48	0.0027	0.00054	0.02411	12.05357
BM15_90TiO ₂ 10CuO_5010_1	2.0	35	2:13:42	0.0004	0.00008	0.00357	1.78571
BM15_90TiO ₂ 10CuO_5010_1	2.0	36	2:17:42	0.0004	0.00008	0.00357	1.78571
BM15_90TiO ₂ 10CuO_5010_1	2.0	37	2:21:38	0.0004	0.00008	0.00357	1.78571
BM15_90TiO ₂ 10CuO_5010_1	2.0	38	2:25:40	0.0004	0.00008	0.00357	1.78571
BM15_90TiO ₂ 10CuO_5010_1	2.0	39	2:29:36	0.0004	0.00008	0.00357	1.78571
BM15_90TiO ₂ 10CuO_5010_1	2.0	40	2:33:33	0.0000 BDL	0.00000	0.00000	0.00000
BM15_90TiO ₂ 10CuO_5010_1	2.0	41	2:37:27	0.0004	0.00008	0.00357	1.78571
BM15_90TiO ₂ 10CuO_5010_1	2.0	42	2:41:22	0.0004	0.00008	0.00357	1.78571
BM15_90TiO ₂ 10CuO_5010_1	2.0	43	2:45:17	0.0004	0.00008	0.00357	1.78571
BM15_90TiO ₂ 10CuO_5010_1	2.0	44	2:49:11	0.0004	0.00008	0.00357	1.78571
BM10_3_90TiO ₂ 10ZnO_5010_1	2.1	1	0:00:00	0.0000 BDL	0.00000	0.00000	0.00000
BM10_3_90TiO ₂ 10ZnO_5010_1	2.1	2	0:03:57	0.0000 BDL	0.00000	0.00000	0.00000
BM10_3_90TiO ₂ 10ZnO_5010_1	2.1	3	0:07:51	0.0000 BDL	0.00000	0.00000	0.00000
BM10_3_90TiO ₂ 10ZnO_5010_1	2.1	4	0:11:47	0.0000 BDL	0.00000	0.00000	0.00000

				CHANNEL 3	20 ml Ar/min	1 mol gas = 22.4 l	
units	mg	-	min	%	ml/min	μmol/min	μmol/min·g catalyst
SAMPLE	CATALYST	REP	Time	Acetaldehyde (CH3CHO)	Acetaldehyde (CH3CHO)	Acetaldehyde (CH3CHO)	Acetaldehyde (CH3CHO)
BM10_3_90TiO210ZnO_5010_1	2.1	5	0:15:39	0.0000 BDL	0.00000	0.00000	0.00000
BM10_3_90TiO210ZnO_5010_1	2.1	6	0:19:32	0.0000 BDL	0.00000	0.00000	0.00000
BM10_3_90TiO210ZnO_5010_1	2.1	7	0:23:31	0.0000 BDL	0.00000	0.00000	0.00000
BM10_3_90TiO210ZnO_5010_1	2.1	8	0:27:26	0.0000 BDL	0.00000	0.00000	0.00000
BM10_3_90TiO210ZnO_5010_1	2.1	9	0:31:17	0.0000 BDL	0.00000	0.00000	0.00000
BM10_3_90TiO210ZnO_5010_1	2.1	10	0:35:12	0.0000 BDL	0.00000	0.00000	0.00000
BM10_3_90TiO210ZnO_5010_1	2.1	11	0:39:08	0.0000 BDL	0.00000	0.00000	0.00000
BM10_3_90TiO210ZnO_5010_1	2.1	12	0:42:59	0.0000 BDL	0.00000	0.00000	0.00000
BM10_3_90TiO210ZnO_5010_1	2.1	13	0:46:53	0.0000 BDL	0.00000	0.00000	0.00000
BM10_3_90TiO210ZnO_5010_1	2.1	14	0:50:47	0.0023	0.00046	0.02054	9.77891
BM10_3_90TiO210ZnO_5010_1	2.1	15	0:54:42	0.004	0.00080	0.03571	17.00680
BM10_3_90TiO210ZnO_5010_1	2.1	16	0:58:37	0.002	0.00040	0.01786	8.50340
BM10_3_90TiO210ZnO_5010_1	2.1	17	1:02:29	0.0019	0.00038	0.01696	8.07823
BM10_3_90TiO210ZnO_5010_1	2.1	18	1:06:28	0.002	0.00040	0.01786	8.50340
BM10_3_90TiO210ZnO_5010_1	2.1	19	1:10:21		0.00000	0.00000	0.00000
BM10_3_90TiO210ZnO_5010_1	2.1	20	1:14:15		0.00000	0.00000	0.00000
BM10_3_90TiO210ZnO_5010_1	2.1	21	1:18:09		0.00000	0.00000	0.00000
BM10_3_90TiO210ZnO_5010_1	2.1	22	1:22:04		0.00000	0.00000	0.00000
BM10_3_90TiO210ZnO_5010_1	2.1	23	1:25:58		0.00000	0.00000	0.00000
BM10_3_90TiO210ZnO_5010_1	2.1	24	1:29:58		0.00000	0.00000	0.00000
BM10_3_90TiO210ZnO_5010_1	2.1	25	1:34:00		0.00000	0.00000	0.00000
BM10_3_90TiO210ZnO_5010_1	2.1	26	1:37:52		0.00000	0.00000	0.00000
BM10_3_90TiO210ZnO_5010_1	2.1	27	1:41:47		0.00000	0.00000	0.00000
BM10_3_90TiO210ZnO_5010_1	2.1	28	1:45:41		0.00000	0.00000	0.00000
BM10_3_90TiO210ZnO_5010_1	2.1	29	1:49:35		0.00000	0.00000	0.00000

				CHANNEL 3	20 ml Ar/min	1 mol gas = 22.4 l	
units	mg	-	min	%	ml/min	μmol/min	μmol/min·g catalyst
SAMPLE	CATALYST	REP	Time	Acetaldehyde (CH3CHO)	Acetaldehyde (CH3CHO)	Acetaldehyde (CH3CHO)	Acetaldehyde (CH3CHO)
BM10_3_90TiO210ZnO_5010_1	2.1	30	1:53:30		0.00000	0.00000	0.00000
BM10_3_90TiO210ZnO_5010_1	2.1	31	1:57:23		0.00000	0.00000	0.00000
BM10_3_90TiO210ZnO_5010_1	2.1	32	2:01:18		0.00000	0.00000	0.00000
BM10_3_90TiO210ZnO_5010_1	2.1	33	2:05:12		0.00000	0.00000	0.00000
BM10_3_90TiO210ZnO_5010_1	2.1	34	2:09:06	0.0018	0.00036	0.01607	7.65306
BM10_3_90TiO210ZnO_5010_1	2.1	35	2:13:03	0.0000 BDL	0.00000	0.00000	0.00000
BM10_3_90TiO210ZnO_5010_1	2.1	36	2:17:00	0.0000 BDL	0.00000	0.00000	0.00000
BM10_3_90TiO210ZnO_5010_1	2.1	37	2:20:56	0.0000 BDL	0.00000	0.00000	0.00000
BM10_3_90TiO210ZnO_5010_1	2.1	38	2:24:53	0.0000 BDL	0.00000	0.00000	0.00000
BM10_3_90TiO210ZnO_5010_1	2.1	39	2:28:45	0.0000 BDL	0.00000	0.00000	0.00000
BM10_3_90TiO210ZnO_5010_1	2.1	40	2:32:40	0.0000 BDL	0.00000	0.00000	0.00000
BM10_3_90TiO210ZnO_5010_1	2.1	41	2:36:39	0.0000 BDL	0.00000	0.00000	0.00000
BM10_3_90TiO210ZnO_5010_1	2.1	42	2:40:34	0.0000 BDL	0.00000	0.00000	0.00000
BM10_3_90TiO210ZnO_5010_1	2.1	43	2:44:41	0.0000 BDL	0.00000	0.00000	0.00000
BM10_3_90TiO210ZnO_5010_1	2.1	44	2:48:46	0.0000 BDL	0.00000	0.00000	0.00000
BM15_90TiO210CdS_5010_1	2.5	1	0:00:00	0.0000 BDL	0.00000	0.00000	0.00000
BM15_90TiO210CdS_5010_1	2.5	2	0:03:58	0.0000 BDL	0.00000	0.00000	0.00000
BM15_90TiO210CdS_5010_1	2.5	3	0:07:52	0.0000 BDL	0.00000	0.00000	0.00000
BM15_90TiO210CdS_5010_1	2.5	4	0:11:48	0.0000 BDL	0.00000	0.00000	0.00000
BM15_90TiO210CdS_5010_1	2.5	5	0:15:48	0.0000 BDL	0.00000	0.00000	0.00000
BM15_90TiO210CdS_5010_1	2.5	6	0:19:44	0.0000 BDL	0.00000	0.00000	0.00000
BM15_90TiO210CdS_5010_1	2.5	7	0:23:39	0.0000 BDL	0.00000	0.00000	0.00000
BM15_90TiO210CdS_5010_1	2.5	8	0:27:35	0.0000 BDL	0.00000	0.00000	0.00000
BM15_90TiO210CdS_5010_1	2.5	9	0:31:32	0.0000 BDL	0.00000	0.00000	0.00000
BM15_90TiO210CdS_5010_1	2.5	10	0:35:24	0.0000 BDL	0.00000	0.00000	0.00000

				CHANNEL 3	20 ml Ar/min	1 mol gas = 22.4 l	
units	mg	-	min	%	ml/min	μmol/min	μmol/min·g catalyst
SAMPLE	CATALYST	REP	Time	Acetaldehyde (CH ₃ CHO)	Acetaldehyde (CH ₃ CHO)	Acetaldehyde (CH ₃ CHO)	Acetaldehyde (CH ₃ CHO)
BM15_90TiO210CdS_5010_1	2.5	11	0:39:19	0.0000 BDL	0.00000	0.00000	0.00000
BM15_90TiO210CdS_5010_1	2.5	12	0:43:16	0.0000 BDL	0.00000	0.00000	0.00000
BM15_90TiO210CdS_5010_1	2.5	13	0:47:13	0.0000 BDL	0.00000	0.00000	0.00000
BM15_90TiO210CdS_5010_1	2.5	14	0:51:10	0.0053	0.00106	0.04732	18.92857
BM15_90TiO210CdS_5010_1	2.5	15	0:55:11	0.0065	0.00130	0.05804	23.21429
BM15_90TiO210CdS_5010_1	2.5	16	0:59:05	0.0043	0.00086	0.03839	15.35714
BM15_90TiO210CdS_5010_1	2.5	17	1:03:00	0.0062	0.00124	0.05536	22.14286
BM15_90TiO210CdS_5010_1	2.5	18	1:06:54	0.0042	0.00084	0.03750	15.00000
BM15_90TiO210CdS_5010_1	2.5	19	1:10:50	0.0062	0.00124	0.05536	22.14286
BM15_90TiO210CdS_5010_1	2.5	20	1:14:44	0.0044	0.00088	0.03929	15.71429
BM15_90TiO210CdS_5010_1	2.5	21	1:18:38	0.0044	0.00088	0.03929	15.71429
BM15_90TiO210CdS_5010_1	2.5	22	1:22:34	0.0043	0.00086	0.03839	15.35714
BM15_90TiO210CdS_5010_1	2.5	23	1:26:29	0.0044	0.00088	0.03929	15.71429
BM15_90TiO210CdS_5010_1	2.5	24	1:30:30	0.0042	0.00084	0.03750	15.00000
BM15_90TiO210CdS_5010_1	2.5	25	1:34:25	0.0063	0.00126	0.05625	22.50000
BM15_90TiO210CdS_5010_1	2.5	26	1:38:20	0.0045	0.00090	0.04018	16.07143
BM15_90TiO210CdS_5010_1	2.5	27	1:42:15	0.0063	0.00126	0.05625	22.50000
BM15_90TiO210CdS_5010_1	2.5	28	1:46:12	0.0065	0.00130	0.05804	23.21429
BM15_90TiO210CdS_5010_1	2.5	29	1:50:05	0.0044	0.00088	0.03929	15.71429
BM15_90TiO210CdS_5010_1	2.5	30	1:54:00	0.0043	0.00086	0.03839	15.35714
BM15_90TiO210CdS_5010_1	2.5	31	1:57:58	0.003	0.00060	0.02679	10.71429
BM15_90TiO210CdS_5010_1	2.5	32	2:01:50	0.0000 BDL	0.00000	0.00000	0.00000
BM15_90TiO210CdS_5010_1	2.5	33	2:05:45	0.0000 BDL	0.00000	0.00000	0.00000
BM15_90TiO210CdS_5010_1	2.5	34	2:09:41	0.0000 BDL	0.00000	0.00000	0.00000
BM15_90TiO210CdS_5010_1	2.5	35	2:13:39	0.0000 BDL	0.00000	0.00000	0.00000

				CHANNEL 3	20 ml Ar/min	1 mol gas = 22.4 l	
units	mg	-	min	%	ml/min	μmol/min	μmol/min·g catalyst
SAMPLE	CATALYST	REP	Time	Acetaldehyde (CH ₃ CHO)	Acetaldehyde (CH ₃ CHO)	Acetaldehyde (CH ₃ CHO)	Acetaldehyde (CH ₃ CHO)
BM15_90TiO210CdS_5010_1	2.5	36	2:17:33	0.0000 BDL	0.00000	0.00000	0.00000
BM15_90TiO210CdS_5010_1	2.5	37	2:21:28	0.0000 BDL	0.00000	0.00000	0.00000
BM15_90TiO210CdS_5010_1	2.5	38	2:25:21	0.0000 BDL	0.00000	0.00000	0.00000
BM15_90TiO210CdS_5010_1	2.5	39	2:33:17	0.0000 BDL	0.00000	0.00000	0.00000
BM15_90TiO210CdS_5010_1	2.5	40	2:37:14	0.0000 BDL	0.00000	0.00000	0.00000
BM15_90TiO210ZnS_5010_1	2.1	1	0:00:00	0.0000 BDL	0.00000	0.00000	0.00000
BM15_90TiO210ZnS_5010_1	2.1	2	0:03:59	0.0000 BDL	0.00000	0.00000	0.00000
BM15_90TiO210ZnS_5010_1	2.1	3	0:07:53	0.0000 BDL	0.00000	0.00000	0.00000
BM15_90TiO210ZnS_5010_1	2.1	4	0:11:55	0.0000 BDL	0.00000	0.00000	0.00000
BM15_90TiO210ZnS_5010_1	2.1	5	0:15:49	0.0000 BDL	0.00000	0.00000	0.00000
BM15_90TiO210ZnS_5010_1	2.1	6	0:19:44	0.0000 BDL	0.00000	0.00000	0.00000
BM15_90TiO210ZnS_5010_1	2.1	7	0:23:49	0.0000 BDL	0.00000	0.00000	0.00000
BM15_90TiO210ZnS_5010_1	2.1	8	0:27:46	0.0000 BDL	0.00000	0.00000	0.00000
BM15_90TiO210ZnS_5010_1	2.1	9	0:31:40	0.0000 BDL	0.00000	0.00000	0.00000
BM15_90TiO210ZnS_5010_1	2.1	10	0:35:34	0.0000 BDL	0.00000	0.00000	0.00000
BM15_90TiO210ZnS_5010_1	2.1	11	0:39:28	0.0000 BDL	0.00000	0.00000	0.00000
BM15_90TiO210ZnS_5010_1	2.1	12	0:43:24	0.0000 BDL	0.00000	0.00000	0.00000
BM15_90TiO210ZnS_5010_1	2.1	13	0:47:20	0.0000 BDL	0.00000	0.00000	0.00000
BM15_90TiO210ZnS_5010_1	2.1	14	0:51:16	0.0000 BDL	0.00000	0.00000	0.00000
BM15_90TiO210ZnS_5010_1	2.1	15	0:55:20	0.0000 BDL	0.00000	0.00000	0.00000
BM15_90TiO210ZnS_5010_1	2.1	16	0:59:16	0.0000 BDL	0.00000	0.00000	0.00000
BM15_90TiO210ZnS_5010_1	2.1	17	1:03:12	0.0000 BDL	0.00000	0.00000	0.00000
BM15_90TiO210ZnS_5010_1	2.1	18	1:07:10	0.0027	0.00054	0.02411	11.47959
BM15_90TiO210ZnS_5010_1	2.1	19	1:11:05	0.0057	0.00114	0.05089	24.23469
BM15_90TiO210ZnS_5010_1	2.1	20	1:14:58	0.0037	0.00074	0.03304	15.73129

				CHANNEL 3	20 ml Ar/min	1 mol gas = 22.4 l	
units	mg	-	min	%	ml/min	μmol/min	μmol/min·g catalyst
SAMPLE	CATALYST	REP	Time	Acetaldehyde (CH3CHO)	Acetaldehyde (CH3CHO)	Acetaldehyde (CH3CHO)	Acetaldehyde (CH3CHO)
BM15_90TiO210ZnS_5010_1	2.1	21	1:18:53	0.0058	0.00116	0.05179	24.65986
BM15_90TiO210ZnS_5010_1	2.1	22	1:22:50	0.0056	0.00112	0.05000	23.80952
BM15_90TiO210ZnS_5010_1	2.1	23	1:26:44	0.004	0.00080	0.03571	17.00680
BM15_90TiO210ZnS_5010_1	2.1	24	1:30:41	0.004	0.00080	0.03571	17.00680
BM15_90TiO210ZnS_5010_1	2.1	25	1:34:36	0.006	0.00120	0.05357	25.51020
BM15_90TiO210ZnS_5010_1	2.1	26	1:38:32	0.006	0.00120	0.05357	25.51020
BM15_90TiO210ZnS_5010_1	2.1	27	1:42:28	0.0059	0.00118	0.05268	25.08503
BM15_90TiO210ZnS_5010_1	2.1	28	1:46:28	0.0041	0.00082	0.03661	17.43197
BM15_90TiO210ZnS_5010_1	2.1	29	1:50:26	0.0041	0.00082	0.03661	17.43197
BM15_90TiO210ZnS_5010_1	2.1	30	1:54:22	0.0062	0.00124	0.05536	26.36054
BM15_90TiO210ZnS_5010_1	2.1	31	2:02:16	0.004	0.00080	0.03571	17.00680
BM15_90TiO210ZnS_5010_1	2.1	32	2:06:13	0.0061	0.00122	0.05446	25.93537
BM15_90TiO210ZnS_5010_1	2.1	33	2:10:05	0.0048	0.00096	0.04286	20.40816
BM15_90TiO210ZnS_5010_1	2.1	34	2:13:59	0.0000 BDL	0.00000	0.00000	0.00000
BM15_90TiO210ZnS_5010_1	2.1	35	2:17:55	0.0000 BDL	0.00000	0.00000	0.00000
BM15_90TiO210ZnS_5010_1	2.1	36	2:21:48	0.0000 BDL	0.00000	0.00000	0.00000
BM15_90TiO210ZnS_5010_1	2.1	37	2:25:52	0.0000 BDL	0.00000	0.00000	0.00000
BM15_90TiO210ZnS_5010_1	2.1	38	2:29:50	0.0000 BDL	0.00000	0.00000	0.00000
BM15_90TiO210ZnS_5010_1	2.1	39	2:33:42	0.0000 BDL	0.00000	0.00000	0.00000
BM15_90TiO210ZnS_5010_1	2.1	40	2:37:38	0.0000 BDL	0.00000	0.00000	0.00000
BM15_90TiO210ZnS_5010_1	2.1	41	2:41:34	0.0000 BDL	0.00000	0.00000	0.00000
BM15_90TiO210ZnS_5010_1	2.1	42	2:45:26	0.0000 BDL	0.00000	0.00000	0.00000
BM15_90TiO210SnO2_5010_1	2.2	1	0:00:00	0.0126	0.00252	0.11250	51.13636
BM15_90TiO210SnO2_5010_1	2.2	2	0:03:55	0.0022	0.00044	0.01964	8.92857
BM15_90TiO210SnO2_5010_1	2.2	3	0:07:50	0.0039	0.00078	0.03482	15.82792

				CHANNEL 3	20 ml Ar/min	1 mol gas = 22.4 l	
units	mg	-	min	%	ml/min	μmol/min	μmol/min·g catalyst
SAMPLE	CATALYST	REP	Time	Acetaldehyde (CH3CHO)	Acetaldehyde (CH3CHO)	Acetaldehyde (CH3CHO)	Acetaldehyde (CH3CHO)
BM15_90TiO210SnO2_5010_1	2.2	4	0:11:45	0.0019	0.00038	0.01696	7.71104
BM15_90TiO210SnO2_5010_1	2.2	5	0:15:40	0.002	0.00040	0.01786	8.11688
BM15_90TiO210SnO2_5010_1	2.2	6	0:19:37	0.0017	0.00034	0.01518	6.89935
BM15_90TiO210SnO2_5010_1	2.2	7	0:23:32	0.0017	0.00034	0.01518	6.89935
BM15_90TiO210SnO2_5010_1	2.2	8	0:27:24	0.0037	0.00074	0.03304	15.01623
BM15_90TiO210SnO2_5010_1	2.2	9	0:31:20	0.0019	0.00038	0.01696	7.71104
BM15_90TiO210SnO2_5010_1	2.2	10	0:35:21	0.0037	0.00074	0.03304	15.01623
BM15_90TiO210SnO2_5010_1	2.2	11	0:39:16	0.0000 BDL	0.00000	0.00000	0.00000
BM15_90TiO210SnO2_5010_1	2.2	12	0:43:09	0.0000 BDL	0.00000	0.00000	0.00000
BM15_90TiO210SnO2_5010_1	2.2	13	0:47:06	0.0000 BDL	0.00000	0.00000	0.00000
BM15_90TiO210SnO2_5010_1	2.2	14	0:51:03	0.0065	0.00130	0.05804	26.37987
BM15_90TiO210SnO2_5010_1	2.2	15	0:54:58	0.0117	0.00234	0.10446	47.48377
BM15_90TiO210SnO2_5010_1	2.2	16	0:58:53	0.0121	0.00242	0.10804	49.10714
BM15_90TiO210SnO2_5010_1	2.2	17	1:02:48	0.0119	0.00238	0.10625	48.29545
BM15_90TiO210SnO2_5010_1	2.2	18	1:06:49	0.0117	0.00234	0.10446	47.48377
BM15_90TiO210SnO2_5010_1	2.2	19	1:10:44	0.0118	0.00236	0.10536	47.88961
BM15_90TiO210SnO2_5010_1	2.2	20	1:14:40	0.0117	0.00234	0.10446	47.48377
BM15_90TiO210SnO2_5010_1	2.2	21	1:18:38	0.0118	0.00236	0.10536	47.88961
BM15_90TiO210SnO2_5010_1	2.2	22	1:22:32	0.0116	0.00232	0.10357	47.07792
BM15_90TiO210SnO2_5010_1	2.2	23	1:26:29	0.0117	0.00234	0.10446	47.48377
BM15_90TiO210SnO2_5010_1	2.2	24	1:30:23	0.0116	0.00232	0.10357	47.07792
BM15_90TiO210SnO2_5010_1	2.2	25	1:34:16	0.0114	0.00228	0.10179	46.26623
BM15_90TiO210SnO2_5010_1	2.2	26	1:38:11	0.0116	0.00232	0.10357	47.07792
BM15_90TiO210SnO2_5010_1	2.2	27	1:42:06	0.0115	0.00230	0.10268	46.67208
BM15_90TiO210SnO2_5010_1	2.2	28	1:46:01	0.0113	0.00226	0.10089	45.86039

				CHANNEL 3	20 ml Ar/min	1 mol gas = 22.4 l	
units	mg	-	min	%	ml/min	μmol/min	μmol/min·g catalyst
SAMPLE	CATALYST	REP	Time	Acetaldehyde (CH3CHO)	Acetaldehyde (CH3CHO)	Acetaldehyde (CH3CHO)	Acetaldehyde (CH3CHO)
BM15_90TiO210SnO2_5010_1	2.2	29	1:49:56	0.0133	0.00266	0.11875	53.97727
BM15_90TiO210SnO2_5010_1	2.2	30	1:53:56	0.0137	0.00274	0.12232	55.60065
BM15_90TiO210SnO2_5010_1	2.2	31	1:58:01	0.0137	0.00274	0.12232	55.60065
BM15_90TiO210SnO2_5010_1	2.2	32	2:02:03	0.0041	0.00082	0.03661	16.63961
BM15_90TiO210SnO2_5010_1	2.2	33	2:06:04	0.002	0.00040	0.01786	8.11688
BM15_90TiO210SnO2_5010_1	2.2	34	2:09:59	0.0036	0.00072	0.03214	14.61039
BM15_90TiO210SnO2_5010_1	2.2	35	2:13:55	0.004	0.00080	0.03571	16.23377
BM15_90TiO210SnO2_5010_1	2.2	36	2:17:50	0.0000 BDL	0.00000	0.00000	0.00000
BM15_90TiO210SnO2_5010_1	2.2	37	2:21:45	0.0000 BDL	0.00000	0.00000	0.00000
BM15_90TiO210SnO2_5010_1	2.2	38	2:25:44	0.0000 BDL	0.00000	0.00000	0.00000
BM15_90TiO210SnO2_5010_1	2.2	39	2:29:41	0.0000 BDL	0.00000	0.00000	0.00000
BM15_90TiO210SnO2_5010_1	2.2	40	2:33:35	0.0000 BDL	0.00000	0.00000	0.00000
BM15_90TiO210SnO2_5010_1	2.2	41	2:37:29	0.0000 BDL	0.00000	0.00000	0.00000
BM10_3_90TiO210SnO2_5010_1	2.1	1	0:00:00	0.0137	0.00274	0.12232	58.24830
BM10_3_90TiO210SnO2_5010_1	2.1	2	0:03:59	0.0049	0.00098	0.04375	20.83333
BM10_3_90TiO210SnO2_5010_1	2.1	3	0:07:50	0.0026	0.00052	0.02321	11.05442
BM10_3_90TiO210SnO2_5010_1	2.1	4	0:11:44	0.0041	0.00082	0.03661	17.43197
BM10_3_90TiO210SnO2_5010_1	2.1	5	0:15:38	0.0024	0.00048	0.02143	10.20408
BM10_3_90TiO210SnO2_5010_1	2.1	6	0:19:33	0.0023	0.00046	0.02054	9.77891
BM10_3_90TiO210SnO2_5010_1	2.1	7	0:23:26	0.0021	0.00042	0.01875	8.92857
BM10_3_90TiO210SnO2_5010_1	2.1	8	0:27:20	0.004	0.00080	0.03571	17.00680
BM10_3_90TiO210SnO2_5010_1	2.1	9	0:31:21	0.004	0.00080	0.03571	17.00680
BM10_3_90TiO210SnO2_5010_1	2.1	10	0:35:15	0.0019	0.00038	0.01696	8.07823
BM10_3_90TiO210SnO2_5010_1	2.1	11	0:39:10	0.0039	0.00078	0.03482	16.58163
BM10_3_90TiO210SnO2_5010_1	2.1	12	0:43:03	0.004	0.00080	0.03571	17.00680

				CHANNEL 3	20 ml Ar/min	1 mol gas = 22.4 l	
units	mg	-	min	%	ml/min	μmol/min	μmol/min·g catalyst
SAMPLE	CATALYST	REP	Time	Acetaldehyde (CH ₃ CHO)	Acetaldehyde (CH ₃ CHO)	Acetaldehyde (CH ₃ CHO)	Acetaldehyde (CH ₃ CHO)
BM10_3_90TiO210SnO2_5010_1	2.1	13	0:46:57	0.0039	0.00078	0.03482	16.58163
BM10_3_90TiO210SnO2_5010_1	2.1	14	0:50:51	0.0018	0.00036	0.01607	7.65306
BM10_3_90TiO210SnO2_5010_1	2.1	15	0:54:45	0.0038	0.00076	0.03393	16.15646
BM10_3_90TiO210SnO2_5010_1	2.1	16	0:58:43	0.0037	0.00074	0.03304	15.73129
BM10_3_90TiO210SnO2_5010_1	2.1	17	1:02:36	0.0038	0.00076	0.03393	16.15646
BM10_3_90TiO210SnO2_5010_1	2.1	18	1:06:31	0.0039	0.00078	0.03482	16.58163
BM10_3_90TiO210SnO2_5010_1	2.1	19	1:10:27	0.0000 BDL	0.00000	0.00000	0.00000
BM10_3_90TiO210SnO2_5010_1	2.1	20	1:14:18	0.0054	0.00108	0.04821	22.95918
BM10_3_90TiO210SnO2_5010_1	2.1	21	1:18:13	0.0076	0.00152	0.06786	32.31293
BM10_3_90TiO210SnO2_5010_1	2.1	22	1:22:08	0.0057	0.00114	0.05089	24.23469
BM10_3_90TiO210SnO2_5010_1	2.1	23	1:26:04	0.0053	0.00106	0.04732	22.53401
BM10_3_90TiO210SnO2_5010_1	2.1	24	1:30:01	0.0073	0.00146	0.06518	31.03741
BM10_3_90TiO210SnO2_5010_1	2.1	25	1:33:55	0.0075	0.00150	0.06696	31.88776
BM10_3_90TiO210SnO2_5010_1	2.1	26	1:37:49	0.0074	0.00148	0.06607	31.46259
BM10_3_90TiO210SnO2_5010_1	2.1	27	1:41:45	0.0073	0.00146	0.06518	31.03741
BM10_3_90TiO210SnO2_5010_1	2.1	28	1:45:37	0.0052	0.00104	0.04643	22.10884
BM10_3_90TiO210SnO2_5010_1	2.1	29	1:49:37	0.0053	0.00106	0.04732	22.53401
BM10_3_90TiO210SnO2_5010_1	2.1	30	1:53:37	0.0072	0.00144	0.06429	30.61224
BM10_3_90TiO210SnO2_5010_1	2.1	31	1:57:36	0.0078	0.00156	0.06964	33.16327
BM10_3_90TiO210SnO2_5010_1	2.1	32	2:01:30	0.0053	0.00106	0.04732	22.53401
BM10_3_90TiO210SnO2_5010_1	2.1	33	2:05:28	0.0072	0.00144	0.06429	30.61224
BM10_3_90TiO210SnO2_5010_1	2.1	34	2:09:19	0.0052	0.00104	0.04643	22.10884
BM10_3_90TiO210SnO2_5010_1	2.1	35	2:13:15	0.0052	0.00104	0.04643	22.10884
BM10_3_90TiO210SnO2_5010_1	2.1	36	2:17:07	0.0072	0.00144	0.06429	30.61224
BM10_3_90TiO210SnO2_5010_1	2.1	37	2:21:01	0.0073	0.00146	0.06518	31.03741

				CHANNEL 3	20 ml Ar/min	1 mol gas = 22.4 l	
units	mg	-	min	%	ml/min	μmol/min	μmol/min·g catalyst
SAMPLE	CATALYST	REP	Time	Acetaldehyde (CH3CHO)	Acetaldehyde (CH3CHO)	Acetaldehyde (CH3CHO)	Acetaldehyde (CH3CHO)
BM10_3_90TiO210SnO2_5010_1	2.1	38	2:25:01	0.0074	0.00148	0.06607	31.46259
BM10_3_90TiO210SnO2_5010_1	2.1	39	2:28:56	0.0072	0.00144	0.06429	30.61224
BM10_3_90TiO210SnO2_5010_1	2.1	40	2:32:50	0.0039	0.00078	0.03482	16.58163
BM10_3_90TiO210SnO2_5010_1	2.1	41	2:36:45	0.0018	0.00036	0.01607	7.65306
BM10_3_90TiO210SnO2_5010_1	2.1	42	2:40:39	0.0017	0.00034	0.01518	7.22789
BM10_3_90TiO210SnO2_5010_1	2.1	43	2:44:35	0.0000 BDL	0.00000	0.00000	0.00000
BM10_3_90TiO210SnO2_5010_1	2.1	44	2:48:27	0.0000 BDL	0.00000	0.00000	0.00000
BM10_3_90TiO210SnO2_5010_1	2.1	45	2:52:21	0.0000 BDL	0.00000	0.00000	0.00000
BM10_3_90TiO210SnO2_5010_1	2.1	46	2:56:21	0.0000 BDL	0.00000	0.00000	0.00000
BM10_3_90TiO210SnO2_5010_1	2.1	47	3:00:16	0.0000 BDL	0.00000	0.00000	0.00000
BM10_3_90TiO210SnO2_5010_1	2.1	48	3:04:23	0.0000 BDL	0.00000	0.00000	0.00000
BM10_3_90TiO210SnO2_5010_1	2.1	49	3:08:18	0.0000 BDL	0.00000	0.00000	0.00000
BM10_3_90TiO210SnO2_5010_1	2.1	50	3:12:14	0.0000 BDL	0.00000	0.00000	0.00000

Table 11. Data from Channel 3.

B Datasheets

B1. FRITSCH Ball Mills - Mini-Mill PULVERISETTE 23 [44]



B2. Agilent 490 Micro Gas Chromatograph [43]



Ball Mills



IDEAL FOR

- CHEMICAL ANALYSIS
- ENVIRONMENTAL RESEARCH
- PHARMACEUTICALS AND MEDICINE
- BIOTECHNOLOGY
- FORENSIC ANALYSIS
- MATERIAL TECHNOLOGY
- ROHS

BALL MILLS

FINE COMMINUTION IN THE LAB

FRITSCH BALL MILLS: THE MOST EFFECTIVE MILLS FOR SMALL AND VERY SMALL QUANTITIES

- For fast batchwise grinding of medium-hard to hard samples
- For achieving the finest particle sizes
- Dry or wet grinding
- For mixing
- For homogenisation



FRITSCH is an internationally respected manufacturer

of application-oriented laboratory instruments. For more

than 80 years, laboratories worldwide have relied on our

FRITSCH. ONE STEP AHEAD.

experience, quality, service and innovation - for fast industrial



applications as well as for especially accurate results in

industry- and research laboratories. See for yourself.

FRITSCH Ball Mills

are the most effective laboratory mills for rapid batchwise comminution of medium-hard to hard samples down to the finest particle size. The grinding can take place dry

or wet. Grinding sets of many different materials are available. **FRITSCH Ball Mills** are also the ideal and reliable lab assistants for mixing and homogenising.

Mini-Mill PULVERISETTE 23	Vibratory Micro Mill PULVERISETTE 0
The smallest instrument for small quantities	Fine comminution and sieving in one unit
	

Operating principle	Impact force	Impact force
Optimal for material type	Medium-hard, brittle, moist	Medium-hard, brittle, temperature-sensitive, moist
Grinding bowl sizes	5, 10, 15 ml	–
Grinding ball diameter	0.1 – 15 mm	50 – 70 mm
Max. feed size (depending on the material)	6 mm	5 mm
Min. sample quantity	0.01 ml	1 ml
Max. sample quantity	5 ml	10 ml
Final fineness (depending on the material)	5 µm	10 µm
Typical grinding time (depending on the material)	2 min	10 min
Cryogenic grinding	Liquid nitrogen can be used for pre-cooling in the PTFE bowl	Yes
Grinding process	Dry/wet	Dry/wet
Grinding bowl oscillations per minute	900 – 3000 at 9 mm amplitude	3000 – 3600 at 1 – 3 mm amplitude
Electrical details	100-240 V/1~, 50-60 Hz, 90 watt	100-240 V/1~, 50-60 Hz, 50 watt
Weight	Net: 7 kg, gross: 8 kg	Net: 21 kg, gross: 22 kg
Dimensions w x d x h	Bench top instrument: 20 x 30 x 30 cm	Bench top instrument: 37 x 40 x 20 cm
Packing details	Cardboard box: 37 x 25 x 34 cm	Cardboard box: 50 x 43 x 30 cm

Grinding in a Ball Mill takes place through impact and friction of the sample between the grinding balls and the inside wall of the grinding bowl respectively the mortar.

For this, the grinding bowl or mortar performs vertically oscillating movements of high amplitude and high frequency, which are transferred to the grinding vessel.



PULVERISETTE 23

THE ULTRA-EFFECTIVE FRITSCH MINI-MILL

- For smallest sample quantities up to 5 ml
- Max. feed size 6 mm, final fineness 5 µm
- Dry, wet and cryogenic grinding in a single unit
- Extremely compelling in price and in performance
- Extremely effective grinding due to spherical grinding bowl with plug-style closure and practical quick clamping system
- Precisely adjustable configurable and reproducible grinding time
- Very simple operation, cleaning and maintenance



PTFE bowl for use in biotechnology

The ultra-compact FRITSCH Mini-Mill is the ideal assistant for fine comminution of smallest quantities – for wet grinding as well as for dry or cryogenic grinding. Its special, spherical grinding bowl ensures much better performance in grinding, mixing and homogenising compared with similar models. With a footprint of just 20 x 30 cm and a weight of 7 kg, it easily fits anywhere. It's smart, is extremely user-friendly, inexpensive, and convinces with impressive results: small, fast, effective.

PTFE bowl

The 5 ml PTFE bowl is specially suited for using the FRITSCH PULVERISETTE 23 in biotechnology applications. For example, it is possible to break up fungus or yeast cells, deep frozen tissue and cells in only a few minutes with this special plastic bowl and a 10 mm steel ball. It is also possible to pre-cool the entire bowl in liquid nitrogen.

UNMATCHED EFFECTIVENESS WITH SPHERICAL GRINDING BOWLS

Available only from FRITSCH: In special consideration of the ball mill grinding concept, we developed for the PULVERISETTE 23 a grinding bowl with interior walls that are spherical instead of cylindrical. Your advantage: Unmatched grinding performance with a significantly improved grinding effect, much easier recovery and simpler cleaning.

Typical FRITSCH!

Especially practical: The spherical grinding bowls of the PULVERISETTE 23 are assembled simply and quickly, just twist and turn!

METAL-FREE GRINDING

With grinding bowls made of zirconium oxide, you can ensure that your samples remain absolutely metal-free.

TECHNICAL DATA

Electrical details

100-240 V/1~, 50-60 Hz, 90 watt

Weight

Net 7 kg

Gross 8 kg

Dimensions w x d x h

Bench top instrument 20 x 30 x 30 cm

Packaging w x d x h

Cardboard box 37 x 25 x 34 cm

Emissions value of workplace according to DIN EN ISO 3746:2005

Approx. 75 dB(A)

(depending on the material to be ground and grinding bowl/balls used)

Order no.

23.1000.00



Practical and effective: Spherical grinding bowls for easy assembly



Operating panel with integrated, easy-to-clean glass keyboard

IDEAL FOR

Chemical analysis

Comminution and homogenisation of grinding samples for creation of compacts for x-ray fluorescence and infrared spectroscopy (e.g. potassium bromide tablets)

Environmental research

Soils in contaminant analysis, humic acid determination, botanical materials in residue analysis of fertilisers and pesticides, pulping of seeds

Pharmaceuticals and medicine

Kidney and gallstone analysis, breaking up tablets, pharmaceutical ingredients

Forensic analysis

Hair analysis for genetic testing and drug tests, preparation of extremely small particles for chemical analysis, textile fibre and bone analysis

Biotechnology

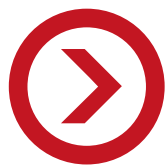
Comminution of deep frozen tissue samples

Material synthesis

Creating mixtures for catalytic tests on polymers, ceramic analysis

FACTS AND ADVANTAGES

- Fast, reproducible comminution
- Small grinding bowl volumes
- Low contact surface area with grinding elements
- Accessories: Grinding bowls and grinding balls in 4 different materials (ordered separately)
- Grinding bowl oscillations: 900 - 3,000 oscillations/min at 9 mm amplitude
- Regulated oscillation frequency (15 - 50 Hz)
- CE mark
- 2-year guarantee



PULVERISETTE 0

THE FRITSCH VIBRATORY BALL MILL

- Max. feed size 5 mm
- Max. sample quantity 10 ml
- Final fineness 10 µm
- Effective comminution in a narrow, homogeneous particle size range
- Loss-free grinding in a closed vessel – dry or in suspension
- Cryogenic grinding and simple embrittling in the cryo-box
- Modular system for simple conversion to dry or wet sieving
- Adjustable oscillation amplitude for easy adaption of the vibration energy to the grinding sample



FRITSCH cryo-box for fast, simple embrittlement

The **FRITSCH PULVERISETTE 0** is the ideal laboratory mill for fine comminution of medium-hard, brittle, moist or temperature-sensitive samples – dry or in suspension – as well as for homogenising of emulsions and pastes.

IMPACT AND FRICTION

The FRITSCH Vibratory Micro Mill PULVERISETTE 0 grinds your sample through impact and friction by which the mortar vibrates electromagnetically and the grinding material transfers the vibrations to the grinding ball.

At the beginning of the grinding, the comminution of the coarse particles is achieved by the impact effect of the grinding ball. Next, the fine particles are comminuted through friction by the tumbling motion of the grinding ball as the vibrations subside. The impact energy of the grinding ball is freely adjustable thus, allowing it to be precisely adapted to the sample being ground.

CRYOGENIC GRINDING

For fast embrittlement of soft, slightly oily, fatty or moist materials for cryogenic grinding, we offer the **FRITSCH cryo-box**: Simply insert the filled grinding set into the cryo-box and fill it with liquid nitrogen with this method even extremely difficult-to-grind samples can be ground down to analysis fineness. And the thick insulation ensures a particularly efficient use of coolant.

GRINDING AND SIEVING IN ONE UNIT

For dry and wet sieving, the FRITSCH PULVERISETTE 0 can be converted to a Vibratory Sieve Shaker for quantitative particle size analysis of solids (measuring range 32 µm – 63 µm) and suspensions (measuring range 20 µm – 10 mm) by simply inserting corresponding sieves. All related information can be found at www.fritsch.de/sieveshakers.

ROHS

The FRITSCH Vibratory Micro Mill PULVERISETTE 0 is recommended for sample preparation of RoHS tests (Restriction of Hazardous Substances).

TECHNICAL DATA

Electrical details

100-240 V/1~, 50-60 Hz, 50 watt

Weight

Net 21 kg

Gross 22 kg

Dimensions w x d x h

Bench top instrument 37 x 40 x 20 cm

Packaging w x d x h

Cardboard box 50 x 43 x 30 cm

Emissions value of workplace according to

DIN EN ISO 3746:2005

Approx. 68 dB(A), with sound absorption hood approx. 53 dB(A)
(depending on the material to be ground and mortar/grinding balls used)

Order no.

00.6020.00



Grinding and sieving in one unit: the PULVERISETTE 0 as ANALYSETTE 3 SPARTAN



Teeth before and after grinding with the FRITSCH PULVERISETTE 0

IDEAL FOR

Chemical analysis	Electron microscopy
Environmental research	Soil samples, comminution of botanical materials – also possible deep frozen
Pharmaceuticals and medicine	Ophthalmological agents, gels, creams, extracts, drugs, pastes, dragées, tablets
Biotechnology	Tissue samples, botanical matter
Forensic analysis	Teeth, bones
Materials technology	Pigments, precious materials, new materials
RoHS	Mobile phone circuit boards, mobile phone cameras, mobile phone LCD glass panels, mobile phone keypads, electronic chips, LCD diffusion panels

FACTS AND ADVANTAGES

- Grinding and sieving in one unit
- Agglomeration phenomena avoided
- Ergonomically positioned membrane keyboard IP65, splash-proofed
- Recyclable plastic housing
- Convertible for cryogenic grinding
- Window for observing the grinding progress
- Digital timer
- Standard equipment includes grinding head (included in price)
- Accessories: Mortars and grinding balls in 6 different materials (ordered separately). All mortars are rimmed in an aluminium shell.
- Grinding bowl oscillations 3,000 – 3,600 oscillations/min at 1 – 3 mm amplitude
- CE mark
- 2-year guarantee



PULVERISETTE 23



GRINDING BOWLS AND GRINDING BALLS

For your FRITSCH Mini-Mill PULVERISETTE 23, you require one grinding bowl and the corresponding number of grinding balls. To avoid undesired contamination of the sample through abrasion, we offer a selection of 4 different material types. Normally, grinding bowls and balls of the same material are used. In principle, the grinding bowl material must be harder than the material to be ground. Important: Pay attention to the specified useful capacity as this is not identical to the bowl volume!

Material data for grinding bowls and grinding balls

Material	Main component of the material*	Density g/cm ³	Abrasion resistance	Use for material to be ground
Zirconium oxide	ZrO ₂	< 5.9	Very good	Fibrous, abrasive samples
Stainless steel	Fe – Cr – Ni	7.8	Fairly good	Medium-hard, brittle samples
Hardened steel	Fe – Cr	7.9	Good	Hard, brittle samples
PTFE	C _x – F _{2x}	2.16	Sufficient	Frozen tissue samples

* At www.fritsch.de, you can find the corresponding element analyses with detailed information about the materials.

Recommended number of balls per grinding bowl

Grinding bowl/ Useful capacity (sample volume)	15 ml 0.5 – 5 ml	10 ml 0.2 – 1 ml	5 ml 0.01 – 1 ml
Balls diameter			
15 mm	2	1	
10 mm	5	3	1
5 mm	60	30	20



PULVERISETTE 0



MORTAR AND GRINDING BALLS

For the FRITSCH Vibratory Micro Mill PULVERISETTE 0, you require a mortar, which must be equipped with a grinding ball. All FRITSCH mortars are rimmed, regardless of the material, in a robust shell of shock-resistant aluminium, which protects the actual mortar. To optimally adapt the grinding to any sample type, you can choose between 6 different materials, whereby mortars and grinding balls of the same material are generally used. Important: The mortar material must always be harder than the material to be ground. For cryogenic grinding, use mortars and grinding balls made of steel or tungsten carbide. The PULVERISETTE 0 can also be converted to a Vibratory Sieve Shaker ANALYSETTE 3 SPARTAN for dry and wet sieving. All related information can be found at www.fritsch.de/sieveshakers – or simply ask us!

Material data for mortars and grinding balls

Material	Main component of material*	Density g/cm ³	Abrasion resistance	Use for material to be ground
Agate ¹⁾	SiO ₂	2.65	Good	Soft to medium-hard samples
Sintered corundum ¹⁾	Al ₂ O ₃	3.8	Fairly good	Medium-hard, fibrous samples
Zirconium oxide	ZrO ₂	< 5.9	Very good	Fibrous, abrasive samples
Stainless steel	Fe – Cr – Ni	7.8	Fairly good	Medium-hard, brittle samples
Hardened steel	Fe – Cr	7.9	Good	Hard, brittle samples
Hardmetal tungsten carbide	WC	14.95	Very good	Hard, abrasive samples

* At www.fritsch.de, you can find the corresponding element analyses with detailed information about the materials.

¹⁾ Grinding sets made of agate and sintered corundum are not suitable for cryogenic grinding.

EXCELLENT GRINDING RESULTS WITH FRITSCH BALL MILLS**ENVIRONMENTAL ROHS – MOBILE PHONES ARE REDUCED TO DUST**

For comminution of individual electronic components, such as mobile phones for RoHS analysis, the FRITSCH Vibratory Micro Mill PULVERISETTE 0 delivers very good results – depending on the sample characteristics at room temperature or with cryogenic grinding after embrittlement with liquid nitrogen in the practical FRITSCH cryo-box.



Mobile phone keypad: Grinding results after embrittlement under freezing conditions

PHARMACEUTICALS – BONE PREPARATION FOR RESEARCH

For comminution of bones, e.g. for XRF analysis for medication development, we recommend the Vibratory Micro Mill PULVERISETTE 0 with mortar and grinding ball made of zirconium oxide or steel. The special advantage: Gentle sample preparation without development of heat or thermal loads.



Bone material before and after grinding with the FRITSCH PULVERISETTE 0

ANALYSIS – DRUG TESTS THROUGH HAIR ANALYSIS

For fast and simple preparation of hair samples for analysis for drug traces, roughly 300-500 mg of hair can be ground to a fine powder (< 100 μm) in just 5 minutes in the FRITSCH Mini-Mill PULVERISETTE 23 using a 15 mm steel ball in a 15 ml steel bowl.



Hair sample before and after grinding with the FRITSCH PULVERISETTE 23

PLASTICS/TEXTILES – FIBRE ANALYSIS WITH KBR TECHNOLOGY

For fibre analysis with infrared spectroscopy, the PULVERISETTE 23 provides the ideal preparation of the sample for creation of homogeneous pellets of potassium bromide (KBr). With addition of 20 mg of KBr, the fibre sample is ground to a homogeneous powder in 3 minutes. With an additional 250 mg of KBr that was ground for 90 seconds to a fine consistency in the PULVERISETTE 23, the ground sample is then ground further and homogenised in only 30 seconds.



KBr pellets for analysis of fibre samples

ORDERING DATA

Order no. Article

MINI-MILL PULVERISETTE 23

PULVERISETTE 23



23.1000.00 **Instrument without grinding bowl and balls**
for 100-240 V/1~, 50-60 Hz

Grinding bowl 15 ml volume
23.1427.00 Zirconium oxide
23.1410.00 Stainless steel
23.1409.00 Tempered steel

Grinding bowl 10 ml volume
23.1327.00 Zirconium oxide
23.1310.00 Stainless steel
23.1309.00 Tempered steel

Grinding bowl 5 ml volume
23.1600.00 PTFE

Grinding balls 15 mm diameter
55.0150.27 Zirconium oxide
55.0150.10 Stainless steel
55.0150.09 Tempered steel

Grinding balls 10 mm diameter
55.0100.27 Zirconium oxide
55.0100.10 Stainless steel
55.0100.09 Tempered steel

Grinding balls 5 mm diameter
55.0050.27 Zirconium oxide
55.0050.10 Stainless steel
55.0050.09 Tempered steel

Smaller grinding balls (0.1 - 3 mm Ø) are also available!

Order no. Article

VIBRATORY MICRO MILL PULVERISETTE 0

PULVERISETTE 0



00.6020.00 **Instrument incl. grinding head, without mortar and grinding ball**
for 100-240 V/1~, 50-60 Hz

Mortars
40.0150.05 Agate
40.0140.06 Sintered corundum (99.7 % Al₂O₃)
40.0220.27 Zirconium oxide
40.0130.10 Stainless steel
40.0120.09 Tempered steel
40.0110.08 Hardmetal tungsten carbide

Grinding balls
40.0170.05 Agate 50 mm diameter, polished
40.0210.05 Agate 70 mm diameter, polished
40.0170.06 Sintered corundum (99.7 % Al₂O₃) 50 mm diameter
40.0230.27 Zirconium oxide 50 mm diameter
40.0180.10 Stainless steel 50 mm diameter
40.0190.09 Tempered steel 50 mm diameter
40.0200.08 Hardmetal tungsten carbide 50 mm diameter

Further accessories
00.2000.00 Cryo-box (device for grinding in liquid nitrogen)
00.0130.17 Sound absorption hood plexiglas

Accessories for dry and wet sieving
Vibratory Sieve Shaker ANALYSETTE 3 SPARTAN

Ask for a detailed brochure! Or have a look at www.fritsch.de/sieveshakers



Grinding reports online!

At www.fritsch.de/solutions, you will find a comprehensive database of grinding reports for various materials and industries. It's worth to take a look!



Alternatively, send us your sample for a free grinding trial. We will then submit you a fully documented grinding report identifying the mill, which is the right one for you.

Do you have questions?
We would be happy to assist you!

+49 67 84 70 0

www.fritsch.de



Fritsch GmbH

Milling and Sizing

Industriestrasse 8

55743 Idar-Oberstein

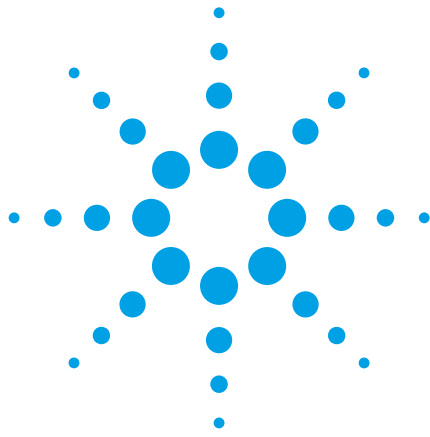
Germany

Phone +49 67 84 70 0

Fax +49 67 84 70 11

info@fritsch.de

www.fritsch.de



Fast and Reliable Trace Gas Analysis – Improved Detection Limits for the Agilent 490 Micro GC

Technical Overview

Trace gas analysis is a challenge in today's world. The ability to analyze lower component levels enables you to do better quality control, and gain more reliable results. To meet your requirement for fast and accurate gas analysis outcomes, we have made continuous product quality improvements resulting in lower limits of detection (LOD) for our gas analysis platform – the Agilent 490 Micro GC.

To match your gas application requirements, you can equip the 490 Micro GC with one to four independently controlled column channels. Each column channel is a complete miniturized gas chromatograph with:

- Electronic carrier gas control,
- Micro-machined injector,
- Narrow-bore analytical column, and
- Micro thermal conductivity detector (μ TCD).

This setup provides fast gas analysis, with typical run times of 30 to 90 seconds.



Agilent Technologies

Up to Five Times Improved Detection Limit

The limit of detection (LOD) for chromatography systems depends on the analyte peak signal compared to the baseline noise. Column type influences chromatographic separation and peak shape. For gas analysis, a wall-coated open tubular (WCOT) column gives the sharpest peaks, and provides the best signal-to-noise ratios (S/N). Porous layer open tubular (PLOT) columns and micro-packed columns have solid stationary phases with less efficiency. They give broader peaks and, therefore, slightly higher detection limits.

Until recently, LOD specifications were set to 1 ppm for WCOT columns and 10 ppm for PLOT and micro-packed columns. The latest enhancements for the Agilent 490 Micro GC show up to five times improved LODs, down to 0.5 ppm for WCOT columns, 2 ppm for PLOT columns, and 10 ppm for micro-packed columns. Table 1 gives an overview of the detection limits per column type. You can find more details about instrument specifications in the 490 Micro GC Data Sheet [1].

Table 1. Agilent 490 Micro GC Specifications for LOD

Column type	LOD (ppm)*
Wall coated open tubular column Agilent CP-Sil 5 CB, CP-Sil 13 CB, CP-Sil 19 CB, and CP-WAX 52 CB	0.5
Porous layer open tubular and micro-packed column Molsieve 5A, PoraPLOT Q, PoraPLOT U, Aluminum oxide, SilicaPLOT, MES, and HayeSep A	2
Micro-packed column CP-CO _x	10

* Detection limits are typical for selected components provided that the proper column length and chromatographic conditions are used.

Example for WCOT Columns — 0.5 ppm Hydrocarbons on the CP-Sil 5 CB Column

Analysis of hydrocarbons is a typical application for the Agilent CP-Sil 5 CB column. This WCOT column is also used to analyze the high end of this sample in the natural gas analyzers that are based on the 490 Micro GC. Agilent Application Note 5991-0275EN [2] highlights this capability. The chromatogram in Figure 1 exhibits baseline separation and substantial peak area for *n*-hexane, *n*-heptane, and *n*-octane at the detection limit (approximately 0.5 ppm per compound).

Repeatability, calculated for 10 replicate analyses at twice the detection limit for *n*-heptane, is 1.3 % relative standard deviation (RSD) for concentration and 0.05 % for retention time. Figure 2 depicts an overlay of five of these replicate runs.

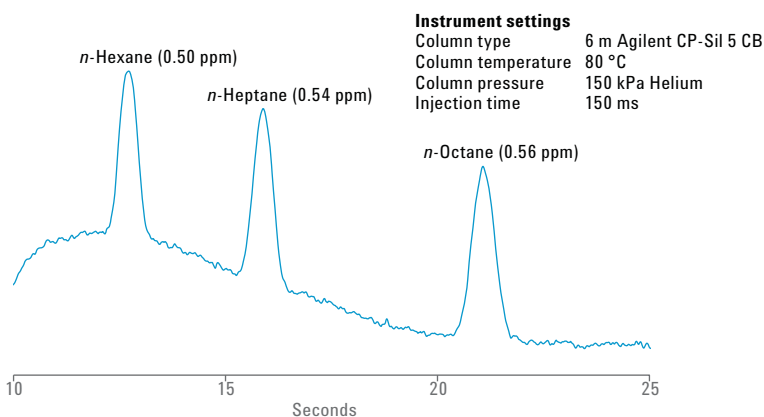


Figure 1. The Agilent CP-Sil 5 CB column channel shows excellent peak area and baseline separation at the detection limit for three alkanes.

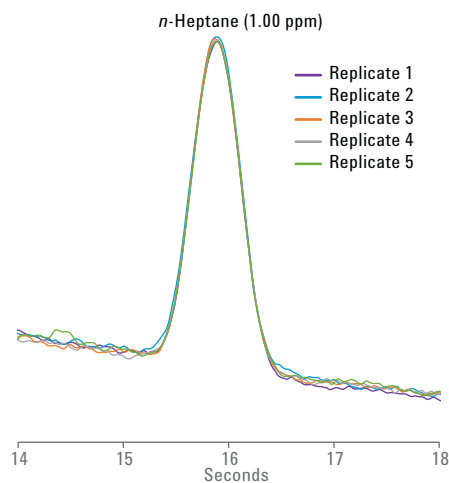


Figure 2. Overlay of five replicate runs at 1.08 ppm *n*-heptane demonstrates reliable repeatability.

Example for PLOT Columns — C2 Hydrocarbons Down to 2 ppm on PoraPLOT U

The 490 Micro GC equipped with an Agilent PoraPLOT U column is used for the fast analysis of nitrogen, carbon dioxide, methane, ethane, and propane. Agilent Application Note 5990-9508EN clearly demonstrates this capability [3]. In addition, this PLOT column delivers baseline separation of the C2 hydrocarbons. Figure 3A shows a chromatogram for ethane, ethylene, and acetylene at the 2 ppm level – its specification for LOD. Compared with the old specification, this is a five-fold improvement. In addition to excellent separation and low-ppm detection limits, the μ TCD on the 490 Micro GC shows outstanding linearity. The R^2 values are 0.999, as depicted in Figure 3B.

A good repeatability is calculated at detection limit level (2 ppm), approximately 5% RSD for ethane, ethylene, and acetylene. These values are significantly decreased at 5 times the detection limit (10 ppm) to 0.55–1.18% RSD. Retention time repeatability over the full range was measured at lower than 0.02 to 0.08% RSD. Tables 2 and 3 give an overview.

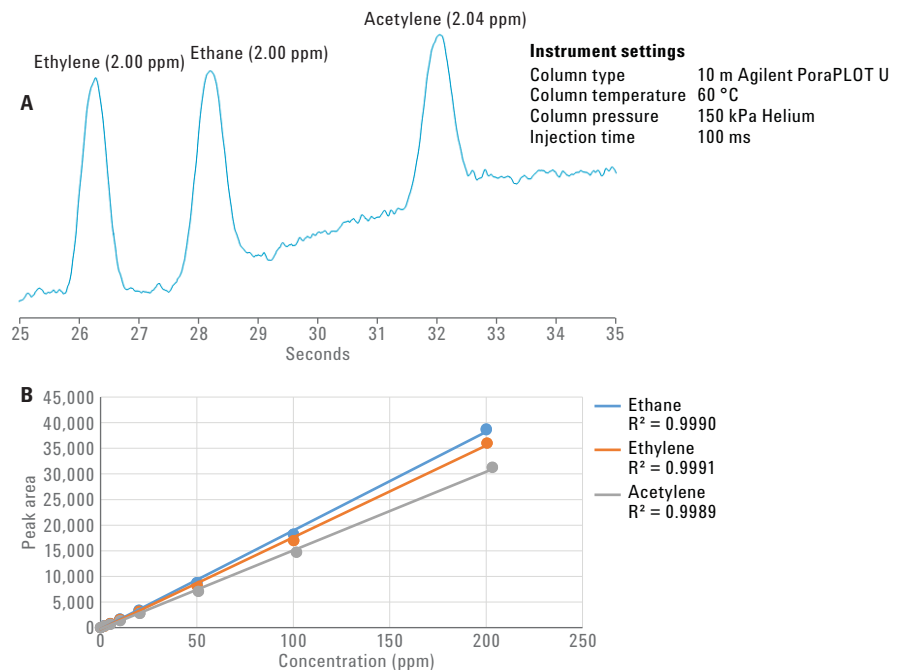


Figure 3. Chromatogram (A) shows excellent peak area and separation at the detection limit of 2 ppm. Calibration curve (B) for these compounds demonstrates good linearity.

Table 2. Repeatability Data for Peak Area for the Ethylene, Ethane, and Acetylene Analysis

RSD % (n = 10) for concentration (ESTD)			
Concentration (ppm)	Ethylene	Ethane	Acetylene
2	5.08	5.37	4.37
10	0.55	1.18	1.14
200	0.12	0.21	0.15

Table 3. Repeatability Data for Retention Time for Ethylene, Ethane, and Acetylene Analysis

RSD % (n = 10) for retention time (RT)			
Concentration (ppm)	Ethylene	Ethane	Acetylene
2	0.071	0.085	0.082
10	0.023	0.019	0.023
200	0.030	0.020	0.017

Example for Micro-packed Columns — 10 ppm Level Carbon Dioxide on CP-CO_x Column

The detection limit specification for micro-packed column type CP-CO_x is set to 10 ppm. This column type is typically used for the analysis of permanent gases, including carbon dioxide. Agilent application note 5990-7054EN shows an example [4]. Figure 4 shows a chromatogram of 10 ppm carbon dioxide using helium carrier gas.

Repeatability for 20 consecutive analyses at 5 times LDL specification (50 ppm) is measured at 0.16% RSD for retention time and 2.6% for external standard concentration, as shown in Table 4. An overlay of five of these runs is given in Figure 5A. Excellent linearity is determined for 10 to 300 ppm carbon dioxide; the regression coefficient for linear curve fitting for this range is 0.9999 (Figure 5B).

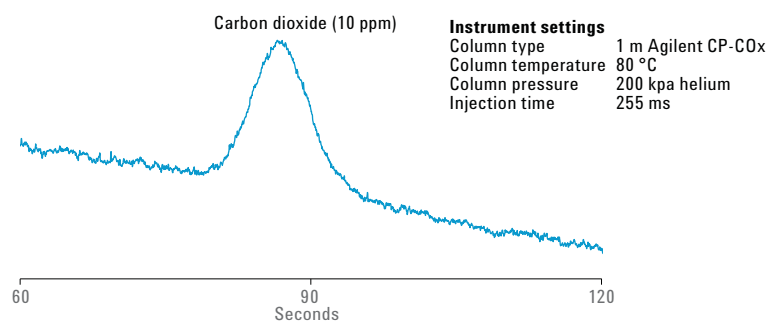


Figure 4. LOD performance of the Agilent CP-CO_x column.

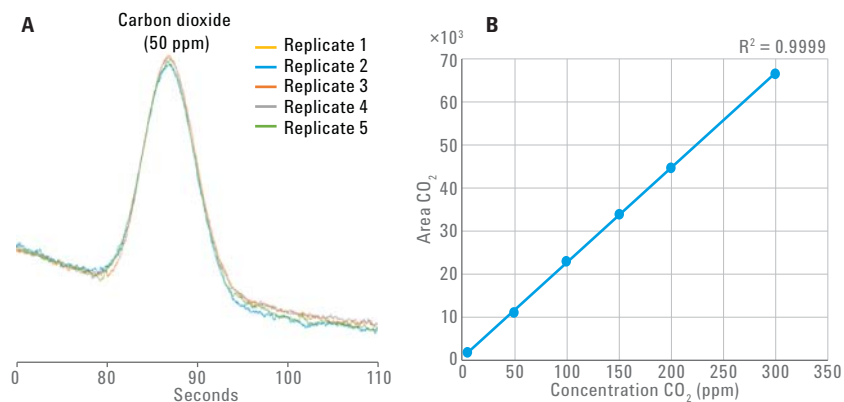


Figure 5. A) Overlay of five replicate runs of carbon dioxide at 50 ppm on an Agilent CP-CO_x column. B) Excellent linearity, with regression coefficient for linear curve (10–300 ppm CO₂) determined at 0.9999.

Table 4. Repeatability Data for Carbon Dioxide on the CP-CO_x Column

Carbon dioxide (50 ppm)	RSD % (n = 20)
Retention time	0.16 %
Concentration; external standard method	2.6 %

Reliable Trace Analysis

The 490 Micro GC delivers sensitive gas analysis in seconds. With the recent detection limit improvements that resulted from product quality enhancements, the 490 Micro GC provides reliable trace gas analysis down to 0.5 ppm for WCOT columns, 2 ppm for PLOT columns, and 10 ppm for micro-packed columns. Contact an Agilent Representative today to find out more about Agilent Micro GC solutions for your application.

References

1. Agilent 490 Micro GC Natural Gas Analyzers, *Agilent Technologies Data Sheet*, publication number 5991-0301EN (2012).
2. R. van Loon, Fast Analysis of Natural Gas Using the Agilent 490 Micro GC Natural Gas Analyzer, *Agilent Technologies Application Note*, publication number 5991-0275EN (2012).
3. R. van Loon, Analysis of Biogas Using the Agilent 490 Micro GS Biogas Analyzer, *Agilent Technologies Application Note*, publication number 5990-9508EN (2011).
4. S. Darphorn-Hooijschuur, *et al.* Permanent Gases on a COX Module Using an Agilent 490 Micro GC, *Agilent Technologies Application Note*, publication number 5990-7054EN (2012).

www.agilent.com/chem

Agilent shall not be liable for errors contained herein or for incidental or consequential damages in connection with the furnishing, performance, or use of this material.

Information, descriptions, and specifications in this publication are subject to change without notice.

© Agilent Technologies, Inc., 2015
Printed in the USA
September 11, 2015
5991-6201EN



Agilent Technologies